THE PROCEEDINGS OF THE PHYSICAL SOCIETY

Section A

VOL. 63, PART 1 1 January 1950 No. 361 A

EDITORIAL

PROCEEDINGS OF THE PHYSICAL SOCIETY SECTIONS A and B

In the light of experience gained over the course of the past year it is now possible to make a clearer statement of the basis on which division into the two Sections of the *Proceedings* is being made.

In general, it has been found that the division which best meets the needs of Fellows is one which brings papers on microphysics and the physics of elementary particles into the one Section, A, and papers on macroscopic physics into the other Section, B. While it is essential to maintain a certain amount of flexibility in the allocation of papers, a paper will, as far as possible, be put in the Section where the main interest lies, e.g. a paper on counter-technique would appear in B if the circuitry is the main interest, but would be in A if the applications to actual counting are of major importance.

A list indicating this subject division is given below.

A. C. STICKLAND,
Secretary–Editor.

Section A

Thermodynamics
Electrodynamics
Statistical mechanics
Quantum theory
Nuclear physics
Electron theory: metals, semiconductors, dielectrics
Molecular and atomic structure
Spectra of atoms and molecules over the whole frequency range
Physics of crystals (including luminescence as a means of investigating this)
Photoconductivity
Theory of solids, liquids and gases
Magnetism (theoretical)
Cosmic rays
Low temperature physics
Standards relevant to this Section

Section B

Thermal, magnetic, electrical, elastic, rheological and other mechanical properties of matter
Hydrodynamics and aerodynamics
Acoustics
Metallography
Geometrical optics, optical design and microscopy
Interferometry, diffraction and classical physical optics generally
Electric and electronic circuits
Dielectrics and semiconductors: measurement and theory of measurement
Electric discharges
Electron optics
Geophysics
Radio
Physics of the atmosphere and ionosphere
Physics of the sensory processes
Colour physics
Astrophysics and solar physics
Applications of spectroscopy (e.g. chemical analysis, structure analysis)
Analysis of crystal structure
Radiography
Luminescence
Photoelectricity
Thermoelectricity
Piezoelectricity
Photoconductivity
Magnetic properties of materials (including methods of measurement)
Production of low temperatures
High pressure physics
Vacuum physics
Thermionic emission
Standards relevant to this Section

Heat Transport in Superconductors

By K. MENDELSSOHN and J. L. OLSEN
Clarendon Laboratory, Oxford

MS. received 6th July 1949

ABSTRACT. The heat conduction processes in superconductors have been discussed on the basis of the analogy with liquid helium II. It is suggested that under certain conditions the superconductive metal can exhibit a type of heat transport corresponding to the heat flow associated with the fountain effect. The heat conductivity of a number of pure metals and alloys has been measured in the normal and in the superconductive state and the results have been analysed with reference to the hypothesis mentioned above. In addition to the change of heat conduction with temperature, the magnetic hysteresis of the heat conduction has been investigated. The use of these phenomena as make-and-break thermal contacts at very low temperatures has been suggested.

---

§ 1. INTRODUCTION

Of the various manifestations of superconductivity the phenomena associated with the transport of heat appear to be particularly difficult to explain. This is due to the fact that the heat resistance of the metal in the superconductive state may be higher *or* lower than in the normal state at the same temperature. While the former case usually applies to a pure metal and the latter to alloys, this in not a general rule. Thus the available experimental material presents a somewhat confused aspect which none of the theoretical work has attempted to explain. A few years ago one of us (Mendelssohn 1946), when discussing the similarity between superconductivity and liquid helium II, suggested a possible mechanism which seems capable of accounting for the qualitatively different behaviour of pure metals and alloys in heat conduction. Indeed, the fact that this difference should have followed as a necessary consequence from the analogy between the two phenomena was taken to be strong support for it.

In order to test our hypothesis of heat transport in superconductors more experimental material than exists at present is required, and it was therefore decided to begin systematic experiments on the heat conduction of superconductive pure metals and particularly of alloys. A considerable amount of work in this field has been carried out in Leiden (cf. de Haas and Bremmer 1936, de Haas and Rademakers 1940) in which the dependence on temperature of the heat resistance of a number of alloys and pure metals was determined. This was supplemented by experiments in this laboratory (Mendelssohn and Pontius 1937) in which the change of heat resistance in the transition between the superconductive and the normal state was studied in some detail for the alloy Pb 90% – Bi 10% and for pure lead. Finally it was found (Daunt and Mendelssohn 1946 a) that the temperature gradient in a superconductor is uninfluenced by the setting up of a persistent current. This fact, which shows that the Thomson coefficient is zero, leads to the important conclusion that the entropy of the electrons in a supercurrent, too, is zero. A survey of this material shows that it would be desirable to extend the work on heat resistance to a greater number of substances, and especially to combine determinations of the temperature dependence with the taking of magnetic cycles similar to the observations of Mendelssohn and Pontius.

A considerable number of measurements of this kind has now been carried out and the present paper gives a survey of the results obtained so far. In view of the extent of the field of research the work to date is far from complete and can only be considered as a first report. However, in view of the conclusions which can be drawn already, and because continuation of the work for several years is anticipated, it seems desirable to publish the first results at this stage.

§ 2. MECHANISMS OF HEAT TRANSPORT

Our hypothesis of the heat transport phenomena is based on the assumption that the electrons in a superconductor can be treated as being made up of two inter-penetrating fluids of different entropy (Mendelssohn 1945) similar to helium II. The normal (n-) constituent has ordinary properties, including finite entropy, while the other (z-) constituent has anomalous properties and zero entropy. The z-fluid makes its first appearance at the transition point and its concentration increases at the expense of the n-fluid as the temperature is lowered. Evidence from magnetic determinations (Daunt, Horseman and Mendelssohn 1939) indicates that at very low temperatures the concentration of the n-fluid in a superconductor approaches the value zero.

Enumerating the processes contributing to the heat transport, we have first to consider in the superconductor the effect of the crystal lattice. Unless we care to liken it to the conduction of the container, this term has no counterpart in the case of helium II. Then comes the conduction of the n-fluid, which is evidently quite small in liquid helium but large in the case of electrons. This, of course, is the ordinary metallic heat conductivity which is related to the electrical conduction by the Wiedemann–Franz law. Compared with the normal state, this term must decrease in the superconductive state with falling temperature as the concentration of the n-fluid decreases. It should tend to zero at absolute zero. The heat conduction of the z-fluid must be zero as it has zero entropy, but this does not mean that the z-fluid cannot contribute to the heat transport. The setting up of a temperature difference within the substance is tantamount to creating a difference in the concentration of the two fluids. This in turn results in a flow of z-fluid towards the hot end*, and in a return flow of n-fluid in the opposite direction. A circulation of this type is accompanied by a large heat transport. It differs from an ordinary convection by the fact that at the warm end the z-fluid is transformed into the n-state and in doing so must take up the *total* entropy at this temperature. This circulation is well known in the case of helium II, where it gives rise to the fountain effect (Allen and Jones 1938, H. London 1939). It is this process which is responsible for the very high heat transport of the liquid.

The question arises whether a similar circulation can take place in a superconductor. In order to maintain it, a super-current must flow in the direction towards the warm end, and it must be compensated by a normal current in the opposite direction. However, here the main difference between helium and a superconductor, the electrodynamic properties of the latter, comes into play. The super-current must be a surface flow while the induction inside the conductor has to be zero. The normal return current and its magnetic field would have to be distributed over the whole cross section of the conductor. Because of the Meissner effect no such field is permitted and the return flow cannot, therefore, take place. It is important to realize that a circulation flow similar to that in helium with its high heat transport is only prohibited by electrodynamics, and that if conditions can be created which allow the induction inside the superconductor to be different from zero, this heat transport should take place.

---

* The mechanism of this flow of z-fluid has been interpreted by us as a kind of diffusion process under its zero point momentum (Mendelssohn 1945), and this assumption has gained support from experiments on the helium film (Daunt and Mendelssohn 1946 b).

Such superconductors with finite magnetic induction do in fact exist. The systematic investigations carried out in this laboratory on the magnetic and thermal properties of superconductors have shown that superconductive alloys are electrodynamically inhomogeneous. Their properties can be described as those of a magnetic 'sponge' (Mendelssohn 1935) whose meshes are made up of superconductive and normal regions. It is, in fact, almost impossible to experiment with a superconductor which does not show traces of this sponge structure since the magnetic properties appear to be extremely sensitive to chemical and physical impurities. According to our views we should therefore expect in impure superconductors and in alloys an entirely new heat transport mechanism which is exactly analogous to the high heat flow in liquid helium II. The observed fact that the heat transport in pure superconductive lead is smaller than in the normal metal, whereas this relation is reversed in lead containing 10% of bismuth (Mendelssohn and Pontius 1937), appears most convincing.

Thus the heat 'conduction' of the metal in the normal and in the superconductive state can be added up as follows. Denoting by L the heat conductivity of the lattice, E the ordinary electronic heat conduction, ρ_z the fraction of electrons in the superconductive state, and G the heat transport by circulation, similar to that in liquid helium II, we can write for the total heat 'conductivity' K of the metal:

(*a*) in the normal state

$$K_n = L + E \qquad \ldots\ldots(1)$$

and

(*b*) in the superconductive state, for (α), $B = 0$

$$K_{s\alpha} = L + Ef(1 - \rho_z), \qquad \ldots\ldots(2)$$

for (β) $B \neq 0$

$$K_{s\beta} = L + Ef(1 - \rho_z) + G, \qquad \ldots\ldots(3)$$

and since $f(1 - \rho_z)$ will vary between 0 and 1,

$$K_n > K_{s\alpha}; \qquad \ldots\ldots(4)$$

but

$$K_n \gtrless K_{s\beta}. \qquad \ldots\ldots(5)$$

In view of the fact that all the terms depend in a complex manner on temperature and structure, numerical evaluation of equations (1), (2) and (3) is clearly out of the question. However, as equations (4) and (5) show, the expressions for K_n and K_s seem to lead to a qualitative interpretation of the heat conduction phenomena in superconductors. For instance, in a very pure metal where the induction is zero we should *always* have a smaller heat conduction in the superconductive than in the normal state. Moreover, near absolute zero in such a metal the heat conduction in the superconductive state must become very small since ρ_z will approach the value 1 and the second term in equation (2) disappears. The assumption that at absolute zero *all* conduction electrons in the metal are in the superconductive state is based on magnetic determinations of the entropy (Daunt, Horseman and Mendelssohn 1939) and appears to be borne out by the observed high heat resistance of pure superconductive lead at the lowest temperature (de Haas and Rademakers 1940). Under these circumstances it is only the lattice which contributes to the heat conductivity.

Whether in cases where the induction is different from zero K_n or K_s is the larger must depend, as equation (3) shows, on the relative importance of the terms $f(1-\rho_z)$ and G. While a proper assessment of $f(1-\rho_z)$ can only be made on the basis of a theoretical model of superconductivity, one has reason to believe that it should decrease as a monotonic function of the temperature. The anomalous heat transport G will depend on a number of factors. It must be proportional to $S\rho_z$, where S is the total electronic entropy of the metal. Since $\rho_z \rightarrow 0$ at the transition point and $S \rightarrow 0$ at absolute zero, G must pass through a maximum with varying temperature. G is inversely proportional to the resistance encountered by the return flow of the circulation in the normal phase, but will also depend on the thermo-electrical properties of the latter.

The whole circulation process might be described as an internal thermocouple consisting of a superconductive and a normal lead. No current will be possible, for instance, if the thermo-E.M.F. between the warm and the cold end is zero since a current in the normal phase depends on the existence of an accelerating potential. In other words, under these circumstances G will become zero, and we think it possible that this influence of the thermo-electric properties may account for the qualitatively different behaviour of different superconductive alloys. This conception appears to be borne out by the results on lead–bismuth and the lead–tin alloy described in this paper.

§ 3. RESULTS

The method employed followed the usual pattern of measuring the temperature at two places on a rod of the metal along which a steady temperature gradient is established. The accuracy at 4° K. was about $\pm 2\%$, but dropped to $\pm 5\%$ at the very lowest temperatures. The temperature differences were of the order of $0{\cdot}1^\circ - 0{\cdot}2^\circ$. A detailed description of the apparatus employed will be given at a later date.

Tantalum. As an example of a pure metal tantalum was chosen because the heat conductivity of this metal has not been measured before. The specimen used was the same rod of very pure metal whose critical fields had been determined by Daunt and Mendelssohn (1937). The results, given in Figure 1, show that at all temperatures the heat conduction in the superconductive state is smaller than that in the normal state, which is in agreement with equation (4). Moreover, the heat conductivity of the superconductive metal decreases rapidly as the temperature is lowered, being less than half of the normal at 2·75° K. Also, the curve for the normal state appears to be the *continuous* one, from which the superconductive curve breaks away at the transition point. All these features agree with previous work on pure metals as well as with our equations (1) and (2). Near the transition point the scatter of our values is considerable and may be larger than is warranted by the experimental errors. A possible explanation of this will be discussed below.

Pb 90%–*Bi* 10%. This alloy, the results for which are given in Figure 2, was of identical composition with the sample used by Mendelssohn and Pontius. As in the pure metal, the heat conductivity in the normal state follows a continuous curve. However, the heat conductivity of the superconductive metal is entirely different. Instead of falling below the normal curve it *rises* steeply. The whole pattern is so different from the pure metals that it appears clear that a new type of heat transport must be operative. At 5° K. the superconductive heat conductivity is three times as large as the normal. Because of the high threshold fields of this alloy the normal curve could not be determined to lower temperatures, but extrapolation suggests that at 3° K. the superconductive value for the heat flow may be six times higher than the normal one. In this temperature region the superconductive curve shows a maximum, indicating a rapid drop to lower temperatures. Since the normal curve is not known, the question has to be left open whether it will also show a drop. However, it may well be that the observed maximum is that predicted in the previous section for the circulation flow, being due to the drop in the electronic entropy.

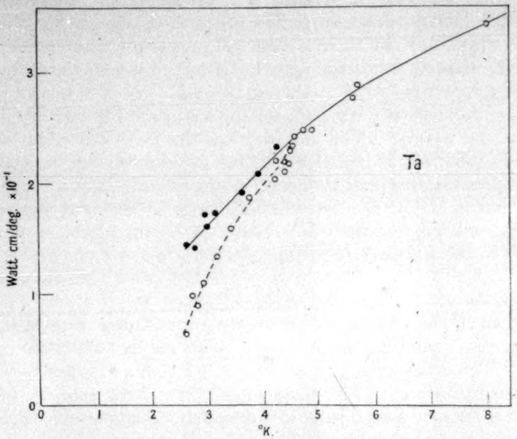

Figure 1. Heat conductivity of tantalum. The continuous curve denotes the normal state of the metal, the broken curve the superconducted state. ○ in zero magnetic field; ● in fields exceeding the threshold value.

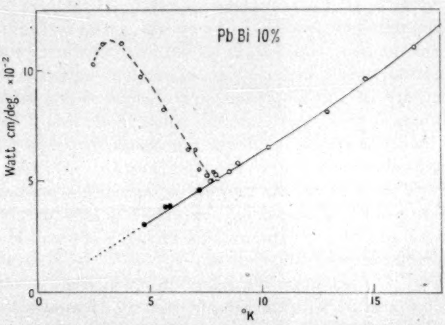

Figure 2 Heat conductivity of Pb–Bi 10% alloy.

Pb 70%–*Sn* 30%. In order to test our assumption concerning the influence of the thermo-electric properties on the circulation flow a lead–tin alloy was measured because it is known (Keesom and Matthijs 1938) that the thermo-E.M.F. between these metals in the helium region is very small. Although the thermo-E.M.F. in the alloy is likely to be different from that between the pure constituents, one may expect that it is much smaller than between lead and bismuth. The results, shown in Figure 3, indeed seem to support this assumption. The superconductive curve lies at all temperatures below the normal, and the results altogether resemble much more those for tantalum than those obtained on the lead–bismuth alloy. In particular, we may assume that the induction in this case was different from zero, and there should, therefore, be a chance for the establishment of a normal current in the metal. That in spite of this no appreciable heat flow by circulation takes place can be taken as a strong indication for the expected thermo-electric influence.

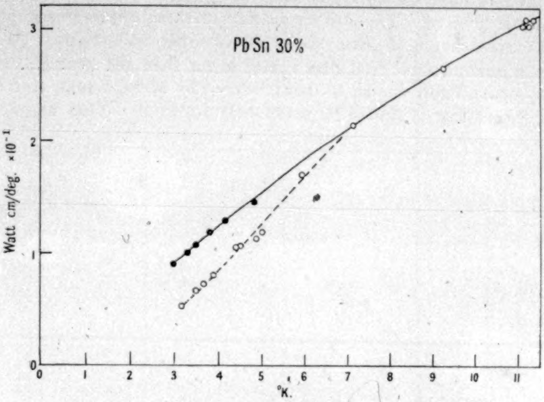

Figure 3. Heat conductivity of Pb–Sn 30% alloy.

Columbium. It seemed interesting to investigate this metal not only because of its similarity to tantalum but also because it has a very high transition point (9·2° K.). The rod used was of high purity ('H.S.' Lab. No. 1919). The results (Figure 4) are complex and differ from all previous observations in that the curves cross over at low temperatures. Immediately below the transition point the superconductive metal, similar to tantalum, exhibits a lower heat conduction than the normal. However, as the temperature is lowered the difference between the two curves decreases again, and below 3·8° K. the superconductive metal becomes the better conductor of heat. It would seem very difficult to account for this peculiar behaviour except by two different, competing processes in the heat flow mechanism. We have seen that, according to our hypothesis, such a mechanism actually exists in the relative influence of the terms $f(1-\rho_z)$ and G in equation (3). In a very pure metal the latter term should always be zero, but it is well known that the induction in the 'hard' superconductors is not always zero. In fact it has been found that a similar columbium rod exhibited more and more the magnetic properties of an alloy as the temperature was lowered (Daunt and Mendelssohn 1937). We had therefore reason to suspect that the crossing over of the curves might be due to the appearance of circulation heat flow at low temperatures. In order to investigate this question more thoroughly, the dependence of the heat flow on the magnetic field was measured in some detail.

The magnetic cycles, given in Figure 5, represent the change of thermal resistance (in arbitrary units) with transverse magnetic field. The dotted curves which give the hysteresis cycles after superconductivity had been destroyed are similar at the two different temperatures (4·4° K. and 2·7° K.), except that there is somewhat less hysteresis at the higher temperatures. This is exactly what would be expected on the strength of the magnetic measurements. It shows that the metal behaves to some extent like an alloy and that this effect increases as the temperature is lowered. The striking feature of these observations, however, is the full curve denoting the first destruction of superconductivity. At 4·4° K., where the superconductive heat flow is still lower than the normal, we might expect a hysteresis figure similar to that observed by Mendelssohn and Pontius on Pb–Bi except that it should be completely inverted. That means in our present figure the beginning of the virgin curve should lie somewhat *above* the two peaks of the hysteresis loop. Instead, however, the virgin curve starts well below this value, which means that during the hysteresis the heat resistance (at about 1,000 gauss) is higher than in either the superconductive or the normal state. This feature is even more pronounced in the hysteresis figure at 2·7° K., where the beginning of the virgin curve is depressed below any other value in the complete cycle.* These results seem to show without doubt that the crossing over of the curves in Figure 4 is due to changes of the heat flow mechanism in the superconductive and not in the normal state. The two hysteresis figures demonstrate the appearance of some additional form of heat transport as the magnetic behaviour of the metal alters with temperature. The evidence offered thus appears to support the hypothetical circulation process.

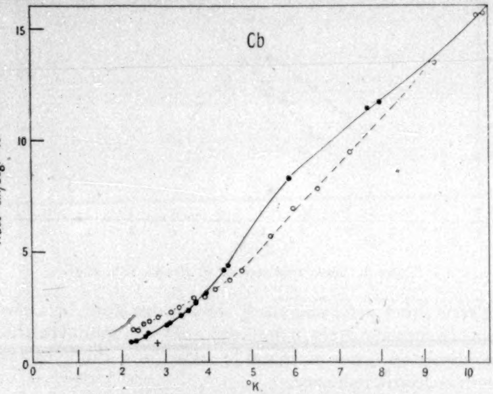

Figure 4. Heat conductivity of columbium.

Pb 99·9%–*Bi* 0·1%. As a further test of our hypothesis it appeared tempting to try to create artificially similar conditions to those which according to our analysis obtained in the columbium specimen. In order to simulate these

---

* It is possible from this figure to extrapolate the heat conductivity in the superconductive state *without* the circulation process, i.e. to place the start of the virgin curve above the maxima. This value is marked by a cross in Figure 4.

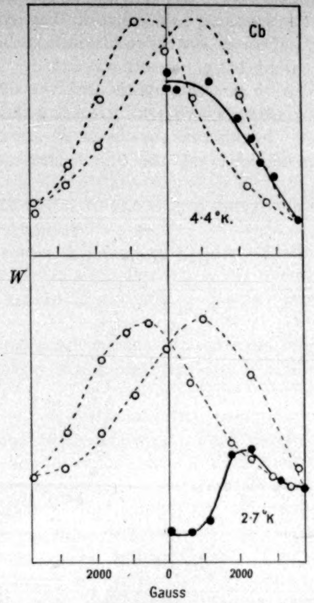

Figure 5. Hysteresis figure (heat resistance W in arbitrary units against magnetic field) for columbium.

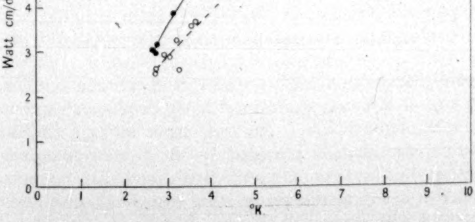

Figure 6. Heat conductivity of Pb–Bi 0·1% alloy.

conditions we decided to add a very small amount of a second constituent to a pure metal. For this purpose we chose lead, since its heat conductivity had been measured in Leiden and in Oxford, and the results indicated a close approximation to ideal conditions. To this 0·1% of bismuth was added. The results (Figure 6) show indeed that, similar to our columbium rod, the difference between the superconductive and the normal curve first increases with lowering temperature and then declines again. In this case the curves do not actually intersect, the superconductive one being lower all the time. However, reasonable extrapolation suggests that the curves may possibly cross over at about 2° K. A slightly higher percentage of bismuth would most likely produce an intersection of the curves at a higher temperature. An even more striking similarity with the observations on columbium is provided by the hysteresis curves (Figure 7). When comparing the curves denoting the first destruction of superconductivity it can be seen that again, as the temperature is lowered, the beginning of this curve is depressed with respect to the rest of the hysteresis cycle. It appears

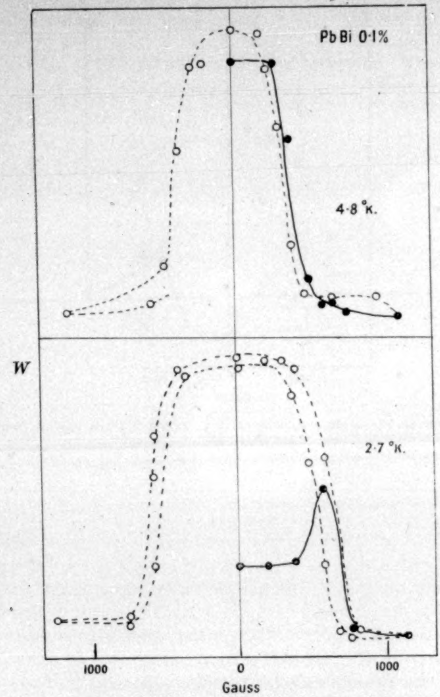

Figure 7. Hysteresis figure for Pb–Bi 0·1% alloy.

almost certain that this anomalous rise in the superconductive heat conduction must be the first indication of the circulation process which in the alloy with 10% bismuth completely overshadows all other effects.

§ 4. CONCLUSION

As already stated, the work has to be regarded as being of a preliminary character, and the results obtained so far emphasize the need for further and more detailed information. On the other hand, the available data seem to provide fairly satisfactory evidence for our qualitative model of heat transport phenomena, especially the existence of a new type of heat transport which can under certain (controllable) circumstances take place in the superconductive metal appears well established. Whether this process is in fact identical with the circulation flow postulated by us and to what extent it is the counterpart to the high heat conduction in liquid helium II can only be decided with certainty when more data are available. It should be pointed out, however, that all the results obtained so far can be regarded as confirmatory. In particular, the fact that the complex and unexpected results on columbium have proved amenable to our interpretation is most encouraging. The positive outcome of the two test experiments, one (Pb–Bi 0·1%) simulating the conditions in columbium and the other (Pb–Sn) the influence of the thermo-electric effects, must also be counted as supporting evidence. However, further experiments on these lines are clearly required.

In order to summarize our results we have plotted the ratio of the superconductive to the normal heat conduction K_s/K_n, against the reduced temperature, T/T_c, where T_c is the transition temperature. In this way our results can be compared with the theory of Heisenberg (1948). The deviation of our curves from the theoretical one can be seen in Figure 8. Apart from tantalum, all our results indicate higher ratios, K_s/K_n, than the theory predicts. In view of our hypothesis, this is not surprising. Heisenberg's theory only considers the process corresponding to our equation (2), making *no* provision for the circulation transport postulated by us. It is therefore interesting to note that all our ratios are higher except for tantalum where, according to our conceptions, the term G should be zero. Moreover, Pb–Sn, which should have the smallest G, also shows the smallest excess, while for Pb–Bi 10%, which will have the highest G, the excess ratio is so large that the scale had to be changed in order to accommodate its curve in the same diagram. These curves, too, therefore seem to provide evidence for a new process carrying large amounts of heat in superconductors. Quite recently Hulm (1949) has summarized some heat conductivity measurements in this type of diagram and concluded that the ratio K_s/K_n may be a characteristic function of temperature. In view of our results and of those obtained by Mendelssohn and Pontius we cannot but regard the mutual agreement between Hulm's curves as rather accidental. It would seem that in none of the cases investigated by him was G appreciable, but an analysis of his results suggests that, if he had further increased the mercury percentage of his Sn–Hg alloys, he might possibly have obtained a ratio K_s/K_n larger than unity.

Finally two possible future developments of this work should be mentioned. Firstly, in our treatment of the term G we have omitted the possibility that the circulation process may be limited at a given temperature by the superconductive threshold current. This would result in a saturation effect and the heat 'conduction' should be larger for small heat currents. No such effect has as yet been established, but it may be responsible for the scatter in the tantalum results mentioned above as well as for the unexplained scatter observed by de Haas and Rademakers (1940) in lead. Secondly, the phenomena of heat flow in superconductors may find a practical application in experiments at very low temperatures. Any cooling process carried out in successive stages will require make-and-break thermal contacts. On the basis of their recent experiments Hudson, Hunt and Kurti (1949) have suggested for this purpose the use of a thin layer of liquid helium between metal contacts. The results described in the present paper now

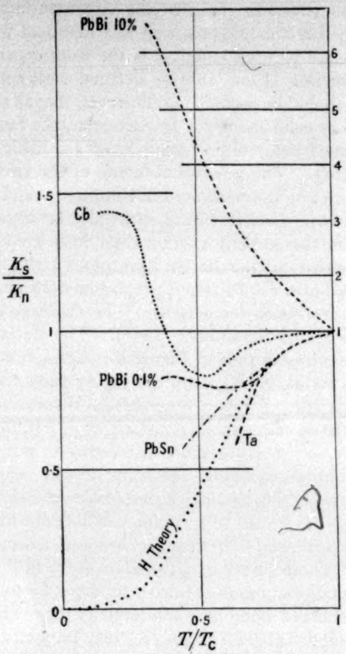

Figure 8. Ratio of heat conductivities against reduced temperature.

seem to offer an alternative or possibly a supplementary solution to this difficult problem. The difference between the heat conduction of a metal in the superconductive and the normal state can in certain cases be considerable, and one has reason to expect that, for instance in pure metals, at very low temperatures the ratio may be of the order of one to twenty or more. Furthermore, judicious adjustment of the amount of a second constituent can probably produce temperature variation of the ratio in such a manner as to suit the particular experiment. Make-and-break thermal contacts consisting of rigid connections of a metal whose heat conduction can be altered by a magnetic field may therefore often be found to be sufficient. They would have the advantage of being free of moving parts, and by a suitable choice of the metal the necessary magnetizing field could in many cases be kept small.

ACKNOWLEDGMENTS

Thanks are due to the Department of Scientific and Industrial Research for providing financial support for one of us (J. L. O.).

REFERENCES

ALLEN, J. F., and JONES, H., 1938, *Nature, Lond.*, **141**, 243.
DAUNT, J. G., HORSEMAN, A., and MENDELSSOHN, K., 1939, *Phil. Mag.*, **27**, 754.
DAUNT, J. G., and MENDELSSOHN, K., 1937, *Proc. Roy. Soc.* A, **170**, 423 ; 1946 a, *Ibid.*, **185**, 225 ; 1946 b, *Nature, Lond.*, **157**, 829.
DE HAAS, W. J., and BREMMER, H., 1936, *Physica*, **3**, 672.
DE HAAS, W. J., and RADEMAKERS, A., 1940, *Physica*, **7**, 992.
HEISENBERG, W., 1948, *Z. Naturforsch.*, **3a**, 65.
HUDSON, R. P., HUNT, B., and KURTI, N., 1949, *Proc. Phys. Soc.* A, **62**, 392.
HULM, J. K., 1949, *Nature, Lond.*, **163**, 368.
KEESOM, W. H., and MATTHIJS, C. J., 1938, *Physica*, **5**, 1.
LONDON, H., 1939, *Proc. Roy. Soc.* A, **171**, 484.
MENDELSSOHN, K., 1935, *Proc. Roy. Soc.* A, **152**, 34 ; 1945, *Proc. Phys. Soc.*, **57**, 371 ; 1946, *Royal Coll. Sci. Journ.*, **16**, 105.
MENDELSSOHN, K., and PONTIUS, R. B., 1937, *Phil. Mag.*, **24**, 777.

The Magnetization of Superconducting Plates in Transverse Magnetic Fields

BY E. R. ANDREW * AND J. M. LOCK
Royal Society Mond Laboratory, University of Cambridge

Communicated by D. Shoenberg ; MS. received 20*th May* 1949, *and in final form* 29*th October* 1949

ABSTRACT. The magnetization curves of thin superconducting tin plates were measured in transverse magnetic fields in order to investigate the nature of the intermediate state in such specimens. The curves showed peak magnetizations much higher than $H_c/4\pi$, indicating the presence of fields much greater than the critical field at the edge of the plates. This effect is qualitatively similar to that predicted by Landau's theory of the intermediate state, but quantitative agreement is not obtained. Resistance measurements on thin strips of tin in transverse fields showed that resistance only reappears for fields considerably greater than those required to start the destruction of superconductivity.

§ 1. INTRODUCTION

THE experiments of Désirant and Shoenberg (1948) on the intermediate state of thin superconducting tin and mercury cylinders in transverse magnetic fields indicate qualitative, and to some extent, quantitative agreement with the model of the intermediate state first suggested by Landau (1943), and worked out in more detail by Andrew (1948). Certain features of the theory suggested, however, that it would be desirable to extend the experiments to superconducting plates in transverse fields in order to test the theory further.

---

* Now at Department of Natural Philosophy, University of St. Andrews, Scotland.

For an ellipsoid whose dimensions are large enough to allow neglect of all surface energy effects, simple argument shows that the magnetization curve consists of two straight lines. For $0 \leqslant h \leqslant H_c(1-n)$, where h is the applied magnetic field, H_c the critical field and $4\pi n$ the demagnetizing coefficient, the ellipsoid is in the superconducting state, and the intensity of magnetization I is given by

$$-4\pi I = h/(1-n). \qquad \ldots\ldots(1)$$

For $H_c(1-n) \leqslant h \leqslant H_c$ the ellipsoid is in the intermediate state, and I is given by

$$-4\pi I = (H_c - h)/n. \qquad \ldots\ldots(2)$$

For $h \geqslant H_c$ the ellipsoid is in the normal state, and $I=0$. This magnetization curve will be described as the 'bulk curve'. For the very oblate ellipsoids to which the flat plates used in the experiments approximate, the value of n is nearly unity and the initial slope of the 'bulk curve' is very great, corresponding to the large value of $1/(1-n)$.

The magnetization curve for an ellipsoid for which surface effects are not negligible, differs from the bulk curve in the manner indicated in Figure 7, where the bulk curve is shown by a broken line. The salient features predicted by the theory, which will be discussed in more detail in § 3, are: (i) the considerable delay in formation of the intermediate state, giving rise to a pronounced peak; (ii) a steeper slope for the intermediate state portion of the curve than that for the bulk curve; (iii) the attainment of the normal state when the applied field is appreciably less than the critical field.

The magnetization curves of thin tin plates of various thicknesses have been determined at various temperatures, and since it was possible to use specimens in which the range of thicknesses extended to much smaller values than was the case with the cylinders used in previous experiments, the departure of the curves from the 'bulk' shape was expected to be considerably greater. This was in fact found and, as with cylinders, qualitative agreement with the theory in certain respects was obtained; in other respects, however, more serious disagreement was found.

§ 2. EXPERIMENTAL DETAILS

All the plates were prepared by rolling spectroscopically pure tin (Johnson and Matthey 2356) to the required thickness. Discs were then cut out, usually with a clean cork borer. One specimen, Sp. 12, was of oblong shape, and this was a small portion of a specimen E3 used in the resistance measurements described later, for which the ratio of the resistance just above the transition temperature (3·8° K.) to that at 18° C. was found to be $3\cdot0 \times 10^{-4}$, indicating a high degree of purity. The discs were about 8 mm. in diameter and their thickness varied from $2\,\mu$ to $400\,\mu$.

In order to prepare the thinnest specimens it was found convenient to allow the strip of tin which was being rolled to stick lightly to the rollers as it passed through, as in this way the smoothest surface could be obtained; most of the tiny wrinkles which appeared could be removed, after the foil had been rolled to the required thickness, by widening the gap between the rollers very slightly and passing the foil through once more.

In all cases the mean thickness of the specimen was calculated from measurements of weight and surface area.

The method of measuring the magnetic moments of the specimens differed in only one way from that used by Désirant and Shoenberg (1948). In the present experiments the initial slope of the magnetization curve was generally so great that the current required for the compensating coil was greater than the solenoid current itself, so that it could not, as in the previous experiments, be taken as a fraction of the solenoid current, but was supplied instead from a separate circuit and was measured directly on a milliammeter. The overall sensitivity of the arrangement was of the order of 3×10^5 mm. scale deflection per E.M.U. of magnetic moment. For the thickest specimens the photoelectric amplifier and second galvanometer were dispensed with, and the magnetic moment was measured directly as a scale deflection of the first galvanometer, using the compensating coil merely for calibration.

All temperatures quoted are deduced from the vapour pressure of the helium bath by means of the 1932 Leiden scale.

The mounting of the foils used for the resistance measurements is described elsewhere (Andrew 1949).

§ 3. MAGNETIZATION CURVES

3.1. *Experimental Results*

Magnetization curves were measured at temperatures of 3·49° K. and 2·99° K. for all specimens, and at 2·50° K. for some specimens. Typical results are shown in Figures 1–6, in which the ordinates are 4π times the magnetization in gauss and the abscissae the applied field in gauss; the full curves are calculated from the theory given below, using the values of the parameter Δ' indicated on p. 22. It will be seen that all the magnetization curves show a considerable peak for low values of the applied field. Certain quantitative features of the curves are exhibited in Table 1 for comparison with theory.

The critical fields of specimens Sp. 5, 12, 15, and 16 have been measured at a number of temperatures in magnetic fields parallel to their surfaces, and from these measurements it is found that the deviations of the transition temperatures of these specimens from 3·72° K. are not greater than 0·01° K. in any case. The critical fields of the other specimens have not been measured, since they are not of decisive importance in comparison of the results with the theory.

3.2. *Theory*

A theory of the intermediate state has been worked out by Landau (1943) and Andrew (1948), and therefore only the results needed here will be quoted. By a calculation similar to that for transverse cylinders, it is found that the point of entry into the intermediate state from the superconducting state should take place at an applied field ρH_c, where ρ is greater than the value $(1-n)$ for the bulk curve. The values of ρ for the laminar and thread models are given by the following relations:

$$\text{Laminar model} \quad \rho_L = \nu + \tfrac{5}{4}(4N\nu)^{3/5}, \qquad \ldots\ldots(3)$$

$$\text{Thread model} \quad \rho_T = \nu + 2(M\nu)^{3/4}, \qquad \ldots\ldots(4)$$

where ν is written for $(1-n)$, and

$$N = \left[\frac{1}{2(\sqrt{2}-1)}\frac{\Delta'}{L}\right]^{2/3}; \qquad M = \left[\frac{2\sqrt{\pi}}{(\sqrt{2}-1)}\frac{\Delta'}{L}\right]^{2/3}.$$

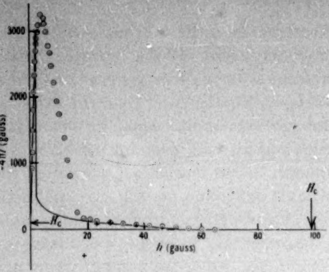

Figure 1. Sp. 11, 2·988° K., $\Delta'/L = 1{\cdot}72 \times 10^{-1}$.

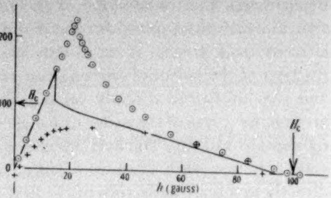

Figure 2. Sp. 16, 2·984° K., $\Delta'/L = 1{\cdot}0 \times 10^{-3}$.

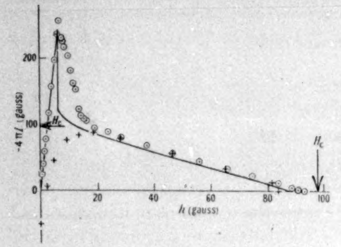

Figure 3. Sp. 15, 2·996° K., $\Delta'/L = 4{\cdot}2 \times 10^{-3}$.

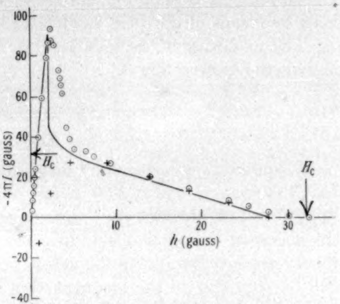

Figure 4. Sp. 15, 3·492° K., $\Delta'/L = 7{\cdot}1 \times 10^{-3}$.

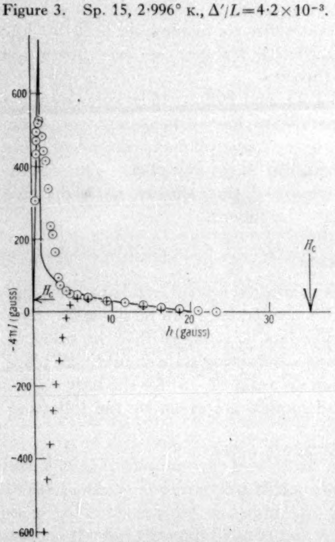

Figure 5. Sp. 5, 3·490° K., $\Delta'/L = 1{\cdot}55 \times 10^{-1}$.

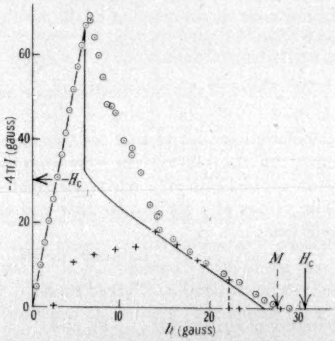

Figure 6. Sp. 12, 3·514° K., $\Delta'/L = 8{\cdot}0 \times 10^{-3}$.

Figures 1–6. Transverse magnetization curves. In each case the full curve is theoretical, assuming values of Δ'/L indicated. ---- discontinuous rise of $-4\pi I$; ⊙ increasing fields; + decreasing fields.

Table 1

Specimen	Description	Diameter d (cm.)	Thickness L (cm. $\times 10^4$)	$1/(1-n)$ (theoretical)	T (° K.)	Initial gradient $-4\pi I/h$	$\frac{-4\pi I(1-n)}{h}$	H_c (gauss)	$\frac{-4\pi I_{\max}}{H_c}$	$\frac{\sigma}{1-n}$
Sp. 11	Disc	0·766	2·1	2280	2·504	1560	0·683		34·3	
					2·988	1600	0·702		32·8	2·88
					3·491	1585	0·695		27·1	3·64
Sp. 4	Disc	0·793	3·3	1520	2·981	1000	0·658		20·4	2·49
					3·486	~1300	~0·85		16·3	3·02
Sp. 5	Disc	0·734	4·1	1150	2·988	769	0·669	105·1	16·9	2·37
					3·490	748	0·651	35·3	15·6	2·66
Sp. 7	Disc	0·647	5·7	720	2·993	484	0·672		8·9	2·02
					3·480	484	0·672		8·0	2·51
Sp. 6	Disc	0·784	6·3	794	2·990	532	0·670		7·9	2·06
					3·488	527	0·663		7·2	2·30
Sp. 3	Disc	0·781	12·6	395	2·987	266	0·673		5·4	1·56
					3·487	~280	~0·71		5·0	1·96
Sp. 8	Disc	0·651	28·0	148	2·509	100·0	0·675		4·15	
					2·985	100·3	0·696		4·31	1·36
					3·488	100·3	0·696		4·58	1·51
Sp. 2	Disc cut with scissors	0·810	71	73	2·982	51·0	0·698		3·15	1·26
Sp. 1	Disc	0·796	77	66	2·995	46·7	0·707		3·48	1·23
					3·492	46·7	0·707		3·19	1·26
Sp. 12	Oblong shape	0·099 × 0·727	79	12·5	2·561	11·3	0·904	155·7	2·31	
					3·201	11·3	0·904	73·7	2·39	1·37
					3·514	11·1	0·888	30·6	2·28	1·22
Sp. 15	Disc polished electrolytically	0·766	89	54·6	2·996	38·0	0·696	98·0	2·62	1·20
					3·492	38·2	0·700	32·2	2·80	1·23
Sp. 9	Disc	0·800	220	23·4	2·506	16·6	0·709		2·34	
					2·987	16·8	0·718		2·43	1·20
					3·490	16·6	0·709		2·41	1·15
Sp. 16	Disc polished electrolytically	0·781	382	13·4	2·984	10·4	0·776	100·0	2·28	1·10
					3·495	10·4	0·776	31·8	2·19	1·02
Sp. 17	Disc	0·793	449	12·1	2·995	9·2	0·760		1·98	1·09
					3·508	9·4	0·777		2·01	0·99

Thus

$$\rho_{\mathrm{L}}/\nu = 1 + 3{\cdot}1\left(\frac{\Delta'}{L\nu}\right)^{2/5} \qquad \ldots\ldots(5)$$

and

$$\rho_{\mathrm{T}}/\nu = 1 + 5{\cdot}9\left(\frac{\Delta'}{L\sqrt{\nu}}\right)^{1/2}. \qquad \ldots\ldots(6)$$

The complete magnetic behaviour of an ellipsoid can be derived from the three equations

$$H = h - 4\pi nI, \qquad B = H + 4\pi I, \qquad H = \partial\Phi/\partial B. \qquad \ldots\ldots(7)$$

For an ellipsoid in the intermediate state, Φ, the free energy multiplied by 4π may be expressed as $H_{\mathrm{c}}B + \phi$, where ϕ is a term which takes interphase surface effects into account. For the laminar model described by Landau,

$$\phi = \frac{3B^{1/3}H_{\mathrm{c}}(H_{\mathrm{c}} - B)^{2/3}}{2^{2/3}(\sqrt{2} - 1)^{2/3}}\left(\frac{\Delta'}{L}\right)^{2/3}, \qquad \ldots\ldots(8)$$

where L is the thickness of the material in the direction of the applied field, and Δ' is given by

$$\Delta' = \frac{8\pi\alpha}{H_{\mathrm{c}}^{2}} - \lambda, \qquad \ldots\ldots(9)$$

where λ is the penetration depth of the field into a superconducting domain, and α is the surface energy per unit area between the normal and superconducting phases. A similar expression for ϕ is derived from the thread model described by Andrew.

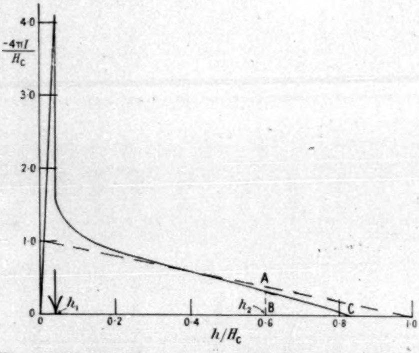

Figure 7. Theoretical magnetization curve. Full curve for $\Delta'/L = 10^{-2}$, $\nu = 10^{-2}$. Broken curve for $\Delta'/L = 0$ (' bulk curve ').

In applying the theory to long cylindrical specimens perpendicular to the field, n is put equal to $\frac{1}{2}$, but it is difficult to decide what value to take for L in the formula for ϕ given above, since it varies from $2r$ in the centre of the specimen to zero at its edges, where r is the radius of the cylinder. The theory can, however, be applied directly to the similar problem of thin plates perpendicular to the field, as here no doubt arises as to the value of L to be inserted. Another difficulty arises, however, because a uniform flat plate with sharp edges does not correspond exactly to the perfect ellipsoid required to give uniform magnetization, so that its behaviour cannot be described completely in terms of a simple demagnetizing coefficient and, as will be mentioned later, the experimental values of the initial gradients of the magnetization curves do in fact differ from those calculated on the assumption that the uniform plate may be treated as its inscribed ellipsoid.

In the limit $\Delta'/L\rightarrow 0$, equations (7) and (8) lead to the bulk curve already mentioned in § 1. For $\Delta'/L=10^{-2}$ and $\nu=10^{-2}$, these equations lead to the curve shown in Figure 7; two discontinuous jumps are predicted at fields h_1 and h_2. The first of these occurs when the free energy of the superconducting state becomes just equal to that of the intermediate state, so that $h_1=\rho H_c$, where ρ is given by equation (8). The second jump AB corresponds to the fact that at a field h_2 the normal state becomes energetically favourable but its attainment would require the sudden expulsion of the remaining superconducting domains in the specimen. Experimentally this is found not to occur, and the curves agree much better with the assumption that the intermediate state persists in a metastable condition giving rise to the continuation of the magnetization curve along AC.

3.3. *Comparison of Theory and Experiment*

From (1) the initial gradient of the magnetization curve, $-4\pi I/h$, should have the value $1/(1-n)$. The demagnetizing coefficient of an oblate ellipsoid of revolution of diameter d and thickness L is given by

$$1-n=\frac{\pi}{2}\frac{L}{d}-2\left(\frac{L}{d}\right)^2+O\left(\frac{L}{d}\right)^3. \qquad\ldots\ldots(10)$$

This relation may be used to calculate the expected value of the initial gradient if it is assumed that the discs behave like their inscribed ellipsoids. The experimentally determined slope was, however, always about 2/3 of the calculated slope for the discs. The reason for this discrepancy is probably as follows. Consider a superconducting specimen in the form of an oblate ellipsoid of revolution thin enough for its demagnetizing coefficient in a field parallel to its axis to be given by the relation

$$1-n=\frac{\pi}{2}\frac{L}{d},$$

where L is the length of its minor axis and d that of the major axes. Then in an applied magnetic field h its magnetic moment M will be given by

$$-4\pi M=\frac{4}{3}\pi\frac{L}{2}\left(\frac{d}{2}\right)^2\frac{2d}{\pi}\frac{h}{L}=\frac{1}{3}d^3h. \qquad\ldots\ldots(11)$$

Thus the magnetic moment of such a specimen in a given field is independent of its thickness; physically this means that the distortion of the magnetic field due to the presence of such a superconducting specimen depends only on its dimensions in the plane perpendicular to the applied magnetic field and not on its dimensions in the direction of that field. It seems reasonable to suppose that for a thin superconducting plate this result holds even if the cross section of the specimen is not elliptical, and in particular that it holds for a thin cylindrical disc; if this is so, then for such a disc the magnetic moment M in a given field will be the same as that of its inscribed ellipsoid.

Since the volume of the disc is $\frac{1}{4}\pi d^2L$ the slope of the magnetization curve will be

$$\frac{-4\pi M}{\frac{1}{4}\pi d^2Lh}=\frac{4}{3\pi}\frac{d}{L}=\frac{2}{3}\frac{1}{1-n}, \qquad \ldots\ldots(12)$$

which is just the value found experimentally. In analysing the results it is this experimental value of the demagnetizing coefficient which has been used throughout.

It will be seen that except for the thickest specimens, after an initial steep rise at constant gradient the peak rounds off somewhat, so that the summit is not attained until a field has been reached considerably higher than would have been required had the gradient remained constant. This effect is on the whole more pronounced in the thinnest specimens, and is presumably due to field penetration at the sharp edges. In comparing the results with the theory, the ratios $-4\pi I_{\max}/H_c$, where $I_{\max}$ is the maximum magnetization, have been compared with the theoretical values of ρ/ν, which is of course equal to $-4\pi I_{\max}/H_c$ for the theoretical curve.

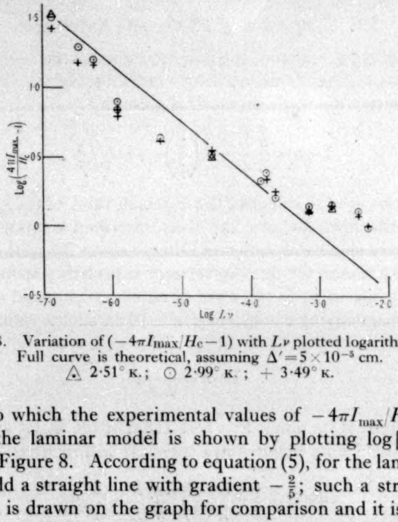

Figure 8. Variation of $(-4\pi I_{\max}/H_c-1)$ with $L\nu$ plotted logarithmically. Full curve is theoretical, assuming $\Delta'=5\times10^{-5}$ cm. △ 2·51° K.; ⊙ 2·99° K.; + 3·49° K.

The extent to which the experimental values of $-4\pi I_{\max}/H_c$ agree with the predictions for the laminar model is shown by plotting $\log[-4\pi I_{\max}/H_c-1]$ against $\log L\nu$ in Figure 8. According to equation (5), for the laminar theory such a plot should yield a straight line with gradient $-\frac{2}{5}$; such a straight line, taking $\Delta'=5\times10^{-5}$ cm., is drawn on the graph for comparison and it is evident that the functional relation is markedly different from that predicted, and the disagreement with theory becomes particularly pronounced for very large values of L, that is to say for thick discs, if we keep the diameter constant. It is this discrepancy which is disturbing from the point of view of the theory, since it is just these specimens which yield the most reliable and the most reproducible experimental results; as can be seen from the magnetization curve of Sp. 16 at 2·984° K., there is no appreciable penetration of the field right up to the top of the sharp peak. The thread model gives no better agreement.

To decide whether the exact shape of the edges of the specimen was critical, two discs, Sp. 15 and Sp. 16, were polished electrolytically; in this way specimens with considerably rounded edges and smooth surfaces were obtained, though slight electrolytic etching as well as electrolytic polishing took place. The magnetization curves obtained, however, indicated no significant change either in the initial gradient of the curve or in the value of $-4\pi I_{\max}/H_c$, as compared with unpolished specimens of the same thickness and diameter.

Another feature of the experimental magnetization curves which can be related quantitatively to the theory concerns the slope of the falling portion of the magnetization curve. From the equations (7) the gradient dI/dh of the magnetization curve is given by

$$4\pi(1-n)\frac{dI}{dh}+1=\frac{dB}{dh}=\left[n+(1-n)\frac{d^2\phi}{dB^2}\right]^{-1}. \qquad \ldots\ldots(13)$$

For the laminar model

$$\frac{d^2\phi}{dB^2}=-\frac{2^{1/3}}{3(\sqrt{2}-1)^{2/3}\gamma^{5/3}(1-\gamma)^{4/3}}\left(\frac{\Delta'}{L}\right)^{2/3}, \qquad \ldots\ldots(14)$$

and for the thread model

$$\frac{d^2\phi}{dB^2}=-\frac{2^{2/3}\pi^{1/3}\left(1-\frac{3\beta}{4}\right)}{3(\sqrt{2}-1)^{2/3}\gamma^{4/3}(1-\beta)^{4/3}}\left(\frac{\Delta'}{L}\right)^{2/3}, \qquad \ldots\ldots(15)$$

where $\gamma=B/H_c$ and $\beta=(2B/\pi H_c)^{\frac{1}{2}}$. For $B=\frac{1}{2}H_c$ both these expressions become very nearly $d^2\phi/dB^2=-6{\cdot}1(\Delta'/L)^{2/3}$.

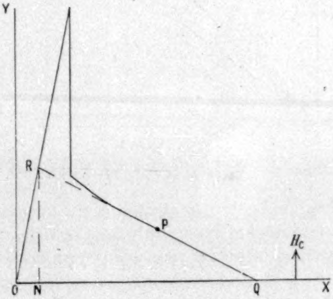

Figure 9. To illustrate how $\sigma/(1-n)$ is obtained.

If we draw the tangent to the magnetization curve at the point P (Figure 9) given by $B=\frac{1}{2}H_c$ and produce it to cut the initial straight line portion of the curve at a field $h=h_R$ and the axis of field at h_Q, and define σ as the ratio of h_R/h_Q, then

$$\sigma=(1-n)\left[1-\frac{d^2\phi}{dB^2}\right]=(1-n)\left[1+6{\cdot}1\left(\frac{\Delta'}{L}\right)^{2/3}\right]. \qquad \ldots(16)$$

Although σ and $(1-n)$ are both small, their ratio $\sigma/(1-n)$ can be calculated by a simple geometrical argument (see Figure 9). We have $\sigma=\mathrm{ON}/\mathrm{OQ}$ and $1-n=\mathrm{ON}/\mathrm{RN}$; hence

$$\sigma/(1-n)=\mathrm{RN}/\mathrm{OQ}. \qquad \ldots\ldots(17)$$

The relative scale along the axes OX and OY for an experimental magnetization curve is independent of the exact critical field of the specimen and depends only on the mass of the specimen, the solenoid constant, and the absolute calibration of magnetic moment, all of which are known to within 1%. The values of $\sigma/(1-n)-1$ calculated from the experimental curves have been plotted against $L^{-2/3}$ for temperatures of 3·49 and 2·99° K. in Figure 10. The points lie fairly accurately on straight lines passing through the origin, and from the gradients of these lines the values of Δ' obtained are $6{\cdot}3\times10^{-5}$ cm. and $3{\cdot}7\times10^{-5}$ cm. at 3·49° K. and 2·99° K. respectively. These values are in good agreement with those obtained by the same procedure as applied to transverse cylinders (Désirant and Shoenberg 1948), namely $6{\cdot}2\times10^{-5}$ cm. and $3{\cdot}6\times10^{-5}$ cm. respectively. The theoretical magnetization curves obtained using these values of Δ' are shown in Figures 1–6, and over the intermediate state range where the magnetization has fallen from its high value at the initial peak the agreement is seen to be fairly good.

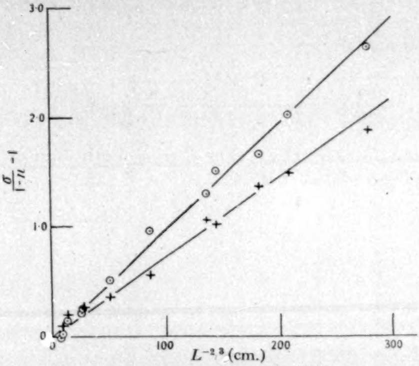

Figure 10. Variation of $\sigma/(1-n)-1$ with $L^{-2/3}$.

We have so far described only that portion of the magnetization curve traced out as the applied field is raised monotonically from zero to a value greater than the critical field. On lowering the field to zero again considerable hysteresis is found; for most specimens the field can be reduced to a value lower than that at which the rising field curve cuts the axis before magnetization reappears, and when it does so it takes place in a jump indicated by a sudden kick of the galvanometer. This 'super-cooling' effect is similar to that observed in the earlier experiments on transverse cylinders. On further reduction of the magnetic field the magnetization curve retraces quite accurately the rising field curve until the base of the initial peak is reached, when it begins to fall fairly sharply and drops to a negative value when the field becomes zero. This 'frozen-in moment' is largest for the thinnest specimens, for some of which it reaches a value whose magnitude is actually greater than that obtaining at the peak of the rising field curve. It is presumably associated with the formation of a stable superconducting ring at the edge of the disc in which a permanent current can flow, and it is noticeable that this hysteresis effect is in fact very similar to that observed with a superconducting annulus. The polished specimen Sp. 16 had a smaller frozen-in moment than the unpolished specimen Sp. 17 of about the same thickness, and this suggests that the formation of a superconducting ring is favoured by the presence of sharp corners, in agreement with the results obtained by Shoenberg (1937) for cylinders whose length was about the same as their diameter. It is also in agreement with the much higher frozen-in moments obtained with the thinnest disc specimens.

If the formation of the intermediate state took place reversibly over the whole range of applied fields, it can be shown quite generally that the area under the (I, h) curve should be exactly $H_c^2/8\pi$ regardless of the particular assumptions which are made concerning the structure of the intermediate state. The theoretical curves have in fact just this area, but it is immediately evident that the experimental results yield a magnetization curve with a far greater area, the discrepancy increasing as we go to thinner specimens. Thus for Sp. 11 at 2·98° K. the area of the increasing field curve is $7 \cdot 0 \times H_c^2/8\pi$. Now irreversible changes will give rise to just such an increase in the area under the magnetization curve as is observed, and since most of the difference is associated with the large initial peak of the curve, and since the drop from this peak is much more gradual than the theory predicts, we must assume that over this range of fields the transitions taking place are not reversible. No theory based on a structure of the intermediate state in which the changes taking place are reversible will therefore be adequate to describe the observed behaviour in this part of the magnetization curve, which must instead be ascribed to the formation of some kind of metastable structure of normal and superconducting domains which breaks up into a stable 'intermediate state' at higher fields. The fact that the decreasing field curve follows the rising field curve accurately for such fields proves that here we are dealing with reversible changes and a stable structure.

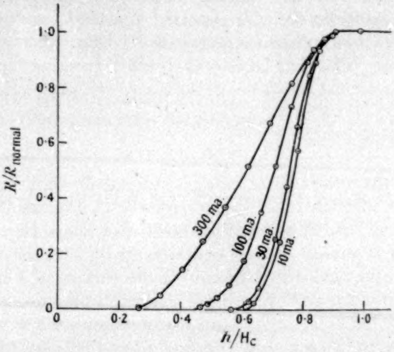

Figure 11. Resistance-field curves for E3 at 3·510° K., using various measuring currents. $L = 7 \cdot 8 \times 10^{-3}$ cm.

§ 4. RESISTANCE MEASUREMENTS

Resistance measurements were made on a number of transverse tin foils in the form of narrow strips about 3 cm. long and 1 mm. wide, varying in thickness from $3 \cdot 4\,\mu$ to $78\,\mu$. Resistance-field curves for the $78\,\mu$ foil, of which a portion was used as Sp. 12 in a magnetization experiment (Figure 6), are shown in Figure 11 for the same temperature and are seen to depend strongly on the measuring current. For a weak measuring current the foil had a superconducting path for applied fields up to $0{\cdot}63H_c$, a value considerably greater than that at which superconductivity begins to be destroyed in Sp. 12 as shown by the peak of the magnetization curve; a similar high value of the field required to cause the reappearance of resistance was found for all the foils. Stronger measuring currents displace the point at which resistance first appears to lower fields.

Since the magnetization measurements were made in the absence of a measuring current they should be compared with the resistance measurements using the smallest current, for which the corresponding field at the edges of the foil was only about $0{\cdot}01H_c$. The absence of resistance in a field greater than that required to start the destruction of superconductivity may be due to the normal domains growing from the edges and running in from both sides of the strip; in this way a central superconducting path can exist along the whole length of the foil until a normal domain actually cuts across its entire cross section. Thus no evidence can be obtained about the initial destruction of superconductivity in plates from such resistance-field measurements. On the other hand, the restoration of complete normal resistance seems to occur as expected at a field very nearly equal to that required to destroy the last traces of superconductivity as indicated by the magnetization reaching zero. Thus in Figure 6 the point M marks the value of the field required to restore normal resistance in the foil of the same thickness from which Sp. 12 was made.

§ 5. DISCUSSION

The theory of the intermediate state considered above is based fundamentally on the hypothesis that the macroscopic laminae or threads of normal material undergo progressive branching until at the surface there results an exceedingly finely divided mixed phase. Recent experiments by Meshkovsky and Shalnikov (1947 b), in which the field distribution over the surface of a sphere in the intermediate state was investigated by means of a very fine bismuth probe, show instead irregularities in the field on just the same macroscopic scale as were found in their previous investigation (Meshkovsky and Shalnikov 1947 a) of the field inside a gap cut across a diametrical plane of the sphere. This result appears to disprove the branching hypothesis for such a specimen, and it is certainly not more likely to be true for the thinnest specimens used in the present experiments, in view of the small distance available for such branching to take place. If this is so, the theory of Landau and Andrew must at least require considerable modification. Where agreement between this theory and the results of the present experiments is found, and particularly in the slopes of the magnetization curves in the nearly linear region shortly before the magnetization has fallen to zero, it is possible that the rôle played in the theory by the branching of the laminae is not decisive. In this case the close agreement between the values of Δ' derived from the σ values obtained in the present experiments and from those obtained by Désirant and Shoenberg in the experiments on cylinders may indicate that in the correct theory of the intermediate state the surface energy between the normal and superconducting phases will play a part similar to that which it plays in the Landau theory. The possibility that the agreement mentioned above is fortuitous must not, however, be neglected.

As already pointed out, the large area of the magnetization curves of the thin tin plates indicates irreversibility, especially in the region where the magnetization begins to fall rapidly. Although the area discrepancy is much smaller in the experiments of Désirant and Shoenberg on transverse cylinders, it is probable that the 'horns' in the magnetization curves found by them are manifestations on a smaller scale of the same process which gives rise to the large peaks in the magnetization curves obtained in the present experiments. Thus little reliance can be placed on the values of Δ' derived from the ρ values for thin cylinders in terms of the equilibrium theory, and perhaps the higher Δ' values suggested by the present work are nearer the truth.

ACKNOWLEDGMENTS

The authors wish to thank Dr. D. Shoenberg, who suggested this problem, for much helpful advice; their thanks are also due to Mr. A. B. Pippard for many valuable discussions. The work was carried out during the tenure by one of them (J.M.L.) of a grant from the Department of Scientific and Industrial Research.

REFERENCES

ANDREW, E. R., 1948, *Proc. Roy. Soc.* A. **194,** 98 ; 1949, *Proc. Phys. Soc.* A, **62,** 88.

DÉSIRANT, M., and SHOENBERG, D., 1948, *Proc. Roy. Soc.* A, **194,** 63.

LANDAU, L., 1943, *J. Phys. U.S.S.R.*, **7,** 99.

MESHKOVSKY, A., and SHALNIKOV, A., 1947 a, *J. Phys. U.S.S.R.*, **11,** 1 ; 1947 b, *J. Exp. Theor. Phys.*, **17,** 851 (in Russian).

SHOENBERG, D., 1937, *Proc. Camb. Phil. Soc.*, **33,** 260.

A Modified Perturbation Procedure for a Problem in Paramagnetism

BY M. H. L. PRYCE
Clarendon Laboratory, Oxford

MS. received 2nd August 1949

ABSTRACT. A modified perturbation technique is described for problems in which second-order effects are comparable in magnitude with first-order effects, where orthodox methods break down. It is applied to the energy levels of paramagnetic ions in a crystal, giving an effective Hamiltonian in which the Stark splitting, the anomalous g-value and the temperature-independent paramagnetism are clearly exhibited.

§ 1. INTRODUCTION

In some applications of perturbation theory it happens that first and second order effects are comparable in magnitude. The straightforward perturbation development then leads to difficulties if the unperturbed state is degenerate, for the first step is to set up the first-order secular equation, from which are derived the zero-order states: while actually a second-order secular equation is necessary to get them correctly in this case.

Such a state of affairs arises in the theory of paramagnetic crystals. Here one has to study the energy levels of paramagnetic ions under the influence of the crystalline electric field, the spin–orbit coupling and the external magnetic field. The problem is usefully attacked in stages, first studying the energy levels under the influence of electrostatic fields only, and ignoring spin forces; and then, with this as the unperturbed system, treating the spin–orbit coupling and external field as perturbations. The contribution of the spin–orbit coupling vanishes in first order, if the unperturbed orbital level is non-degenerate, leaving only the contribution from the external field. This may, in practical cases, according to the strength of the field, be larger than, comparable with or smaller than the second-order contribution from the spin–orbit coupling. Higher order terms are smaller.

The purpose of this note is to show how to set up the required second-order secular equation in a form applicable to the paramagnetic problem. Here the unperturbed system is characterized by certain configurational variables and has energy levels which may conveniently be called orbital levels. Owing to the spin each orbital level is $(2S+1)$-fold degenerate. It will be assumed that the lowest orbital level, in which one is primarily interested, is non-degenerate apart from the spin degeneracy. The perturbation Hamiltonian is

$$\mathscr{H}^1 = \lambda \mathbf{L} \,.\, \mathbf{S} + \beta(\mathbf{L} + 2\mathbf{S}) \,.\, \mathbf{H}. \qquad \ldots\ldots(1)$$

It will be shown that the energy levels, correct to the second order, are the eigenvalues of an observable involving only the spin variables, namely

$$E_0 + 2\beta(\delta_{ij} - \lambda\Lambda_{ij})S_iH_j - \lambda^2\Lambda_{ij}S_iS_j - \beta^2\Lambda_{ij}H_iH_j. \qquad \ldots\ldots(2)$$

In these expressions β is the Bohr magneton, $\mathbf{H}$ the external magnetic field, λ the spin–orbit coupling constant and Λ_{ij} is a real, symmetrical, positive definite tensor defined in terms of the matrix elements of the orbital angular momentum $\mathbf{L}$ by

$$\Lambda_{ij} = \sum_{n \neq 0} \frac{\langle 0|L_i|n\rangle \langle n|L_j|0\rangle}{(E_n - E_0)}. \qquad \ldots\ldots(3)$$

The tensor indices i, j refer to Cartesian coordinates and the summation convention is assumed for them. The indices $0, \ldots. n, \ldots.$ refer to the orbital levels, 0 being the lowest; summation for these will be written explicitly.

One can readily interpret each term in (2). The first, E_0, is the unperturbed energy. The second

$$2\beta(\delta_{ij} - \lambda\Lambda_{ij})S_iH_j \qquad \ldots\ldots(4)$$

is the magnetic energy of a spin system with a (in general anisotropic) g-factor represented by the tensor

$$g_{ij} = 2(\delta_{ij} - \lambda\Lambda_{ij}), \qquad \ldots\ldots(5)$$

in the external field $\mathbf{H}$. The third,

$$-\lambda^2\Lambda_{ij}S_iS_j, \qquad \ldots\ldots(6)$$

is the second-order contribution of the spin–orbit coupling. If Λ_{ij} is isotropic (i.e. a multiple of δ_{ij}) it merely represents an equal downward shift of all the $2S+1$ levels; if not, there is in addition a splitting of the levels, even in the absence of an external magnetic field. The last term

$$-\beta^2\Lambda_{ij}H_iH_j \qquad \ldots\ldots(7)$$

which is spin-independent and quadratic in $\mathbf{H}$, corresponds to a temperature-independent paramagnetic susceptibility.

§ 2. THE GENERAL CASE

The perturbation procedure will first be described in terms of a more general system. For purely descriptive purposes the terms 'orbital levels' and 'spin multiplicity' will be retained, though the argument could equally be applied to systems whose unperturbed levels were characterized by other than orbital variables and in which the degeneracy arose in other ways. The unperturbed Hamiltonian will be denoted by $\mathscr{H}^0$, with eigenvalues $E_0, \ldots, E_n, \ldots$ Eigenstates of $\mathscr{H}^0$, will be denoted by $|0\rangle, \ldots, |n\rangle, \ldots$ Each set $\{|n\rangle\}$ is a linear manifold of dimensionality equal to the spin multiplicity. The total Hamiltonian will be written

$$\mathscr{H} = \mathscr{H}^0 + \mathscr{H}^1. \qquad \ldots\ldots(8)$$

The eigenvalue equation is

$$\mathscr{H}\,|\,\rangle = E\,|\,\rangle. \qquad \ldots\ldots(9)$$

One now expands $|\,\rangle$ in terms of eigenstates of $\mathscr{H}^0$:

$$|\,\rangle = |0\rangle + \sum_{n \neq 0} |n\rangle. \qquad \ldots\ldots(10)$$

For a solution of (9) whose eigenvalue is approximately E_0, $|0\rangle$ is of zero order, while the $|n\rangle$ are of first order. Part of the problem is to determine the appropriate $|0\rangle$ (secular equation). The eigenvalue equation (9) can be rewritten

$$(E^0 - E + \mathscr{H}^1)|0\rangle + \sum_{n \neq 0} (E_n - E + \mathscr{H}^1)|n\rangle = 0. \qquad \ldots\ldots(11)$$

The left hand side of (11) will now be decomposed into eigenstates of $\mathscr{H}^0$. This is conveniently done by means of the projection operators P_n of the linear manifold $\{|n\rangle\}$. Operating on (11) with P_0, P_n, one has

$$(E_0 - E + P_0\mathscr{H}^1)|0\rangle + \sum_{n \neq 0} P_0\mathscr{H}^1|n\rangle = 0, \qquad \ldots\ldots(12)$$

$$(E_n - E)|n\rangle + P_n\mathscr{H}^1|0\rangle + \sum_{m \neq 0} P_n\mathscr{H}^1|m\rangle = 0. \qquad \ldots\ldots(13)$$

Equation (13) shows that $|n\rangle$ is indeed of first order in $\mathscr{H}^1$, and allows one to solve for it in *first* order as follows:

$$|n\rangle = -\frac{P_n\mathscr{H}^1}{(E_n - E)}|0\rangle. \qquad \ldots\ldots(14)$$

Substituting (14) into (12) one has, to *second* order,

$$\left(E_0 + P_0\mathscr{H}^1 - \sum_{n \neq 0} \frac{P_0\mathscr{H}^1 P_n \mathscr{H}^1}{(E_n - E_0)} - E\right)|0\rangle = 0, \qquad \ldots\ldots(15)$$

or, in a more symmetrical form,

$$\left(E_0 + P_0\mathscr{H}^1 P_0 - \sum_{n \neq 0} \frac{P_0\mathscr{H}^1 P_n \mathscr{H}^1 P_0}{(E_n - E_0)} - E\right)|0\rangle = 0. \qquad \ldots\ldots(16)$$

E_0 has been written for E in the denominators of (15) and (16) since the difference involved is of third order. (16) is the required second order secular equation determining $|0\rangle$. It shows that to this order the eigenvalues E are the eigenvalues of the operator

$$\widetilde{\mathscr{H}} = E_0 + P_0\mathscr{H}^1 P_0 - \sum_{n \neq 0} \frac{P_0\mathscr{H}^1 P_n \mathscr{H}^1 P_0}{(E_n - E)}, \qquad \ldots\ldots(17)$$

which is Hermitian and operates entirely within the manifold $\{|0\rangle\}$.

One may also determine the eigenstate to the second order. A straightforward substitution of (14) into (13) gives $|n\rangle$ correct to *second* order, from which it is possible to give the following expression for $|\,\rangle$, correct to *second* order,

$$|\,\rangle = T|0\rangle, \qquad \ldots\ldots(18)$$

where

$$T=\left(1-\sum_{n\neq 0}\frac{P_n\mathscr{H}^1}{(E_n-E_0)}+\sum_{m\neq 0}\sum_{n\neq 0}\frac{P_n\mathscr{H}^1P_m\mathscr{H}^1}{(E_n-E_0)(E_m-E_0)}-\sum_{n\neq 0}\frac{P_n\mathscr{H}^1P_0\mathscr{H}^1+\frac{1}{2}P_0\mathscr{H}^1P_n\mathscr{H}^1}{(E_n-E_0)^2}\right)P_0. \qquad \ldots\ldots(19)$$

To derive this, $1/(E_n-E)$ has been expanded as $1/(E_n-E_0)+(E-E_0)/(E_n-E_0)^2$ and (15) has been used to eliminate E. The last term in T, with the factor $\frac{1}{2}$, has been included to ensure the normalization

$$\langle|\rangle=\langle 0|0\rangle, \quad \text{i.e.} \quad T^*T=P_0. \qquad \ldots\ldots(20)$$

The factor P_0 on the right of the definition of T is not essential, but as it restricts T to the manifold $\{|0\rangle\}$ it has some advantages.

As a corollary it may be seen that the expectation value of any observable ξ in the state $|\,\rangle$ can be written

$$\langle|\xi|\,\rangle=\langle 0|\tilde{\xi}|0\rangle, \qquad \ldots\ldots(21)$$

where

$$\tilde{\xi}=T^*\xi T. \qquad \ldots\ldots(22)$$

A similar result is also true for the matrix elements connecting any two states $|\,\rangle$ belonging to the unperturbed level E_0. In calculations dealing with the system in its lowest orbital level one may therefore use $\tilde{\xi}$ and the states $|0\rangle$, instead of ξ and the states $|\,\rangle$; this frequently has practical advantages. One example is the operator $\widetilde{\mathscr{H}}$, which is related to $\mathscr{H}$ in this way. Another, which will be discussed below, is the magnetic moment, $-\beta(\mathbf{L}+2\mathbf{S})$, in the paramagnetic problem, which can be expressed in terms of spin variables alone, the orbital moment being linked to the spin by the spin–orbit coupling.

§ 3. THE PARAMAGNETIC PROBLEM

These general results may now be applied to the paramagnetic problem, for which the perturbation Hamiltonian has the form (1). The Schroedinger equation for the unperturbed problem does not contain spin dependent terms, but only the kinetic and electrostatic potential energies, both of which are real operators. The wave functions for the states $|n\rangle$ may therefore be chosen to be real. From this it follows that the matrix elements of $\mathbf{L}$, which is represented in the Schroedinger representation by the operator $-i\Sigma\mathbf{r}\wedge\partial/\partial\mathbf{r}$, are purely imaginary, and, since $\mathbf{L}$ is Hermitian, diagonal elements vanish and off-diagonal elements are antisymmetrical ($\langle m|\mathbf{L}|n\rangle=-\langle n|\mathbf{L}|m\rangle$). One therefore has

$$\begin{aligned}P_0\mathscr{H}^1P_0&=P_0[\lambda\mathbf{L}.\mathbf{S}+\beta(\mathbf{L}+2\mathbf{S}).\mathbf{H}]P_0\\&=2\beta\mathbf{S}.\mathbf{H}\,P_0,\end{aligned} \qquad \ldots\ldots(23)$$

$$P_0\mathscr{H}^1P_n\mathscr{H}^1P_0=\langle 0|L_i|n\rangle\langle n|L_j|0\rangle(\lambda S_j+\beta H_j)(\lambda S_i+\beta H_i)P_0. \quad (n\neq 0). \qquad \ldots\ldots(24)$$

Hence

$$\widetilde{\mathscr{H}} = E_0 + 2\beta \mathbf{S}\,.\,\mathbf{H} - \sum_{n\neq 0} \frac{\langle 0|L_i|n\rangle\langle n|L_j|0\rangle}{(E_n-E_0)}(\lambda S_j+\beta H_j)(\lambda S_i+\beta H_i). \qquad \ldots\ldots(25)$$

(The factor P_0 has been omitted since it is to be understood that $\widetilde{\mathscr{H}}$ operates within $\{|0\rangle\}$.) On simplification and the introduction of the tensor Λ_{ij} defined by (3) this reduces to (2). That Λ_{ij} is real and symmetrical follows from the fact that $\langle 0|L|n\rangle$ is imaginary and equal to $-\langle n|L|0\rangle$. That it is positive definite, provided E_0 is the lowest eigenvalue, is also easily proved.

One may also derive expressions for the effective magnetic moment. In this connection one seldom requires the second-order correction, which is small (provided λ is small compared with the $E_n - E_0$, which is the condition for the perturbation procedure to be a good approximation in this problem); it is therefore sufficient to quote the first-order results. They are

$$\widetilde{L}_i = -2\Lambda_{ij}(\lambda S_j + \beta H_j), \qquad \ldots\ldots(26)$$

$$\widetilde{S}_i = S_i, \qquad \ldots\ldots(27)$$

$$\widetilde{M}_i = -\beta(\widetilde{L}_i + 2\widetilde{S}_i) = -2\beta(\delta_{ij} - \lambda\Lambda_{ij})S_j + 2\beta^2\Lambda_{ij}H_j. \qquad \ldots\ldots(28)$$

They exhibit the temperature independent susceptibility and the contribution of the spin-linked orbital moment to the g-tensor.

The Paramagnetic Resonance from Nickel Fluosilicate

By R. P. PENROSE and K. W. H. STEVENS
Clarendon Laboratory, Oxford

Communicated by M. H. L. Pryce ; MS. received 2nd August 1949

ABSTRACT. The paramagnetic resonance from the nickel ion in nickel fluosilicate has been investigated at a number of frequencies and temperatures. It has previously been suggested that the ion is in an electric field of trigonal symmetry. The results obtained are in good agreement with this hypothesis. It is also found that the magnitude of the splitting of the levels varies with temperature.

§ 1. INTRODUCTION AND CRYSTALLOGRAPHY

DURING the last two years a new means has been developed for elucidating the properties of paramagnetic ions in crystals. This is the method of paramagnetic resonance, which, in principle, is very simple. A magnetic field is applied to the paramagnetic ions, so that the energy levels undergo a Zeeman effect. The ions are also subjected to a high-frequency magnetic field at right-angles to the steady field, so that transitions may be induced between the Zeeman levels when they have the appropriate energy separations, provided that the transitions are allowed. The consequent absorption of energy therefore shows a series of maxima as the static magnetic field is varied. By repeating the experiment for a series of different values of the frequency of the high-frequency field, it is possible to plot out the energy levels as functions of the static field. In particular, one can estimate the splitting of the energy levels in the absence of magnetic fields.

The situation is frequently complicated by the presence of several non-equivalent ions in the unit cell; here each type of ion contributes its own absorption spectrum. The fluosilicates of the iron group salts constitute a particularly simple case, however, since the unit cell contains only one paramagnetic ion. These salts form hexagonal crystals whose structure is known from the work of Pauling (1930); the paramagnetic ion is surrounded by six water molecules which form a slightly distorted octahedron. These give rise to an electrostatic field acting on the ion which is of nearly cubic symmetry but on which, owing to the distortion, a small trigonal component is superimposed. The distortion is in the direction of the hexagonal axis of the crystal, so that the axis of the trigonal field coincides with this crystalline axis.

The behaviour of the Ni^{++} ion [$(3d)^8$, ^3F; $\lambda = -335\,cm^{-1}$] under the influence of crystalline fields was investigated theoretically by Schlapp and Penney (1932). A cubic field splits the F state into two triplets and a singlet; the singlet lies lowest and the triplets are of the order of $10{,}000\,cm^{-1}$ higher in energy. The lowest level has a further threefold degeneracy because of the spin. When the combined effects of the non-cubic part of the crystalline field and the spin–orbit coupling are included, the spin sublevels undergo a small splitting of the order of $1\,cm^{-1}$. At room temperature and below, only the spin triplet of the lowest orbital level is appreciably populated. The higher orbital levels are important as they enter into the perturbation calculations.

Some of the magnetic properties of nickel fluosilicate have already been investigated by Becquerel and Van den Handel (1939), who measured the temperature variation of the Verdet constant. Their experimental results were interpreted by Opechowski (Becquerel and Opechowski 1939), who investigated theoretically the behaviour of the Ni^{++} ion under the influence of a cubic field with a trigonal distortion. Opechowski found that in the absence of a magnetic field the basic spin triplet is resolved into a doublet and a singlet. The experimental results indicated that the singlet is $0{\cdot}30\,cm^{-1}$ above the doublet, and that the levels diverge with a g-value of $2{\cdot}25_2$ when a magnetic field is applied parallel to the hexagonal axis. By making certain assumptions about the form of the crystalline field, Opechowski obtained some information about the position of the higher orbital levels.

The paramagnetic resonance experiments described in this paper cover the temperature range 14°–195°K. Some necessary extensions of the theory of Opechowski have been made by one of us (K.W.H.S.). The experimental results support the theory, and they reveal an interesting temperature variation of the position of the energy levels.

§ 2. EXPERIMENTAL METHOD

The experimental technique will be described here only in outline, as it has already been discussed elsewhere (Bagguley, Bleaney, Griffiths, Penrose and Plumpton 1948). A single crystal of the salt under investigation lay at the bottom of a cavity resonator, in which oscillations of fixed frequency were excited by means of a klystron oscillator. A variable external magnetic field was applied at right angles to the radio-frequency magnetic field to which the crystal was subjected. The absorption of radio-frequency energy by the specimen reduced the Q-value of the cavity and was registered as a diminution in the power transmitted through it, which is proportional to Q^2.

At wavelengths of 3 cm. and 1·2 cm. the resonator was a cylindrical cavity excited in the H_1 mode. For longer wavelengths, quarter-wavelength concentric lines were employed. The resonator was immersed in a suitable constant-temperature bath, e.g. solid carbon dioxide in acetone, or liquid oxygen.

It was necessary to use crystals of different sizes for the different wavelengths in order to obtain a suitable intensity of absorption—the 10 cm. crystal had a volume of 0·5 cm³, while the one for 1·2 cm. occupied 0·05 cm³. In some cases it was possible to use two crystals under the same conditions to afford a check.

§ 3. EXPERIMENTAL RESULTS AND DISCUSSION

In most of the experiments the magnetic field was applied parallel to the optic axis (*c*-axis and hexagonal axis) of the crystal, because the magnetic behaviour is then particularly simple, the energy levels diverging linearly (see § 4)

$$W_1 = +g_{\parallel}\beta H - \delta; \qquad W_2 = -g_{\parallel}\beta H - \delta; \qquad W_3 = 0.$$

where δ is the initial separation, $g_{\parallel}$ the '*g*-value', and β is the Bohr magneton. It is assumed that the doublet is lower than the singlet, so that δ is positive, in agreement with the findings of Becquerel, Van den Handel and Opechowski. The paramagnetic resonance experiments give no evidence on this point; they are consistent with either the doublet or the singlet being the lower.

It can be shown that in the present case transitions are not allowed between W_1 and W_2. The transitions $W_1 \longleftrightarrow W_3$ and $W_2 \longleftrightarrow W_3$ are permitted, however, and they give rise to absorption peaks for values of the magnetic field given by

$$|g_{\parallel}\beta H - \delta| = h\nu \qquad \text{and} \qquad |g_{\parallel}\beta H + \delta| = h\nu.$$

The absorption spectrum was investigated at wavelengths near 1·25, 3·2, 7 and 9 cm. The results for a temperature of 90° K. are presented graphically in Figure 1. They confirm the expected linear divergence of the levels, and yield the value 0·17 cm⁻¹ for the initial splitting. The mean *g*-value is $2{\cdot}25_5$.

When the paramagnetic resonance experiments were repeated at other temperatures, it was found that the initial splittings changed considerably. The values for g and δ for different temperatures are given in the Table.

Temperature (° K.)	195	90	60	20	14
$g_{\parallel} = g_{\perp}$	2·29	2·26	—	2·29	—
δ (cm⁻¹)	0·32	0·17	0·14	0·12	0·12

Evidently g is independent of the temperature, within the limits of experimental error; δ, on the other hand, varies by a factor of 2·5 in the range of temperature investigated.

In attempting to explain these phenomena one must anticipate some of the conclusions reached in the theoretical section, where Opechowski's calculation is extended. He has shown that

$$\delta = (A - B)\lambda^2 \qquad \ldots\ldots(1)$$

and

$$g_{\parallel} = 2(1 - \lambda A), \qquad \ldots\ldots(2)$$

where A and B are parameters which depend in a complicated way on the electric field acting on the ion. The spin–orbit coupling coefficient, λ, is known from the work of Laporte (1928) to be $-335\,\mathrm{cm}^{-1}$. Combining this with our value for δ at 90° ($0{\cdot}17\,\mathrm{cm}^{-1}$) one finds

$$A=(2-g_{\shortparallel})/2\lambda=(2{\cdot}26-2)/2\times 335\simeq 3{\cdot}9\,.\,10^{-4}\,\mathrm{cm.},$$

while

$$(A-B)=\delta/\lambda^2=0{\cdot}17/(335)^2\simeq 1{\cdot}5\,.\,10^{-6}\,\mathrm{cm.},$$

which is about 250 times smaller than A. δ thus represents the difference between two much larger quantities which are determined by the field parameters.

If the electrostatic field were purely of cubic symmetry, δ would be zero; this, however, is not so, and the actual value of δ depends in a rather complicated way on the magnitudes of the cubic and the trigonal terms in the electric field acting on the ion. It is not determined solely by the magnitude of the trigonal field. The variation in δ with temperature could thus be due to changes in the internal field due to thermal expansion of the crystal.

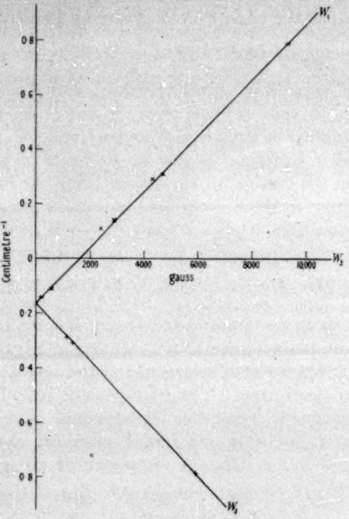

Figure 1. H parallel to hexagonal axis. Temperature 90° K.

In another series of experiments the magnetic field was applied at right angles to the hexagonal axis, to provide a further test of the theory. The energy levels do not now diverge linearly with magnetic field but are given by

$$W_1=-\delta;\qquad W_2=-\tfrac{1}{2}[\delta-\surd(\delta^2+4g_\perp{}^2\beta^2H^2)];\qquad W_3=-\tfrac{1}{2}[\delta+\surd(\delta^2+4g_\perp{}^2\beta^2H^2)],$$

where $g_\perp=2(1-\lambda B)$. As we have already mentioned, $(A-B)/A\sim 1/250$, so that $(g_{\shortparallel}-g_\perp)/g_{\shortparallel}\sim 1/250$. Thus for practical purposes we can say that $g_{\shortparallel}=g_\perp$.

In strong magnetic fields ($4g\beta H \gg \delta$) the energy levels can be written as, approximately,

$$W_1 = -\delta; \qquad W_2 = -\tfrac{1}{2}\delta + g_\perp \beta H; \qquad W_3 = -\tfrac{1}{2}\delta - g_\perp \beta H.$$

The selection rules for transitions between these levels induced by an oscillating magnetic field at right angles to the steady field are that the transitions $W_1 \longleftrightarrow W_2$ and $W_1 \longleftrightarrow W_3$ are allowed, but that the transition $W_2 \longleftrightarrow W_3$ will be very weak. Thus at a given frequency ν two strong absorption lines will be observed at values of H such that $h\nu = g_\perp \beta H - \tfrac{1}{2}\delta$ and $h\nu = g_\perp \beta H + \tfrac{1}{2}\delta$.

Here again it was possible to plot the behaviour of the energy levels (Figure 2). The curves which have been fitted were calculated using for $g_\perp$ the value found for $g_\parallel$ in the previous experiments. The curved part could not be properly verified on account of the low intensity of absorption at the long wavelengths concerned. The available points, however, lie satisfactorily on the curves.

§ 4. THEORY

In order to explain the results of Becquerel and Van den Handel, Opechowski considered the energy levels of the nickel ion in the presence of a steady magnetic field directed along the hexagonal axis. To explain the results given graphically in Figures 1 and 2 it was thought desirable to extend his work and to calculate

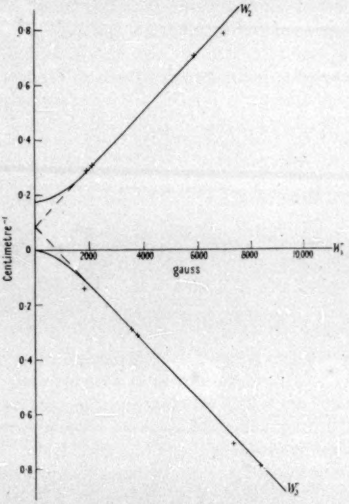

Figure 2. *H* perpendicular to hexagonal axis. Temperature 90° K.

the energy levels as functions of the external field and also of its orientation with respect to the hexagonal axis. This requires a somewhat different treatment from that given by Opechowski, as the energy levels do not, in general, diverge linearly with increase of magnetic field, and also the changes in the energies are often large compared with the separation of the levels in the absence of the field.

The effect of the electric field on the orbital states is the same as that given by Opechowski, and his work is applicable thus far. To find the combined effect of the spin–orbit coupling and the magnetic field, for any direction, it is necessary to take them together and to treat them as a perturbation on the lowest spin multiplet. A straightforward application of first order perturbation theory shows that, while there is a contribution from the magnetic energy, the contribution from the spin–orbit coupling is zero. In proceeding to the second order change in energy it would not, in general, be correct to use the zero order states which make the magnetic energy diagonal, except when the change in energy due to the magnetic field is large compared with that due to spin–orbit coupling. When the magnetic field is along the hexagonal axis, it is found that the zero order states which make the magnetic energy diagonal are also those for which a straightforward application of perturbation theory is valid. As Opechowski was only interested in this case, he avoided the difficulty given above.

A method suitable for dealing with this type of problem has been given by Van Vleck and is described in a paper by Jordahl (1934). Another method is described in a note by Pryce (1950).

The perturbation is taken as

$$\lambda\mathbf{L}\,.\,\mathbf{S}-\beta\mathbf{H}\,.\,(\mathbf{L}+2\mathbf{S}),$$

where λ is the spin–orbit coupling coefficient, $\hbar\mathbf{L}$ is the orbital angular momentum operator, $\hbar\mathbf{S}$ is the spin angular momentum operator, β is the Bohr magneton, and $\mathbf{H}$ is the steady magnetic field. Using the second of the above methods, to second order, it is found that the energy levels of the lowest spin multiplet are the same as the eigenvalues of

$$\begin{aligned}-2\beta\mathbf{H}\,.\,\mathbf{S}-A(\lambda^2S_z^{\,2}-2\lambda\beta H_zS_z+\beta^2H_z^{\,2})\\ -B[\lambda^2(2-S_z^{\,2})-2\beta\lambda(H_xS_x+H_yS_y)+\beta^2(H_x^{\,2}+H_y^{\,2})],\end{aligned}$$

where A and B are constants which, in Opechowski's notation, are given by

$$A=\frac{\tau^2}{\Delta_5{}^E-\Delta_2{}^E}\qquad\text{and}\qquad B=\frac{\sigma^2}{\Delta_4-\Delta_2{}^E}+\frac{\rho^2}{\Delta_5-\Delta_2{}^E}$$

and where the hexagonal axis is taken as Oz. The spin-independent term

$$-A\beta^2H_z^{\,2}-B[2\lambda^2+\beta^2(H_x^{\,2}+H_y^{\,2})],$$

can be dropped, since it corresponds to a displacement of all the levels, though it is of interest in that it shows that there is a displacement proportional to the square of the magnetic field, which will give rise to a constant term in the magnetic susceptibility. By writing $2(1-\lambda A)=g_{\parallel}$, $2(1-\lambda B)=g_{\perp}$ and $(A-B)\lambda^2=\delta$, the energy levels are the eigenvalues of

$$-\delta S_z^{\,2}-\beta H_zg_{\parallel}S_z-\beta g_{\perp}(H_xS_x+H_yS_y). \qquad \ldots\ldots(3)$$

The significance of δ is apparent since it represents the separation of the levels in zero magnetic field.

In order to find the selection rules governing transitions between the components of the lowest spin multiplet, it is necessary to determine their states. A good approximation to the actual states will be given by taking them as products of the lowest orbital state with the eigenstates of the operator (3) given above.

The states on which measurements are made have been obtained for the two directions $\theta=0$ and $\theta=\pi/2$, where θ is the angle between the direction of the magnetic field and the hexagonal axis. It is convenient to take the hexagonal axis as axis of quantization, so that S_z is diagonal with eigenstates $|1\rangle$, $|0\rangle$ and $|-1\rangle$. For the direction $\theta=0$, the energy levels and states are

$$\begin{aligned} W_1 &= g_{\parallel}\beta H-\delta; && |-1\rangle, \\ W_2 &= -g_{\parallel}\beta H-\delta; && |1\rangle, \\ W_3 &= 0; && |0\rangle, \end{aligned}$$

where the orbital state has been omitted as it is the same for each level. The matrix elements of all components of **L** are zero between these states, so the selection rules for an oscillating magnetic field perpendicular to Oz are such that the transitions $W_1 \longleftrightarrow W_3$ and $W_2 \longleftrightarrow W_3$ only are allowed.

For the direction $\theta=\pi/2$, (Ox), the energy levels and states are

$$\begin{aligned} W_1 &= -\delta; && \{|1\rangle-|-1\rangle\}, \\ W_2 &= -\tfrac{1}{2}[\delta-\sqrt{(\delta^2+4g_{\perp}^2\beta^2H^2)}]; && g_{\perp}\beta H\{|1\rangle+|-1\rangle\}+\sqrt{2}W_3|0\rangle, \\ W_3 &= -\tfrac{1}{2}[\delta+\sqrt{(\delta^2+4g_{\perp}^2\beta^2H^2)}]; && g_{\perp}\beta H\{|1\rangle+|-1\rangle\}+\sqrt{2}W_2|0\rangle. \end{aligned}$$

It is to be noted that the states are not normalized. The oscillating field may now be along either Oz or Oy, but in either case it is found that the allowed transitions are $W_1 \longleftrightarrow W_2$ and $W_1 \longleftrightarrow W_3$.

For a general direction of the magnetic field the energy levels are given by the roots of the secular equation:

$$\begin{vmatrix} -\delta-\beta g_{\parallel}H\cos\theta-W & -\dfrac{1}{\sqrt{2}}\beta g_{\perp}H\sin\theta & 0 \\ -\dfrac{1}{\sqrt{2}}\beta g_{\perp}H\sin\theta & -W & -\dfrac{1}{\sqrt{2}}\beta g_{\perp}H\sin\theta \\ 0 & -\dfrac{1}{\sqrt{2}}\beta g_{\perp}H\sin\theta & -\delta+\beta g_{\parallel}H\cos\theta-W \end{vmatrix}=0$$

This is a cubic and does not in general factorize.

§ 5. CONCLUSION

The results of the paramagnetic resonance experiments are entirely consistent with the crystalline field theory developed by Opechowski and extended in this paper. The magnetic properties of nickel fluosilicate have also been investigated by two other methods. Becquerel and Van den Handel (1939) and Becquerel and Opechowski (1939) measured the temperature variation of the Verdet constant in the temperature range 1·5° K.–290° K., and found that the magnetic moment of the ion is 2·25 Bohr magnetons when the magnetic field is parallel to the hexagonal axis of the crystal. The deviations of the Verdet constant from a $1/T$ law enabled them to compute a value for δ. Their measurements are sensitive to δ only at the lowest temperature; hence their value (0·30 cm^{-1}) refers to the helium region. On the other hand Benzie and Cooke (1950) find $\delta=0{\cdot}15-0{\cdot}16$ cm^{-1} at similar temperatures. This can be reconciled with our own measurements at higher temperatures.

The experimental work described in this paper was done in the summer of 1948 by Dr. Penrose, working at the Clarendon Laboratory, Oxford. He subsequently moved to Leiden where he intended to continue these experiments at helium temperatures. Owing to his illness, from which he has recently died, the experiments were not done, but it has seemed worth while to publish these results, though they are not as complete as originally intended.

Note added in proof. Holden, Kittel and Yager (*Phys. Rev.*, 1949, **75**, 1443) have reported a measurement at room temperature and 1·25 cm. wavelength on $\mathrm{Ni\,Si\,F_6, 6H_2O}$. The data for magnetic field parallel and perpendicular to the trigonal axis are not quite consistent with the assumption of trigonal symmetry, but yield the values $\delta = 0{\cdot}49 - 0{\cdot}52\ \mathrm{cm}^{-1}$, $g = 2{\cdot}29 - 2{\cdot}36$. The value of δ falls on a smooth curve with our measurements at lower temperatures.

REFERENCES

Bagguley, D. M., Bleaney, B., Griffiths, J. H., Penrose, R. P., and Plumpton, B. I., 1948, *Proc. Phys. Soc.*, **61**, 542, 551.

Becquerel, J., and Opechowski, W., 1939, *Physica*, **6**, 1039.

Becquerel, J., and Van den Handel, J., 1939, *Physica*, **6**, 1034.

Benzie, R. J., and Cooke, A. W., 1950, *Proc. Phys. Soc.* A, **63**, in the press.

Jordahl, O. M., 1934, *Phys. Rev.*, **45**, 87.

Laporte, O., 1928, *Z. Phys.*, **47**, 761.

Pauling, L., 1930, *Z. Kristallogr.*, **72**, 345.

Pryce, M. H. L., 1950, *Proc. Phys. Soc.* A, **63**, 25.

Schlapp, R., and Penney, W. G., 1932, *Phys. Rev.*, **42**, 666.

The Theory of Magnetic Resonance-Line Widths in Crystals

By M. H. L. PRYCE and K. W. H. STEVENS

Clarendon Laboratory, Oxford

MS. received 3rd *August* 1949

ABSTRACT. A theory is developed for calculating the mean displacements and mean square widths of resonant absorption lines in crystals for which the spin–lattice relaxation time is long compared with the spin–spin relaxation time. The theory is applied to a number of different cases; in particular, the effects of nuclear hyperfine structures and exchange forces in ionic resonances are discussed at length. It is shown that the theory holds, provided that the temperature is high compared with the Curie temperature.

§ 1. INTRODUCTION

The recent development of the method of magnetic resonance has provided a new and powerful method for studying the properties of magnetic systems in solids and liquids. Its application to crystals containing paramagnetic ions has led to a considerable increase in our knowledge of the fields acting on the ions, most of which had previously been obtained from magnetic susceptibility measurements.

The principle of the method is very simple. If an ion possessing a magnetic moment, and therefore having a degenerate ground state, is placed in a steady magnetic field, the degeneracy is lifted and the levels undergo a Zeeman splitting. An oscillating magnetic field will be able to induce transitions between the Zeeman levels if it has the right frequency and if the transition is not forbidden. Thus, if the frequency of the oscillating field is varied, the absorption of energy from it will show a series of maxima as the frequency passes through the characteristic frequencies of the ion. For a free ion there will be only one characteristic frequency, but when the ion is not free there may be more than one frequency of absorption.

For paramagnetic ions in fields of order several thousand gauss the characteristic frequencies usually fall in the microwave region, while for magnetic nuclei in similar fields they fall in the radio-frequency region. The experimental methods have been described by a number of observers (Bagguley *et al.* 1948, Bloembergen, Purcell and Pound 1948) and will not be given here.

As is well known (Van Vleck 1932), ions in crystals are usually in strong electric fields. For a paramagnetic ion the fields distort the orbital motion of the electrons and are also coupled to the resultant spin through the spin–orbit coupling. The effect of this is that the ground state of the ion in a crystal is often very different from that of a free ion and its magnetic properties are correspondingly altered. Usually the orbital motion is 'quenched' and the magnetic moment of the ion is anisotropic with a value near that of the 'spin-only' value.

Magnetic resonance experiments have confirmed these ideas and have given accurate values for the magnetic moments of ions in different crystals. They have also shown that the widths of the absorption lines (usually of order several hundred gauss) are much greater than the natural widths which would be expected if the ions could be regarded as independent systems placed in suitable steady electric and magnetic fields. In other words, the models which have usually been used in calculations of the positions of the resonance lines and the magnetic susceptibilities are not good enough approximations to give the line widths.

§ 2. A GENERAL SURVEY OF THE PROBLEM

In a theory of line widths in crystals it is necessary to consider the interactions between the ions themselves and also between the ions and the thermal motion of the lattice. A general treatment on these lines has not yet been given. In this paper an account will be given of a method which can be used when the interaction between the ions and the lattice is very small compared with interactions between the ions themselves. Under these conditions a good approximation is given by regarding the magnetic ions as located at fixed positions and interacting through their couplings with each other. The thermal motion will modulate the interactions and the approximation is equivalent to assuming that the extra width from the modulation is small compared with that which would be found were there no thermal motions. This is not an unrealistic approximation, as there are many crystals in which the widths of the resonance lines are determined almost entirely by the static interactions. These are crystals in which the spin–lattice relaxation time is long compared with the spin–spin relaxation time.

Before giving the quantum mechanical treatment of the line widths under these conditions, it is instructive to consider the way in which broadening arises, from a semi-classical point of view. Each ion is regarded as a gyroscopic magnet; that is, its angular and magnetic moments are parallel. We consider a system of such magnets, each located at a fixed point in space and all in a uniform steady external magnetic field, directed along Oz. Each magnet will precess about Oz and can be regarded as equivalent to a magnet fixed in the direction of Oz together with a magnet rotating in a plane perpendicular to Oz. If a magnet A is considered, the steady field on it will not be equal to the external field but will be the resultant of the external field and an internal steady field from the fixed magnets associated with all the other magnets. A will therefore precess about this resultant field with a frequency equal to γH, where γ is its gyromagnetic ratio and H is the resultant steady field. The value and orientation of H will vary from one magnet to another, with the result that there will be a spread in the precessional frequencies. This will appear as a broadening of the resonant absorption line. It is to be noted that this type of broadening does not depend on the magnets all having the same gyromagnetic ratios, and may be termed 'steady field broadening'.

It is next necessary to consider whether the fields set up by the rotating magnets can have any broadening effects. If two magnets have the same precessional frequencies, the rotating field from one will be at the right frequency to induce transitions in the other (the transition frequency is equal to the precessional frequency), whereas if the two magnets have different precessional frequencies, the rotating fields will have little effect. This shows that magnets with the same resonance frequencies will tend to induce transitions in each other and reduce their life-times in given states. This will appear as a broadening of the resonance line. There is no way in which the total energy of the system can change, so these transitions will only occur if they are energetically allowed. They can be pictured as transitions in which one magnet gives energy to another. This type of broadening will be referred to as 'resonance broadening'.

In the quantum mechanical treatment of the line widths the expressions obtained are usually fairly complicated, but it is often found that the matrix elements which occur can be interpreted as arising either from resonance broadening or from steady field broadening. Further reference to this will be made after the quantum mechanical treatment.

The semi-classical treatment has been given under the assumption that the only type of coupling between the ions is magnetic dipole–dipole coupling; in actual crystals there may also be exchange couplings. There is no difficulty in taking exchange into account in the theory to be given; the interaction used can include both exchange and magnetic coupling.

The method used is a perturbation method in which the energy of interaction is taken as a perturbation to the energy of an uncoupled system of ions. For this, it is convenient to assume that the energy levels of a single ion, under the influence of the crystalline electric and the applied magnetic field, fall into a low-lying group with separation small compared with $\boldsymbol{k}T$, and that the other levels are so far removed in energy that their populations are negligible at the temperatures used. These higher levels play no part in the theory and it is convenient to forget them and assume that the ions have only the low-lying levels. This restriction is not severe, as it usually happens that the levels are arranged in this way.

It is found that, provided $\boldsymbol{k}T$ is large compared with the energy differences between the states in the low-lying group, the mean square width of the absorption lines is effectively independent of temperature, and that the centre of the broadened line is undisplaced from the position it would have were there no inter-ionic couplings. At temperatures for which $\boldsymbol{k}T$ is of the same order of magnitude as the energy separations, both the displacement and the line width may be temperature dependent, and there is also a dependence on the shape of the crystal, an effect closely connected with the demagnetization factor (see below).

The theory is also applicable to calculating the widths found in nuclear resonance experiments, and it is useful to have a notation which can refer to either ions or nuclei. To this end we shall use the word 'dipole' to mean either a nuclear or an ionic magnetic moment. The magnetic coupling between dipoles will be referred to as 'dipolar coupling'.

The oscillating magnetic field is usually at right angles to the steady field in resonance experiments. It is not necessary to assume this in the theory and the formulae hold for any angle between the fields.

§3. THE DERIVATION OF GENERAL FORMULAE FOR THE MOMENTS

In this section, formulae of general application are obtained for the total area of an absorption line, and its first and second moments about the position it would have were there no inter-dipole couplings. From these quantities the mean displacement and mean-square width can be found by taking the appropriate ratios. The absorption curve is taken as a curve in which the absorption $A(\nu)$ at frequency ν is plotted against ν. $A(\nu)$ can be measured in arbitrary units, since in taking the ratios any common factors will disappear. The method is readily extended to calculating higher moments, but the relevant formulae will not be given, as they are, in principle, easily derived, though cumbersome.

It is supposed that the crystal contains dipoles which have a number of possible transitions, one of which occurs at a frequency ν, and it is the width of the line at ν which has to be calculated. In the absence of any coupling, the energy levels of the dipole system will consist of a large number of highly degenerate levels, and there will be many pairs of levels with separations $\boldsymbol{h}\nu$. One such pair is chosen, and their energies are denoted by E_α and E_β, so that $\boldsymbol{h}\nu = E_\beta - E_\alpha$. The manifold of degenerate states in E_α is described by a projection operator P_α, and that for E_β by P_β. If the effect of a coupling is now considered, the degeneracies are largely removed, and instead of the levels E and E_β giving a sharp line at ν, the states which have come from them will give transitions which are spread about ν. This process will occur for all pairs of levels with initial separations $\boldsymbol{h}\nu$, and in determining the total width it is necessary to average over all such pairs, with appropriate weighting factors. It is assumed that all the width is due to this cause, and that there are no contributions from states which were initially at separations other than $\boldsymbol{h}\nu$. If such contributions were appreciable the spectra observed would not consist of the distinct lines found, but, instead, the lines would be broadened into each other.

The inter-dipole coupling is represented by a term W in the Hamiltonian of the system, and the zero order states in the perturbation calculation are chosen to be those eigenstates of the total energy which make W diagonal in the manifolds P_α and P_β. Then, if $|a\rangle$ represents such a state in P_α and $|b\rangle$ a state in P_β, the change in energy of $|a\rangle$ when W is introduced is, to a first approximation, $\langle a|W|a\rangle$, and that of $|b\rangle$ is $\langle b|W|b\rangle$.

In order to study the resonant absorption when an oscillating magnetic field of frequency near to ν is applied to the crystal, it is necessary to consider its contribution to the Hamiltonian of the system. This will be denoted by M, and it can be regarded as inducing transitions between the various states of the dipole system. It will cause transitions between states $|a\rangle$ and $|b\rangle$ if the frequency of oscillation is $\nu + \{\langle b|W|b\rangle - \langle a|W|a\rangle\}/\boldsymbol{h}$, with a transition probability proportional to $|\langle a|M|b\rangle|^2$. The probability that the crystal is in the state $|a\rangle$ is different from that for state $|b\rangle$, and it is this difference which makes the rate of absorption of energy greater than the rate of stimulated emission. When allowance is made for this, the spectrum from states $|a\rangle$ and $|b\rangle$, apart from constant multiplying factors, can be expressed as:

$$\{\exp(-E_a/\boldsymbol{k}T)-\exp(-E_b/\boldsymbol{k}T)\}(E_b-E_a)|\langle a|M|b\rangle|^2$$
$$\times\,\delta\{\nu'-\nu-\{\langle b|W|b\rangle-\langle a|W|a\rangle\}/\boldsymbol{h}\}/\Sigma_s\exp(-E_s/\boldsymbol{k}T),$$

where E_a is the energy of the state $|a\rangle$, E_b is the energy of the state $|b\rangle$, T is the absolute temperature, $\boldsymbol{k}$ is Boltzmann's constant, the summation is to be taken over all possible values of E_s, ν' is the varying frequency, and $\delta(\nu')$ is a function of ν' which is sharply peaked at $\nu'=0$. $\delta(\nu')$ is introduced to represent the shape of the absorption line. If this expression could be summed over all pairs of states such as $|a\rangle$ and $|b\rangle$, it would give the shape of the complete absorption curve as a function of the frequency ν'. This, however, is not possible, but by making certain approximations it is possible to obtain a good deal of information about the shape of the curve, for it appears that the area, mean centre, mean square width, and higher moments can be written in invariant forms which can be evaluated without knowledge of the zero-order states. It is not practicable to calculate more than the first few moments, as the labour involved increases rapidly with increasing order.

The expression

$$\{\exp(-E_a/\boldsymbol{k}T)-\exp(-E_b/\boldsymbol{k}T)\}(E_b-E_a)$$

can be written as:

$$\exp(-E_\alpha/\boldsymbol{k}T)\exp(-\langle a|W|a\rangle/\boldsymbol{k}T)[1-\exp\{-(\boldsymbol{h}\nu+\langle b|W|b\rangle-\langle a|W|a\rangle)/\boldsymbol{k}T\}]$$
$$\times\,[\boldsymbol{h}\nu+\langle b|W|b\rangle-\langle a|W|a\rangle],$$

where E_α is the energy of the manifold P_α. As $\langle b|W|b\rangle-\langle a|W|a\rangle$ is small compared with $\boldsymbol{h}\nu$ for all the pairs of states which make appreciable contributions to the width, the error will be small if the above expression is replaced by

$$\exp(-E_\alpha/\boldsymbol{k}T)\exp(-\langle a|W|a\rangle/\boldsymbol{k}T)\boldsymbol{h}\nu\{1-\exp(-\boldsymbol{h}\nu/\boldsymbol{k}T)\}.$$

This approximation involves no assumption about the magnitude of the temperature. If it is now assumed that the temperature is much greater than the changes in energy caused by the interaction, a further approximation is to replace $\exp\{-\langle a|W|a\rangle/\boldsymbol{k}T\}$ by unity. The error introduced by this approximation will be considered below. The absorption curve for the states $|a\rangle$ and $|b\rangle$ can then be written as:

$$\exp(-E_\alpha/\boldsymbol{k}T)\boldsymbol{h}\nu(1-\exp\{-\boldsymbol{h}\nu/\boldsymbol{k}T\})|\langle a|M|b\rangle|^2$$
$$\times\,\delta[\nu'-\nu-\{\langle b|W|b\rangle-\langle a|W|a\rangle\}/\boldsymbol{h}]/\Sigma_s\exp(-E_s/\boldsymbol{k}T).$$

In finding the mean displacement and mean square width of the absorption line, it will ultimately be necessary to consider the ratios of expressions derived from the above formula, so it is convenient to drop the factor

$$\boldsymbol{h}\nu\{1-\exp(-\boldsymbol{h}\nu/\boldsymbol{k}T)\}/\Sigma_s\exp(-E_s/\boldsymbol{k}T),$$

as it does not depend on the particular choice of the states $|a\rangle$ and $|b\rangle$. The total area of the absorption curve is then found by summing the areas given by all pairs of states such as $|a\rangle$ and $|b\rangle$. If the integral of $\delta(\nu')$ for all values of ν' is taken to equal unity, and if the summation is first taken over all pairs of states coming from manifolds $\boldsymbol{h}\nu$ apart, the area can be written as:

$$\Sigma_{\alpha,\beta} \exp(-E_\alpha/\boldsymbol{k}T) \operatorname{Spur} P_\alpha M P_\beta M, \qquad \ldots\ldots(1)$$

where the summation is to be taken over all values of α and β such that $E_\beta - E_\alpha = \boldsymbol{h}\nu$. In the same way, the first moment about the undisplaced position is found to equal

$$\Sigma_{\alpha,\beta} \exp(-E_\alpha/\boldsymbol{k}T) \operatorname{Spur}(P_\beta W P_\beta M P_\alpha M - P_\alpha W P_\alpha M P_\beta M), \qquad \ldots\ldots(2)$$

and the second moment:

$$\Sigma_{\alpha,\beta} \exp(-E_\alpha/\boldsymbol{k}T) \operatorname{Spur}(P_\beta W P_\beta W P_\beta M P_\alpha M - 2 P_\alpha W P_\alpha M P_\beta W P_\beta M + P_\alpha W P_\alpha W P_\alpha M P_\beta M). \qquad \ldots\ldots(3)$$

The ratio of (2) to (1) gives the mean displacement of the line from $\boldsymbol{h}\nu$, and the ratio of (3) to (1) gives the mean square width. In taking these ratios, it is seen that the various constants which have been dropped would disappear had they still been present, a result which justifies their earlier removal.

§4. ONE TYPE OF DIPOLE

The above formulae are most easily applied to the case of a crystal in which there is just one type of dipole present, and in which the energy levels of the single dipole are such that there are only two states with energy difference $\boldsymbol{h}\nu$. It is supposed that each dipole has R states which are denoted by $|a_1\rangle, |a_2\rangle, \ldots . |a_R\rangle$, with corresponding energies $a_1, a_2, \ldots . a_R$, and that the transition of interest is that between $|a_1\rangle$ and $|a_2\rangle$, so that $a_2 - a_1 = \boldsymbol{h}\nu$. The energies of the manifolds P_γ can then be specified by the number of dipoles in the various states, and if N is the total number of dipoles in the crystal, a particular pair of levels E_α and E_β may be specified by the sets of numbers $(n_1, n_2, n_3, \ldots . n_R)$ and $(n_1 - 1, n_2 + 1, n_3, \ldots . n_R)$ where

$$E_\alpha = n_1 a_1 + n_2 a_2 + n_3 a_3 + \ldots . + n_R a_R$$

and

$$E_\beta = (n_1 - 1) a_1 + (n_2 + 1) a_2 + n_3 a_3 + \ldots . + n_R a_R$$

with $\Sigma_{r=1}^{r=R} n_r = N$. This replaces the summations over the α's and β's by summations over the n's.

Before carrying out the summations, it is convenient to decompose M and W into their component parts, and to write $M = \Sigma_s m_s$ and $W = \Sigma_{p<q} W_{pq}$, where m_s is the coupling of the radio-frequency field to the sth dipole and W_{pq} is the inter-dipole coupling between dipoles p and q. In order to simplify the notation, it is useful to write expressions of the form

$$\langle a_r a_s \ldots . | W | a_p a_q \ldots . \rangle$$

as

$$\langle r, s \ldots . | W | p, q \ldots . \rangle,$$

where the a's are omitted altogether. This leads to no confusion as long as there is only one type of dipole present, and it so happens that even when there are several types present, the final results can be written in this form without ambiguity. For dipolar and exchange couplings (which are of most interest), expressions of the form $\Sigma_s \langle\, , s | W_{ij} |\, , s\rangle$, being of the nature of spurs over the states of the jth ion, are zero. It will therefore be assumed that all such expressions are zero. The summations can be carried out without this assumption, but it is convenient to make it, as it leads to a good deal of simplification.

The results of the summations are that (1) and (3) give constant terms together with temperature dependent terms which are completely negligible if $\boldsymbol{k}T$ is large compared with the a's, whereas (2) gives terms of order $a_1/\boldsymbol{k}T$. This means that for the temperatures normally used, the mean displacement of the line is small, and that the area and width may be calculated as if the temperature is infinite.

It is readily seen that

$$\text{Spur}\, P_\alpha m_s P_\beta m_t = 0$$

for $\text{Spur}\, P_\alpha m_s P_\beta m_t = \Sigma_{a,b,c,\ldots.} \langle a, b, c, \ldots. | P_\alpha m_s P_\beta m_t | a, b, c, \ldots. \rangle$,

and each term is certainly zero unless the tth dipole is in the state $|1\rangle$; but in this case the operator $P_\beta m_t$ changes it into the orthogonal state $|2\rangle$, and as there are no other operators acting on the tth dipole, these terms also vanish. It also follows by symmetry that

$$\text{Spur}\, P_\alpha m_s P_\beta m_s = \text{Spur}\, P_\alpha m_1 P_\beta m_1$$

and

$$\begin{aligned}\text{Spur}\, P_\alpha m_1 P_\beta m_1 &= \Sigma_{a,b,c,\ldots.} \langle 1, a, b, \ldots. | P_\alpha m_1 P_\beta m_1 | 1, a, b, \ldots. \rangle \\ &= \Sigma_{a,b,c,\ldots.} |\langle 1|m|2\rangle|^2 \langle 1, a, b, \ldots. | P_\alpha | 1, a, b, \ldots. \rangle \\ &= |\langle 1|m|2\rangle|^2 \frac{(N-1)!}{(n_1-1)!\, n_2!\, n_3! \ldots. n_R!},\end{aligned}$$

so that:

$$\Sigma_{\alpha,\beta} \exp(-E_\alpha/\boldsymbol{k}T)\, \text{Spur}\, P_\alpha M P_\beta M = N |\langle 1|m|2\rangle|^2 \exp(-a_1/\boldsymbol{k}T) A^{N-1},$$

where

$$A = \Sigma_{r=1}^{r=R} \exp(-a_r/\boldsymbol{k}T) \simeq R.$$

Coming now to the first and second moments, it is probably simplest to evaluate (2) and (3) by writing them as summations of the form:

$$\Sigma_{i,j,k,\ldots.} \text{Spur}\,(P_\beta W_{ij} P_\beta m_k P_\alpha m_l - P_\alpha W_{ij} P_\alpha m_k P_\beta m_l)$$

and

$$\begin{aligned}\Sigma_{i,j,k,\ldots.} \text{Spur}\,(&P_\alpha W_{ij} P_\alpha W_{kl} P_\alpha m_p P_\beta m_q - 2 P_\alpha W_{ij} P_\alpha m_p P_\beta W_{kl} P_\beta m_q \\ &+ P_\beta W_{ij} P_\beta W_{kl} P_\beta m_p P_\alpha m_q),\end{aligned}$$

and then to evaluate each term separately. This is quite long, so only the results will be given. With $\boldsymbol{k}T$ large compared with the a's, (2) vanishes to first order in $a/\boldsymbol{k}T$. No terms of type $W_{ij}W_{kl}$ survive in (3), and terms of type $W_{ij}W_{jk}$ survive with factors of order $a_1/\boldsymbol{k}T$, compared with those of type $W_{ij}W_{ij}$, and can thus be neglected. The value of (3) is then given by the expression:

$$|\langle 1|m|2\rangle|^2 R^{N-2} \Sigma_i \Sigma_j \left[\begin{array}{l} |\langle 1,1|W_{ij}|1,1\rangle - \langle 2,1|W_{ij}|2,1\rangle - \langle 2,1|W_{ij}|1,2\rangle|^2 \\ + |\langle 1,2|W_{ij}|1,2\rangle - \langle 2,2|W_{ij}|2,2\rangle + \langle 2,1|W_{ij}|1,2\rangle|^2 \\ + \Sigma_{s>2}^{s=R} \left\{\begin{array}{l} |\langle 1,s|W_{ij}|1,s\rangle - \langle 2,s|W_{ij}|2,s\rangle|^2 \\ + |\langle 1,s|W_{ij}|s,1\rangle - \langle 2,s|W_{ij}|s,2\rangle|^2 \end{array}\right\} \end{array}\right].$$

If the summation over all i and j of the terms in the square bracket is denoted by X, the mean square width is seen to equal X/NR.

For the sake of uniformity with the expressions found for the areas and second moments in more complicated cases, it is useful to write the above expressions in the forms:

$$\textit{Area}\quad D\frac{N}{R}|\langle 1|m|2\rangle|^2. \qquad \ldots\ldots(4)$$

Second Moment

$$D\frac{1}{R^2}\Sigma_i\Sigma_j\left[\begin{array}{r|l|}\Sigma_s & \{\langle 1,s|W_{ij}|1,s\rangle-\langle 2,s|W_{ij}|2,s\rangle\}\langle 2|m|1\rangle \\ & +\Sigma_{l,k}\langle 2,l|P_{1s}W_{ij}P_{1s}|1,k\rangle\langle k|m|l\rangle \\ & -\Sigma_{l,k}\langle 2,l|P_{2s}W_{ij}P_{2s}|1,k\rangle\langle k|m|l\rangle \\ \end{array}^{2} \begin{array}{r|l|}+\Sigma_s{}' & \{\langle 1,s|W_{ij}|s,1\rangle-\langle 2,s|W_{ij}|s,2\rangle\}\langle 2|m|1\rangle \\ & +\Sigma_{l,k}\langle 2,l|P_{1s}W_{ij}P_{1s}|k,1\rangle\langle k|m|l\rangle \\ & -\Sigma_{l,k}\langle 2,l|P_{2s}W_{ij}P_{2s}|k,1\rangle\langle k|m|l\rangle \end{array}^{2}\right]. \qquad \ldots\ldots(5)$$

Here, D denotes the total number of states of the crystal and the dash on the second summation over s means that the values 1 and 2 of s are to be excluded. This avoids the repetition of terms which are already included in the first sums. The operators P_{1s} and P_{2s} are to be interpreted as the projection operators of the states of two dipoles corresponding to energies a_1+a_s and a_2+a_s. The possible values of l and k are then severely restricted, and the whole expression is exactly equal to that given earlier.

§ 5. TWO TYPES OF DIPOLE

In this section it will be supposed that the crystal contains two types, A and B, of dipoles, and that no transition frequencies of the dipoles coincide. As before, the states of the dipoles of type A (R in number) are denoted by $|a_1\rangle, |a_2\rangle, \ldots. |a_R\rangle$, and those of type B ($S$ in number) by $|b_1\rangle, |b_2\rangle, \ldots. |b_S\rangle$, with corresponding energies $a_1, a_2, \ldots. a_R$; $b_1, b_2, \ldots. b_S$. The transitions between states $|a_1\rangle$ and $|a_2\rangle$ are considered, and it is again supposed that the partial spurs $\Sigma_s\langle\ ,s|W_{ij}|\ ,s\rangle$ are zero, where dipole j may be of either type.

With the same approximations as before, the first moment is zero, and the others are:

$$\textit{Area}\quad D\frac{N_A}{R}|\langle 1|m_A|2\rangle|^2.$$

Second Moment

$$D\frac{1}{R^2}|\langle 1|m_A|2\rangle|^2X$$
$$+D\frac{1}{RS}|\langle 1|m_A|2\rangle|^2\Sigma_i\Sigma_j\{\Sigma_s|\langle 1,s|W_{ij}|1,s\rangle-\langle 2,s|W_{ij}|2,s\rangle|^2\},$$

where D is equal to the total number of states of the crystal, N_A is the number of dipoles of type A, X is equal to the same expression as before with dipoles i and j both of type A, and the second summation over i and j is to be made with dipoles i of type A and dipoles j of type B.

The general expressions (4) and (5) will include these results if N_A is used for N, and the summations over s are given a wider interpretation, so that s stands for states of both kinds of dipoles, and dipole i is always taken to be of type A, whereas dipole j can be of either type. When dipoles i and j are of the same type, there is a factor $1/R^2$, and when they are of different types the factor has to be altered to $1/RS$. Certain of the terms which then appear have no meaning, since a dipole can only be of one type, and it is necessary to take all such terms as zero. The extensions which have to be made if there are more than two types of dipoles present, and there are no coincident lines, are readily made. All that is necessary is to let s range over the states of all the dipoles, and to change the factor $1/R^2$ in an obvious manner.

§ 6. COINCIDENT LINES

It frequently happens in the case of nuclear resonance, and sometimes in paramagnetic resonance, that a number of transition frequencies for a single dipole coincide. When this occurs, there are resonance effects between the states (as discussed earlier), and the above formulae have to be modified.

In this section it will be supposed that there is only one type of dipole present and, with notation as before, it will be assumed that $a_2 - a_1 = a_4 - a_3$, so that the transitions $a_2 \longleftrightarrow a_1$ and $a_4 \longleftrightarrow a_3$ coincide. The area of the line is found to be equal to the sum of the areas calculated as if the lines were distinct and the mean displacement is, as usual, zero. The second moment is found to be given by the sum of two expressions such as (5), one for the transition $a_2 \longleftrightarrow a_1$, and the other for the transition $a_4 \longleftrightarrow a_3$. The summations over l and k will not now be quite so restricted, and it is to be noted that the width of the line will depend on the matrix elements of the magnetic moments of the dipoles. If more than two lines coincide, there must be a term of type (5) for each coincidence.

A similar result is found when the coincidence is of the form given by $a_2 - a_1 = a_3 - a_2$, so that the transitions $a_2 \longleftrightarrow a_1$ and $a_3 \longleftrightarrow a_2$ coincide. The area is again equal to the sum of the areas calculated as if the lines were distinct, the mean displacement is zero, and the second moment is given as a sum of expressions like (5), with one for each transition.

If other types of dipoles are also present, the formula for the area is unchanged, except that the value of D is altered, and in the second moment it is necessary to let s range over the states of the dissimilar dipoles as well as the similar dipoles, as before.

§ 7. LINES FROM DIFFERENT TYPES OF DIPOLES COINCIDING

In crystals which have two non-equivalent dipoles in unit cell, there are usually orientations of the applied magnetic field for which the two types of dipoles have the same energy levels. When this case is examined, formulae (4) and (5) are still found to hold, each coincidence giving its own contribution. In the cases previously considered, the summations over l and k give zero for dissimilar dipoles, but in this case they give non-vanishing contributions.

It thus appears that formulae (4) and (5) can, with appropriate interpretations of the summations, cover many of the cases actually met with experimentally. The areas are always directly additive, and the second moments are also additive, with the difference that the actual expressions to be added depend on the problem under consideration. As the changes to be made always take place in the summations over l and k, it is reasonable to interpret these terms as the contributions arising from the precessional resonances described earlier.

§8. DEGENERATE AND NEARLY DEGENERATE LEVELS

The external magnetic field is usually sufficient to ensure that the states of the dipoles are non-degenerate, and this has been assumed in the preceding work. It is possible, however, that for some values of the applied field two energy levels coincide. This happens, for instance, in chrome alum for certain orientations and magnitudes of the field (Bagguley and Griffiths 1947). It is necessary to consider this case separately. Let it be assumed that only two levels coincide and that they have energy a_2. The basic states for this level may be chosen to be any two mutually orthogonal combinations of the states in a_2, say $|a_2\rangle$ and $|a_3\rangle$. The expressions for the intensity and the width will depend, *inter alia*, on $\langle a_1|m|a_2\rangle$ and $\langle a_1|m|a_3\rangle$. It is convenient to choose as basic states those linear combinations which make $\langle a_1|m|a_3\rangle=0$. The results must be, of course, independent of the choice of basic states, and can be written in general form when the result for the restricted choice is known.

The *area* of the absorption curve is

$$D\frac{N}{R}|\langle 1|m|2\rangle|^2,$$

and the *second moment* is

$$\frac{D}{R^2}|\langle 1|m|2\rangle|^2$$

$$\times\left[X+\Sigma_i\Sigma_j\left\{\begin{array}{l}2|\langle 2,1|W_{ij}|3,1\rangle-\langle 2,2|W_{ij}|3,2\rangle+\langle 1,2|W_{ij}|3,1\rangle|^2\\+|\langle 2,1|W_{ij}|3,1\rangle|^2+|\langle 2,1|W_{ij}|1,3\rangle|^2\\+|\langle 2,2|W_{ij}|3,3\rangle|^2+|\langle 2,2|W_{ij}|2,3\rangle|^2\end{array}\right\}\right]. \qquad \ldots\ldots(6)$$

X is the same as previously defined for the transition $a_2\longleftrightarrow a_1$. The extra terms giving the effect of the degeneracy are not given by (5) and have therefore been written out in full.

If a dipole has two energy levels, say a_2 and a_3, which are very near to each other, the transitions $a_1\longleftrightarrow a_2$ and $a_1\longleftrightarrow a_3$ give two lines with a small frequency separation, equal to $|a_3-a_2|/\boldsymbol{h}$. When, however, a system containing such dipoles is considered, the lines are broadened by the inter-dipole couplings and it may happen that the widths are comparable with the separation $|a_3-a_2|/\boldsymbol{h}$, so that the lines overlap and can no longer be regarded as distinct. It is then incorrect to calculate the second moment as if the lines are distinct, for if this is permissible, the result so obtained should be independent of $|a_3-a_2|/\boldsymbol{h}$, and as this tends to zero should go into (6). This does not happen. Similarly, it is incorrect to calculate the second moment as if the levels are degenerate, using (6), for if W is put equal to zero, the result is certainly wrong. In order, then, to deal with nearly degenerate levels, the theory has to be extended, as follows.

Consider, first, the Hamiltonian of a single uncoupled dipole, and let its eigenvalues be a_1, a_2, a_3, a_4, ... etc., where a_2 and a_3 are nearly equal. If the corresponding eigenstates $|a_1\rangle$, $|a_2\rangle$, $|a_3\rangle$, ... etc. of the energy are chosen as basic states, the Hamiltonian is diagonal, with elements a_1, a_2, a_3, ... etc., and can be written as the sum of two diagonal matrices, one (H_1) with elements $a_1, a_2', a_2', a_4, \ldots.$, and the other (H_2) with elements $0, a_2-a_2', a_3-a_2', 0, 0, \ldots.$, where a_2-a_2' and a_3-a_2' are small. Regarding H_2 as a small perturbation on H_1, it is seen that the basic states appropriate to the matrix H_1 are also $|a_1\rangle, |a_2\rangle, |a_3\rangle \ldots$. Thus, the quantum mechanical description of a dipole with two nearly degenerate levels is equivalent to regarding the dipole as being slightly perturbed from a description in which the levels actually coincide.

The reasoning which led to formulae (1), (2) and (3), was not dependent on the form of W; the assumption that W was of the form $\Sigma_{p<q} W_{pq}$ was only made to find the moments due to inter-dipole couplings. In dealing with nearly degenerate levels, it is more convenient to regard the dipoles as having levels which actually coincide, and to take the perturbation as a sum of internal couplings, such as H_2, and external couplings, such as dipolar couplings, and write $W = W_{\mathrm{int}} + W_{\mathrm{ext}}$. The formulae (1), (2) and (3) are then directly applicable. The area, which does not depend on W, is given, as usual, by a sum of terms like that in (4), with one for each transition. The first moment may be written as

$$\Sigma_{\alpha,\beta}\left[\begin{array}{l}\exp(-E_\alpha/\boldsymbol{k}T)\,\mathrm{Spur}\,(P_\beta W_{\mathrm{int}} P_\beta M P_\alpha M - P_\alpha W_{\mathrm{int}} P_\alpha M P_\beta M)\\ \quad +\exp(-E_\alpha/\boldsymbol{k}T)\,\mathrm{Spur}\,(P_\beta W_{\mathrm{ext}} P_\beta M P_\alpha M - P_\alpha W_{\mathrm{ext}} P_\alpha M P_\beta M)\end{array}\right],$$

and gives the first moment about $\nu = (a_2' - a_1')/\boldsymbol{h}$. The first summation can be evaluated as if there are no inter-dipole couplings, and therefore gives N times the moments of the transitions $a_2 \longleftrightarrow a_1$ and $a_3 \longleftrightarrow a_1$ of a single dipole about $(a_2' - a_1)/\boldsymbol{h}$. The second term is the first moment of a system whose dipoles have a degenerate energy level, and, as usual, is zero. It has not yet been necessary to give a value to a_2', except to require that $a_2 - a_2'$ and $a_3 - a_2'$ are small, but if it is now chosen so that the first summation also vanishes, the total displacement vanishes, and the frequency $\nu = (a_2' - a_1)/\boldsymbol{h}$ gives the centre of the absorption.

In the same way, the second moment can be written as the sum of four terms, which may be characterized by the notation $(W_{\mathrm{int}} W_{\mathrm{int}})$, $(W_{\mathrm{ext}} W_{\mathrm{ext}})$, $(W_{\mathrm{ext}} W_{\mathrm{int}})$ and $(W_{\mathrm{int}} W_{\mathrm{ext}})$ where

$$\begin{aligned}(W_p W_q) = \Sigma_{\alpha,\beta} \exp(-E_\alpha/\boldsymbol{k}T)\,\mathrm{Spur}\,(&P_\alpha W_p P_\alpha W_q P_\alpha M P_\beta M\\ &-2P_\alpha W_p P_\alpha M P_\beta W_q P_\beta M + P_\beta W_p P_\beta W_q P_\beta M P_\alpha M),\end{aligned}$$

where W_p and W_q can be W_{int} and W_{ext}. $(W_{\mathrm{int}} W_{\mathrm{int}})$ is the expression for the second moment which would be obtained if there were no couplings between the dipoles, and is thus N times the second moment about $(a_2' - a_1)/\boldsymbol{h}$ for the transitions $a_2 \longleftrightarrow a_1$ and $a_3 \longleftrightarrow a_1$ of a single dipole. $(W_{\mathrm{ext}} W_{\mathrm{ext}})$ is the second moment which would be obtained if the dipoles had a degenerate energy level a_2', and is a case which has already been treated. When $(W_{\mathrm{ext}} W_{\mathrm{int}})$ and $(W_{\mathrm{int}} W_{\mathrm{ext}})$ are evaluated it is found that they vanish. Taking the ratio of the second moment to the area, it is seen that the mean square width is equal to $\overline{\Delta W_1^2} + \overline{\Delta W_2^2}$, where $\overline{\Delta W_1^2}$ is the mean square width of the system when there are no inter-dipole couplings, and $\overline{\Delta W_2^2}$ is the mean square width for a related system with a degenerate energy level a_2', as discussed above.

§ 9. HYPERFINE STRUCTURE

In applying these results to the widths of the resonance lines given by paramagnetic ions, it is usually assumed that an ion can be completely specified by its electronic states, whereas, in fact, if there are couplings between the electronic system and the nucleus, a complete description will be a sum of products of nuclear and electronic states. If the nuclear–electronic coupling is zero, the ionic states can be taken as $|e\rangle\,|n\rangle$ where $|e\rangle$ is an electronic state and $|n\rangle$ is a nuclear state, so that each level, instead of being non-degenerate, as has usually been assumed, has actually a degeneracy arising from the nuclear states. If formulae (1) and (2) and (3) are evaluated, taking into account the nuclear states, and assuming that W is purely electronic in nature, it is readily seen that the only effect is to increase the degeneracies of P_α and P_β by factors which disappear when the ratios giving the mean displacements and mean square widths are taken. Thus the omission of the nuclear states does not affect the results of the previous work, provided that there is no coupling between the nucleus and the electronic motion. The assumption that this is so, is not, however, always justified. For example, the magnetic field at the nucleus of the Cu^{++} ion, arising from the electronic system, is of the order of hundreds of thousands of gauss, and the interaction between its nuclear magnetic moment and the electronic system produces splittings of the nuclear levels of the order of $0{\cdot}03\ \mathrm{cm}^{-1}$. If the microwave resonances of the copper ions in a diluted crystal of copper potassium sulphate are observed, a hyperfine structure, with an overall separation of this order of magnitude, is found. It is necessary to use a diluted crystal since, in an undiluted crystal, the broadening due to inter-ionic couplings is also of this order, with the result that the lines in the hyperfine structure are broadened into each other, and are no longer resolved. Evidently then, in calculating the mean square width of the line in an undiluted crystal, it is incorrect to neglect the nuclear–electronic couplings.

The necessary extensions of the theory in order to include the effects arising from hyperfine structures, are readily made. As for the case of nearly degenerate dipole levels, W is taken as a sum of external and internal couplings, W_{ext} (assumed to be entirely electronic), representing the couplings between the different ions, and W_{int} representing the electronic–nuclear couplings which have given rise to the hyperfine structures of the levels. It is then found that the centre of the absorption line is at the same frequency as the centre of the hyperfine structure for the resonance of a single ion, and that the mean square width is equal to the sum of the mean square widths of the system with no electronic–nuclear couplings and the mean square width with no inter-ionic couplings. Thus the results are completely analogous to those found for the case of overlapping absorptions caused by near degeneracies in the electronic levels.

§ 10. DEPENDENCE ON THE SHAPE OF THE CRYSTAL AND ON TEMPERATURE

The double summations of the form $\Sigma_{i,j}|\langle|W_{ij}|\rangle|^2$ which appear in the expressions for the main, temperature independent, part of the mean square width can be replaced by summations over a single index provided that the crystal is reasonably large. For, if a dipole i in the interior of the crystal is considered and the summation over j is performed, the series is so rapidly convergent that its sum depends, effectively, on only those dipoles in the immediate neighbourhood of i. It will therefore be the same for all dipoles of the same type in the crystal, except for those within a few atomic distances of the surface, which, in general, form only a negligible proportion of the whole. The double sum is thus N times the single sum. It will be noted that for dipolar interactions, $|\langle|W_{ij}|\rangle|^2$ falls off as the inverse sixth power of the distance between the dipoles; for exchange it falls off exponentially. The convergence is therefore very rapid, and the final sum does not depend on the shape of the crystal.

The terms of order $1/\boldsymbol{k}T$ which appear in both the mean displacement and the mean square width of the line, contain summations of type $\Sigma_{i,j}\langle|W_{ij}|\rangle$. For exchange interactions such sums are rapidly convergent, but for dipolar interactions the convergence is no longer so rapid, and it is no longer possible to treat the double sum as N times a single sum. The contributions of the surface dipoles are, in fact, appreciable in the interior of the crystal, and the total sum will depend on the shape of the boundary.

In deriving the general formulae for the moments it was assumed that the temperature was so high that it was a good approximation to assume that $\exp\{-\langle a|W|a\rangle/\boldsymbol{k}T\}$ could be replaced by unity. In discussing terms in $1/\boldsymbol{k}T$ this approximation is no longer valid. A more accurate procedure would have been to expand $\exp\{-\langle a|W|a\rangle/\boldsymbol{k}T\}$ in powers of $1/\boldsymbol{k}T$, retaining all the terms. When this is done it is still possible to write the moments in invariant forms though they are a good deal more complicated. The expression for the area is quoted as an example.

Area

$$\Sigma_{\alpha,\beta}\exp(-E_\alpha/\boldsymbol{k}T)\left\{\mathrm{Spur}\,P_\alpha MP_\beta M-\frac{1}{\boldsymbol{k}T}\,\mathrm{Spur}\,P_\alpha WP_\alpha MP_\beta M\right.$$
$$\left.+\frac{1}{2!\,\boldsymbol{k}^2T^2}\,\mathrm{Spur}\,P_\alpha WP_\alpha WP_\alpha MP_\beta M\ldots\right\}.$$

In principle any sum of the form

$$\Sigma\exp(-E_\alpha/\boldsymbol{k}T)\,\mathrm{Spur}\,Z,$$

where Z contains P_α, P_β, W and M in any combination, can be reduced to a summation of matrix elements of the couplings between pairs of dipoles. In practice only the simplest expressions can be evaluated without prohibitive labour. A general type of sum will have the form

$$\Sigma_{i,j,\ldots}\langle|W_{ij}|\rangle\langle|W_{kl}|\rangle\langle|\ldots|\rangle.$$

If there is a suffix occurring once only, summation over that suffix will lead to a shape-dependent sum. If the suffix is repeated, summation over it will give a sum which is independent of shape. The approximation $\exp\{-\langle a|W|a\rangle/\boldsymbol{k}T\}\simeq 1$ is therefore likely to be a good approximation provided that a summation like $\Sigma_j\langle|W_{ij}|\rangle$ remains small compared with $\boldsymbol{k}T$, for this ensures that each term in the series for the moments is smaller than the preceding term, or that the series are rapidly convergent. The first term is then a good approximation to the actual value of the series.

On a classical model, a summation like $\Sigma_j W_{ij}$ measures the energy of the ith dipole in the field of all the other dipoles. This internal field varies as $1/\boldsymbol{k}T$ and is small at temperatures well above the Curie temperature. It is also shape-dependent and is usually described, for a uniformly magnetized body, in terms of a demagnetizing factor. Thus it is reasonable to assume that the formulae obtained for the moments are good approximations provided that the temperature is well above the Curie temperature. Near the Curie temperature the line shape and its displacement are likely to depend on the temperature and on the shape of the crystal.

In a first approximation the effect may be regarded macroscopically as arising from the magnetic field of the moment induced by the external field (which is proportional to $1/\boldsymbol{k}T$). The steady component (i.e. the demagnetizing field), superimposed on the external field, changes the effective steady field on a dipole. The demagnetizing field corresponding to the oscillating component depends on frequency in a resonant way, and taken with the oscillating applied field causes a shift in the resonance frequency.

§ 11. FREE SPINS

The simplest application of these formulae is to the case of dipole–dipole coupling between free spins, such as occurs in nuclear resonance experiments. It will be assumed that the system consists of a mixture of spins, some with spin S_1 and g-factors g_1 and others with spin S_2 and g-factors g_2. In the absence of any couplings, the microwave spectrum will consist of two lines at frequencies $g_1\beta H/\boldsymbol{h}$ and $g_2\beta H/\boldsymbol{h}$ where β is the Bohr magneton and H is the external magnetic field. Assuming that all the spins of the same type are equivalent, and using the forms of equations (7) and (8) appropriate to the cases in which several transitions of the same spin occur at the same frequency, the mean square width of the line at $g_1\beta H/\boldsymbol{h}$ is

$$\frac{3}{4}\frac{g_1{}^4\beta^4 S_1(S_1+1)}{\boldsymbol{h}^2}\Sigma_j\left(\frac{1-3\cos^2\theta_{1j}}{r_{1j}{}^2}\right)^2+\frac{1}{3}\frac{g_1{}^2g_2{}^2\beta^4S_2(S_2+1)}{\boldsymbol{h}^2}\Sigma_k\left(\frac{1-3\cos^2\theta_{1k}}{r_{1k}{}^3}\right)^2.$$

Here, r_{1j} is the distance between spins 1 and j, θ_{1j} is the angle between the radius vector r_{1j} and the direction of the external D.C. magnetic field, spin 1 is a typical spin of the first kind, j ranges over its similar and k over its dissimilar surrounding spins. This formula is due to Bloembergen *et al.* (1948). It then appears that, apart from the factors $g_1{}^2S_1(S_1+1)$ and $g_2{}^2S_2(S_2+1)$, similar ions give 9/4 times more contribution to the square width than do dissimilar spins, a difference due to the resonance effect.

§ 12. EXCHANGE INTERACTIONS

An interaction of particular interest is that which arises from electron exchange between ions. For the present discussion we confine ourselves to ions whose spin is $\frac{1}{2}$. The exchange energy of two ions, i and j, can then be written as:

$$W_{ij}=2J_{ij}\mathbf{S}_i\,.\,\mathbf{S}_j$$

(where J_{ij} is independent of the spins).

If all the ions are identical and this form of interaction is inserted into the appropriate form of (5) the second moment is found to be zero. This implies that exchange interactions alone give rise to no broadening effects. That this is so can also be seen from the following general argument. The exchange energy of the system

$$W_{\text{ex}}=\Sigma_{i<j}2J_{ij}S_i\,.\,S_j$$

commutes with all symmetrical functions of the ionic spin variables, and hence with the unperturbed Hamiltonian, $\mathscr{H}_0$ (the Hamiltonian of an uncoupled system). The total Hamiltonian is therefore the sum of two commuting terms and its eigenvalues are the sums of the eigenvalues of $\mathscr{H}_0$ and W_{ex}. The corresponding eigenstates are simultaneously eigenstates of $\mathscr{H}_0$ and W_{ex}. The probability of a transition being induced by a weak transverse oscillating magnetic field is determined by the matrix elements of the transverse magnetic moment. This is also a symmetric function of the spin variables and therefore commutes with W_{ex}. Thus it has no non-vanishing matrix elements connecting states of different exchange energies, or, in other words, the selection rules are $\Delta W_{\text{ex}}=0$, $\Delta\mathscr{H}_0=\pm g\beta H$, giving rise to one sharp line.

If the ions are not all identical the above discussion is no longer applicable. There are two cases of practical interest: (i) the resonance frequencies of the ions are not all the same, (ii) the ions have the same resonance frequency but are magnetically anisotropic with their principal axes not all the same. We consider these two cases in some detail using a system in which there are two types of ions. The effect of exchange in the first case is to give a broadening proportional to the 'exchange frequency', $J/\boldsymbol{h}$. Just as an isotropic ion can be regarded as precessing about the direction of the magnetic field, so an anisotropic spin precesses about an axis which, in general, is different in direction from that of the magnetic field. In the second case the two types of ions have the same precessional frequencies but are precessing about different axes. The broadening is then proportional to $J/\boldsymbol{h}$ and to $\sin^2 \frac{1}{2}\theta$, where θ is the angle between the two precessional axes.

In the first case we suppose that there are two types of ions, one type precessing with frequency ν about the z-axis and the other with frequency ν' about an axis inclined at an angle θ to Oz. The relevant matrix elements of W_{ij} are

$$\begin{aligned}\langle 1,1|W_{ij}|1,1\rangle &= \langle 2,2|W_{ij}|2,2\rangle \\ = -\langle 2,1|W_{ij}|2,1\rangle &= -\langle 1,2|W_{ij}|1,2\rangle = \tfrac{1}{2}J_{ij}\cos\theta,\end{aligned}$$

where ions i and j are of different types. Inserting these values into the appropriate form of (5), the mean square width of the line at ν is found to be

$$\overline{\Delta\nu^2} = \cos^2\theta\, \Sigma_j J_{1j}^2/\boldsymbol{h}^2,$$

where ion 1 is a typical ion of the first type and the summation is to be taken over all ions of the second type. This analysis is of course only valid if the two lines are distinct, i.e. provided that $J\cos\theta$ is sufficiently smaller than $\boldsymbol{h}|\nu-\nu'|$. When J is larger the two lines fuse and the width can be calculated by another method (Pryce 1948).

In the second case the frequencies of the two types of ions are the same and the appropriate form of (5) now contains the matrix element

$$\langle 1,2|W_{ij}|2,1\rangle = J_{ij}\cos^2 \tfrac{1}{2}\theta.$$

In this case

$$\overline{(\Delta\nu^2)} = \sin^4 \tfrac{1}{2}\theta \,.\, \Sigma_j {J_{1j}}^2/\boldsymbol{h}^2.$$

Reverting now to the case of identical ions, it has been shown by van Vleck (1948 a) and Gorter (1947) that the combined effect of dipolar and exchange interactions is to make the resonance narrower than it would have been with dipolar coupling alone. The narrowing effect of exchange interactions can now be compared with the narrowing effect in nuclear magnetic resonance in liquids arising from the rapid molecular motions. Their argument is that the second moment is unchanged by the presence of exchange but that the fourth moment is increased. This can only happen if the absorption consists of a peak which is sharpened and wings which are simultaneously extended by the exchange.

The argument can be extended to indicate that when the exchange energy is much larger than the dipolar interaction energy, the absorption is nearly all concentrated in a narrow peak, a small fraction being spread out into the wings over a frequency range of order $J/\boldsymbol{h}$.

To see this, an interaction energy

$$W = \lambda W_{\text{ex}} + \mu W_{\text{dip}},$$

is considered, where λ and μ are parameters which will eventually be put equal to unity. It is readily seen that the $2n$th moment will be a polynomial in λ and μ of the form

$$\boldsymbol{h}^{2n}\overline{(\Delta\nu)^{2n}} = A\lambda^{2n-2}\mu^2 + B\lambda^{2n-3}\mu^3 + \ldots + C\mu^{2n},$$

where A, B, C etc. depend on n and on the coefficients in the exchange and dipolar energies. The term in λ^{2n} is absent, for if $\mu = 0$ it is known that $\overline{(\Delta\nu)^{2n}} = 0$ (exchange only). The term in $\lambda^{2n-1}\mu$ is absent because the polynomial must be non-negative for all values of λ and μ. If the exchange effects predominate over the magnetic, the polynomial is dominated by the term in $\lambda^{2n-2}\mu^2$, whose coefficient will contain a factor $J^{2n-2}\beta^2 H_1^2$, where J, β, and H_1 are typical values of the exchange interaction, magnetic moment, and internal magnetic field. Setting λ and μ equal to unity gives

$$\boldsymbol{h}^{2n}\overline{(\Delta\nu)^{2n}} \simeq a_n J^{2n-2}\beta^2 H_1^2,$$

where a_n is some numerical factor of order of magnitude near unity. This is consistent with a resonance in which nearly all the intensity is in the central peak, which does not contribute appreciably to moments above the second, together with an intensity of order $\beta^2 H_1^2/J^2$ spread over a range of frequency of order $J/\boldsymbol{h}$.

This argument throws no light on the width of the central peak.

§ 13. ORIENTATION OF THE OSCILLATING MAGNETIC FIELD

When there are no coincident frequencies it is readily seen that the transition probabilities $|\langle 1|m|2\rangle|^2$ drop out of the mean square width; the mean square width does not then depend on the orientation of the oscillating magnetic field. If, however, there are coincident transition frequencies, they do not drop out, and further they occur as actual matrix elements rather than as square moduli of matrix elements. Although the oscillating magnetic field may be at right angles to the steady magnetic field, so that the transition probabilities are the same for all positions of the oscillating field, the actual matrix elements will change as the direction of the oscillating field is changed in the plane perpendicular to the steady field. This means that the mean square width will depend on the orientation of the oscillating field.

§ 14. CONCLUSION

The purpose of this paper has been to give the principles and general results of the method rather than apply it to specific cases. There are a number of cases for which the widths have been measured experimentally and the comparison of the theoretical predictions with the experimental widths will be given later.

The subject of this paper has recently also been treated in an important paper by Van Vleck (1948 b), which covers much the same ground. Our method of approximation differs in detail from Van Vleck's, and in some directions our results are more general than his, while conversely, in other directions, notably the explicit calculation of the fourth moment, his results are more complete than ours.

REFERENCES

BAGGULEY, D. M. S., and GRIFFITHS, J. H. E., 1947, *Nature, Lond.*, **160**, 532.

BAGGULEY, D. M. S., BLEANEY, B., GRIFFITHS, J. H. E., PENROSE, R. P., and PLUMPTON, B. I., 1948, *Proc. Phys. Soc.*, **61**, 542.

BLOEMBERGEN, N., PURCELL, E. M., and POUND, R. V., 1948, *Phys. Rev.*, **73**, 679.

GORTER, C. J., 1947, *Phys. Rev.*, **72**, 1128.

PRYCE, M. H. L., 1948, *Nature, Lond.*, **62**, 538.

VAN VLECK, J. H., 1932, *Theory of Electric and Magnetic Susceptibilities* (Oxford : University Press) ; 1948 a, *Phys. Rev.*, **73**, 1229; 1948 b, *Ibid.*, **74**, 1168.

On the Capture of Particles into Synchrotron Orbits

By T. R. KAISER
Clarendon Laboratory, Oxford

Communicated by Lord Cherwell ; MS. received 11*th July* 1949

ABSTRACT. A theory is developed for the capture of particles into synchrotron orbits when the radio-frequency accelerating voltage rises from zero to its maximum value in a finite time. It is shown that if this time of rise is sufficiently long, all particles originally occupying a band of width $1/\sqrt{2}$ times the maximum width of the final stable region for synchrotron phase oscillations will be captured, irrespective of the initial phase at which they enter the accelerating gap. This conclusion would seem to be in agreement with the observed characteristics of existing electron synchrotrons.

---

§ 1. INTRODUCTION

PARTICLE acceleration employing radio-frequency accelerating voltages combined with a magnetic field to define circular orbits was first achieved in the form of the cyclotron. In recent years the principle has been extended to the acceleration of electrons (electron synchrotron) and of heavy particles to higher energies (synchrocyclotron and proton synchrotron).

Because of relativistic effects it is in general necessary to vary two of the parameters H, r and ω (magnetic field, orbit radius, and angular radio frequency) during the course of the acceleration. In the synchrocyclotron, r and ω are varied, except in the case of non-relativistic particles (cyclotron), when ω may be kept constant, while in the synchrotron, H and ω are varied, the exception this time being for extreme relativistic particles (electron synchrotron), when only H need vary. The particular advantage of the synchrotron is that with the constant equilibrium orbit radius the magnetic field need only be established in a restricted region about this orbit, resulting in a considerable saving for high energy accelerators.

In the electron synchrotrons operating at the present time it has been convenient to inject the particles at velocities considerably less than the velocity of light, and to accelerate them to extreme relativistic energies (of the order of 2 MEV.) by a betatron mechanism. As this betatron action slowly diminishes (by magnetic saturation) the betatron orbit contracts, and when its radius matches the synchrotron equilibrium radius, the R.F. accelerating voltage is applied to a resonator surrounding the orbit. As the betatron action further diminishes, the deficit is made up by the R.F. voltage.

Not all of the particles initially present can in general be captured into stable synchrotron orbits, and this paper discusses the effect on the capture efficiency of the time of rise of the accelerating voltage, a lower limit to which is in practice set by the selectivity of the resonator.

In general it is found that if this time of rise is above a certain limit, considerably more particles may be captured than would otherwise be the case, which in fact would account for the capture efficiencies approaching 100% observed in all existing electron synchrotrons. This is of greatest importance for schemes involving repeated capture, i.e. handing over of the particles from one resonator or R.F. harmonic to another, as is necessary, for instance, in the accelerator proposed by Kaiser and Tuck (1948).

In the case of the proton synchrotron, the critical point is likely to be in the initial stages of acceptance and acceleration. Some relief from these critical conditions seems to be possible by selecting the time of injection and the rate of rise of the R.F. voltage.

§2. THEORY OF PARTICLE CAPTURE

The theory of particle stability and bunching in the synchrotron has been developed by several authors (Bohm and Foldy 1946, Frank 1946, Dennison and Berlin 1946). The most useful treatment, giving a clear physical picture of the process, is probably that of Bohm and Foldy, who consider a particle of charge $\mathbf{e}$ moving with a velocity β times the velocity of light in the r, θ plane of a cylindrical polar coordinate system. In this plane the magnetic field has only a z component defined as a function of r by

$$n = -\frac{\partial(\ln H)}{\partial(\ln r)}. \qquad \ldots\ldots(1)$$

The phase at which the particle enters the accelerating gap (relative to the R.F. phase) is

$$\phi = \theta - \int_0^t \omega_s\, dt, \qquad \ldots\ldots(2)$$

while a particle which always travels on the equilibrium orbit must enter at the equilibrium phase given by

$$\sin\phi_s = v/V, \qquad \ldots\ldots(3)$$

where ω_s is the angular velocity of the equilibrium particle (and the angular frequency of the R.F.), V is the peak R.F. accelerating voltage, and v is that part of the total accelerating voltage per turn required to maintain a particle on the equilibrium orbit not supplied by betatron induction.

For a particle to be successfully accelerated its phase must execute damped oscillations about ϕ_s, and the equation defining these oscillations is

$$\frac{d}{dt}\left(\frac{2\pi E_s}{\mathbf{e}\omega_s^2 K}\right) + V\sin\phi = V\sin\phi_s, \qquad \ldots\ldots(4)$$

where E is the total energy of the particle (including the rest energy) and

$$K = 1 + \frac{n}{\beta_s^2(1-n)},$$

the subscript, s, everywhere referring to the equilibrium values of the quantities.

Equation (4) is analogous to that defining the equation of motion of a pendulum of moment of inertia $I = 2\pi E_s/\mathbf{e}\omega_s^2 K$, restoring torque $V\sin\phi$, and constant bias torque $v = V\sin\phi_s$. Since E_s will in general remain substantially constant over a period of the phase oscillation, we can, for the quasi-static case, rewrite (4) as

$$\ddot{\phi} + kV\sin\phi = kV\sin\phi_s \qquad \ldots\ldots(5)$$

with $k = \mathbf{e}\omega_s^2 K/2\pi E_s$, which, on integration, gives

$$\dot{\phi}^2/2kV = \cos\phi - \cos\phi_m + (\phi - \phi_m)\sin\phi_s, \qquad \ldots\ldots(6)$$

where ϕ_m is the maximum phase reached during the oscillation.

Associated with the phase oscillation is a radial oscillation defined by (6) and

$$\frac{\epsilon}{r_s} = \frac{\dot{\phi}}{\beta_s^2(1-n)K\omega_s}, \qquad \ldots\ldots(7)$$

where $\epsilon = r - r_s$.

We can rewrite (5) as

$$\frac{\ddot{\phi}}{kV} = -\frac{\partial U(\phi)}{\partial \phi}, \qquad \ldots\ldots(8)$$

where $U(\phi)$ is the potential function defined by

$$U(\phi) = -(\cos\phi + \phi\sin\phi_s), \qquad \ldots\ldots(9)$$

and is plotted for various values of ϕ_s in Figure 1. The maxima in these curves occur at $\phi = \pi - \phi_s$ and the minima at $\phi = \phi_s$.

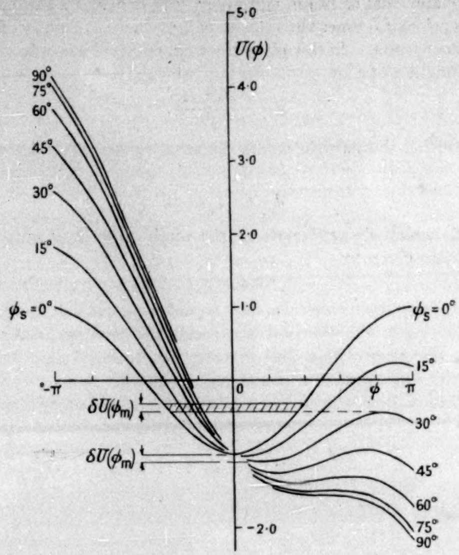

Figure 1. The potential function, $U(\phi)$, for various values of ϕ_s.

The limiting condition for stable oscillation is found by putting $\phi_m = \pi - \phi_s$ in (6), and we find that stable orbits only occur for ϕ and $\dot{\phi}$ within the region of phase space enclosed by

$$\dot{\phi} = \pm\{2kV[(\cos\phi + \cos\phi_s) - (\pi - \phi - \phi_s)\sin\phi_s]\}^{\frac{1}{2}}, \qquad \ldots\ldots(10)$$

which equation actually defines the shape of the bunch of particles, taking ϕ as azimuth relative to the bunch centre.

The limits of the stable region defined by (10) are plotted in Figure 2 for various values of ϕ_s, while Figure 3 gives an idea of the motion of the particles in phase space for both zero and non-zero values of ϕ_s.

The maximum half-width of the stable region is found by putting $\phi = \phi_s$ in (10), giving

$$\dot{\phi}_M = (4kV\Phi)^{\frac{1}{2}}, \qquad \ldots\ldots(11)$$

where $\Phi = \cos\phi_s - [(\pi/2) - \phi_s] \sin\phi_s$, and $\dot{\phi}_M$ is the maximum possible phase velocity within the stable region. Figure 4 gives $\Phi^{\frac{1}{2}}$ as a function of V/v.

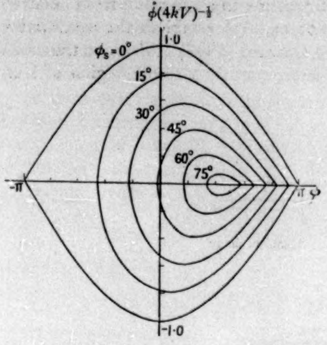

Figure 2. Envelopes of the region within which stable phase oscillations are possible for various values of ϕ_s.

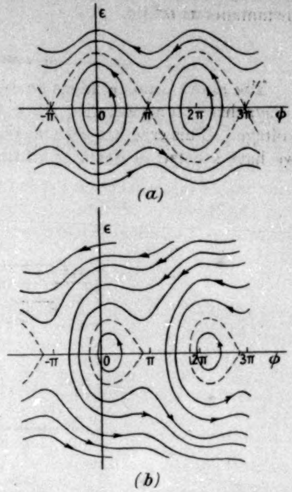

Figure 3. Particle trajectories in phase space for (*a*) $\phi_s = 0°$, (*b*) $\phi_s = 30°$. The dotted curves give the boundaries of the stable regions.

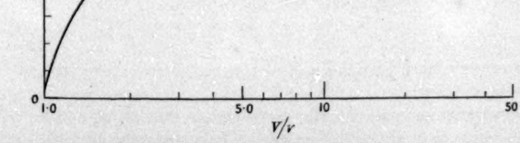

Figure 4. $\Phi^{\frac{1}{2}} = \dot{\phi}_M/(4kV)^{\frac{1}{2}}$ as a function of V/v.

As well as the radial oscillations associated with the phase oscillations there are also rapid free oscillations (betatron oscillations) which, however, have been neglected in arriving at equation (4), since the coupling between the two motions is in general negligible. Because of this, in the whole of the following the free oscillations will be neglected and the particles will be considered to be travelling on their instantaneous orbits, even when pure betaton acceleration is considered; thus, by the width of the betatron beam will be meant the spread of betatron instantaneous orbits.

(i) *Instantaneous Capture*

The above considerations enable us to determine the transition from betatron to synchrotron acceleration when we instantaneously* establish the accelerating voltage. This case has been worked out by Goward (1947). Prior to transition we have a betatron beam of width ϵ_0 and subsequently a stable region of half-width ϵ_M, and only those particles will be trapped which at the instant of transition lie within this stable region. At this instant the betatron acceleration will generally be almost adequate to maintain the acceleration, so that ϕ_s can be taken as zero and the process is as depicted in Figure 5. It is clear that for efficient capture we need $\epsilon_M \gg \epsilon_0$, while for $\epsilon_M \gtrsim \epsilon_0$ we only get about 60% capture. Subsequent to transition the particles will oscillate about the equilibrium radius with radial

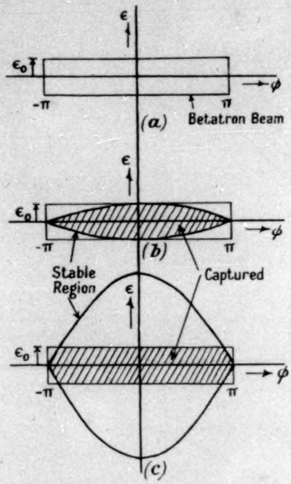

Figure 5. Illustrates particle capture with an instantaneously established R.F. voltage, for the ideal case $\phi_S=0°$.

(*a*) Betatron beam of half-width ϵ_0.

(*b*) $\epsilon_M=\epsilon_0$, 64% capture efficiency.

(*c*) $\epsilon_M=5\epsilon_0$, 94% capture efficiency.

---

* Actually equation (4) is derived by making a Fourier decomposition of the accelerating gap voltage into a series of travelling waves and selecting the component in step with the particle motion, which is the only effective term over a few revolutions. This, however, represents an averaging process, so that the term 'instantaneous' implies 'in the shortest time for which (4) will be valid'—in fact, in the time of a few revolutions.

amplitudes from zero to ϵ_M, and as the betatron flux saturates further, ϕ_s increases and the stable region contracts, both in azimuth and in radial width, causing a fraction of the particles to be lost. For an increase in ϕ_s of from zero to 30° the fraction lost may amount to 40%.

(ii) *Finite Time of Rise of the R.F. Voltage*

An examination of the parameters of a number of existing electron synchrotrons shows that in no case does the R.F. voltage rise instantaneously in the sense indicated above, and that in a conventional machine it may be difficult to satisfy this condition.

In the following, an attempt is made to solve the phase equation (5) for the case in which V rises from zero to a value V_1 in a time t_1. While a general solution would seem impossible, we can obtain an approximate solution, subject to restrictions to be placed on t_1, as follows:

From (5) we have

$$\frac{d\dot{\phi}^2}{d\phi}+2kV\sin\phi=2kv, \qquad \ldots\ldots(12)$$

and integrating,

$$\dot{\phi}^2=\dot{\phi}_0{}^2+2kV\cos\phi+2kv(\phi-\phi_0)-\int_{\phi_0}^{\phi}\frac{2k\dot{V}\cos\phi}{\dot{\phi}}\,d\phi, \qquad \ldots\ldots(13)$$

where at time $t=0$, $\phi=\phi_0$, $\dot{\phi}=\dot{\phi}_0$, $V=0$.

The problem now is to determine the range of values of ϕ_0 and $\dot{\phi}_0$ which a particle may have in order that it may be captured by the time $t=t_1$. Capture actually occurs when $\dot{\phi}$ becomes bounded, i.e. the motion becomes oscillatory. Inspection of (13) shows that it consists of a term $\dot{\phi}_0{}^2+2kv(\phi-\phi_0)$, which is a linear function of ϕ plus an oscillating function of ϕ consisting of two terms, the predominant one being $2kV\cos\phi$ if $\dot{V}$ is sufficiently small, with amplitude increasing with time. Thus $\dot{\phi}^2$ has a series of minima, and capture may be said to occur at that minimum when $\dot{\phi}^2$ just becomes zero, since after this it will be bounded and ϕ will oscillate about ϕ_s.

From (12) these minima occur at values of ϕ given by

$$\left.\begin{aligned}\sin\phi&=\sin\phi_s\\ \cos\phi&=\cos\phi_s\end{aligned}\right\} \qquad \ldots\ldots(14)$$

or

$$\phi=(2q+1)\pi-\phi_s, \qquad \ldots\ldots(15)$$

where

$$q=0,\ \pm1,\ \pm2,\ \pm3,\ \ldots.$$

Substitution of (15) (with the appropriate value of q), plus the simultaneous condition $\dot{\phi}^2=0$, into (13) then gives the final result that a particle with initial coordinates ϕ_0 and $\dot{\phi}_0$ will be trapped when the voltage V satisfies

$$0=\dot{\phi}_0{}^2-2kV\cos\phi_s+2kv\,[(2q+1)\pi-\phi_s-\phi_0]-R, \qquad \ldots\ldots(16)$$

where

$$R=\int_{\phi}^{(2q+1)\pi-\phi_s}\frac{2k\dot{V}\cos\phi}{\dot{\phi}}\,d\phi.$$

It may seem that for particles which are not trapped the above conditions are satisfied at the point where they cross the equilibrium orbit and ϕ changes sign (see Figure 3). In such cases, however, $d\dot{\phi}^2/d\phi$ is non-zero and hence (14) is not satisfied.

Equation (15) is not satisfactory since we do not know the appropriate value of q (i.e. the number of phase revolutions prior to capture); however, one thing that is clear is that by making $\dot{V}$ sufficiently small (i.e. t_1 sufficiently long), R can be made negligible compared with the term $2kV\cos\phi_s$. In what follows, then, R will be treated as negligible and later an estimate will be made of its magnitude for various initial conditions, and the restrictions to be placed on t_1 determined.

Returning to (13) and writing $\phi_\nu = (2\nu + \frac{1}{2})\pi$ (ν integral, positive or negative), we get, neglecting the integral term,

$$\dot{\phi}_\nu^2 = \dot{\phi}_0^2 + 2kv(\phi_\nu - \phi_0),$$

and thus

$$\dot{\phi}^2 = \dot{\phi}_\nu^2 + 2kV\cos\phi + 2kv(\phi - \phi_\nu), \qquad \ldots\ldots(17)$$

which with (15) and $\dot{\phi}_0^2 = 0$ gives the trapping condition

$$0 = \dot{\phi}_q^2 - 2kV\cos\phi_s + 2kv\left(\frac{\pi}{2} - \phi_s\right).$$

For final conditions $V = V_1$, $\phi_s = \phi_{s1}$, all particles will be trapped which lie within the limits of $\dot{\phi}_q$ defined by

$$\dot{\phi}_q^2 = 2kV_1\cos\phi_{s1} - 2kv\left(\frac{\pi}{2} - \phi_{s1}\right) = 2kV_1\Phi_1. \qquad \ldots\ldots(18)$$

Now $\dot{\phi}_q^2$ is obtained by putting $\phi = \phi_q$ in

$$\dot{\phi}^2 = \dot{\phi}_0^2 + 2kv(\phi - \phi_0),$$

corresponding to $\ddot{\phi} = kv$, i.e. $\dot{\phi} = \dot{\phi}_0 + kvt$, and since the time corresponding to $\phi = \phi_q$ is approximately t_1 (for $\dot{V}$ sufficiently small) we can write

$$\dot{\phi}_q \simeq \dot{\phi}_0 + kvt_1.$$

Thus all those particles will be trapped which have $\dot{\phi}_0$ within the range

$$\dot{\phi}_0 = -kvt_1 \pm (2kV_1\Phi_1)^{\frac{1}{2}}. \qquad \ldots\ldots(19)$$

The important point of this result is that it does not contain ϕ_0. Further, by comparison with (11), the range of radii corresponding to this range of $\dot{\phi}_0$ is just $1/\sqrt{2}$ times the width of the final stable region, and all particles within this range will be trapped, irrespective of the initial phases at which they enter the resonator gap. This means that for 100% capture the resonator voltage only needs to be sufficient to make

$$\epsilon_M = \sqrt{2}\epsilon_0 \qquad \ldots\ldots(20)$$

instead of $\epsilon_M \gg \epsilon_0$ for instantaneous capture.

The term $-kvt_1$ in (19) represents the average orbit contraction during the time t_1 of establishing the R.F. voltage. This will set an upper limit (which will be trivial for most electron synchrotrons) to the time of rise, since this amount of contraction must be possible within the orbit space.

We can now determine the equation of motion, immediately subsequent to capture of a particle whose initial phase velocity satisfies (19). At the instant of capture we have

$$\dot{\phi}_q^{\,2} = 2kV_1\left[\cos\phi_{s1} - \left(\frac{\pi}{2} - \phi_{s1}\right)\sin\phi_{s1}\right],$$

$$\dot{\phi}^2 = \dot{\phi}_q^{\,2} + 2kV\cos\phi + 2kv(\phi - \phi_q).$$

Substituting for $\dot{\phi}_q^{\,2}$ and putting $\phi' = \phi - 2q\pi$, we get

$$\dot{\phi}^2 = 2kV_1[\cos\phi_{s1} + \cos\phi' - (\pi - \phi_{s1} - \phi')\sin\phi_{s1}], \qquad \ldots\ldots(21)$$

which reveals by comparison with (10) that such particles, as we would expect, oscillate with the maximum stable amplitude, i.e. on the perimeter of the stable region defined by (10).

An estimation of the conditions under which the integral term R (equation (16)) may be neglected, and thus (19) is valid, is given in the Appendix. The most important result is that if $V_1/v \gg 1$, R is negligible when

$$t_1(2kV_1)^{\frac{1}{2}} \gg \tfrac{1}{2}, \qquad \ldots\ldots(22)$$

and further, that if

$$2V_1/v \gg t_1(2kV_1)^{\frac{1}{2}} \gg \tfrac{1}{2} \qquad \ldots\ldots(23)$$

both R and kvt_1 are negligible and (19) becomes

$$\dot{\phi}_0 = \pm(2kV_1)^{\frac{1}{2}}. \qquad \ldots\ldots(24)$$

Equations (23) and (24) are equivalent to the statement that if the time of rise of the resonator voltage is long compared with $1/4\pi$ times the period of phase revolution of the extreme particles prior to capture, and yet sufficiently short that the orbit contraction during this time may be neglected, then all particles with initial phase velocity within the limits of (24) will be captured, irrespective of their initial phases.

Equation (22) will be the condition for most electron accelerators, since at the time of transition v in general will be small and $V_1/v \gg 1$. If this is not so (as may be the case for accelerators in which initial betatron acceleration is not employed) the appropriate condition may be found from the treatment in the Appendix.

(iii) *Suppression of the Resonator Voltage*

In a similar fashion to the above, we can show that if the R.F. voltage falls from V_1 to zero in a time t_1 satisfying (22) (or the appropriate criterion given in the Appendix if $V_1/v \not\gg 1$) the particles will be spread into a beam, uniformly distributed in phase, of width $1/\sqrt{2}$ times the width of the stable region prior to suppression.

On the other hand, if the R.F. were instantaneously suppressed, the particle bunch would retain its shape immediately subsequent to the suppression, but would then rapidly become uniform in phase, its width being equal to that of the stable region prior to suppression.

(iv) *Saturation of the Betatron Flux and Damping*

Subsequent to capture of the particles into stable orbits there are two major effects. The first is the contraction of the stable region due to the magnetic saturation and the second is the phase oscillation damping as the magnetic field (and particle energy) increases.

The phase oscillation damping for the case $\phi_s \simeq 0$ is given by

$$B^{\frac{1}{2}}(\phi_m/2)\sin(\phi_m/2) \propto \left[\frac{\omega_s{}^2 K}{E_s V}\right]^{\frac{1}{4}}, \qquad \ldots\ldots(25)$$

where B is the complete elliptic integral defined by

$$B(\phi_m/2) = \int_0^{\pi/2} \frac{\cos^2 u\,du}{\{1-\sin^2(\phi_m/2)\sin^2 u\}^{\frac{1}{2}}}.$$

Equation (25), together with

$$\dot{\phi}_m/\dot{\phi}_M = \epsilon_m/\epsilon_M = \sin(\phi_m/2), \qquad \ldots\ldots(26)$$

defines the damping of the associated radial oscillations relative to the stable region (where ϵ_m is the radial amplitude and ϵ_M is the maximum half-width of the stable region).

For small oscillations $B \simeq \pi/4 = \text{constant}$, and we get

$$\phi_m \propto \left[\frac{\omega_s{}^2 K}{E_s V}\right]^{\frac{1}{4}} \qquad \ldots\ldots(27)$$

and

$$\epsilon_m/\epsilon_M \propto \left[\frac{\omega_s{}^2 K}{E_s V}\right]^{\frac{1}{4}}. \qquad \ldots\ldots(28)$$

The damping corresponding to increasing particle energy is plotted in Figure 6, in which the energy has been normalized to unity at $\epsilon_m/\epsilon_M = 1$. The broken line corresponds to $\epsilon_m/\epsilon_M \propto E_s^{-\frac{1}{4}}$, and inspection shows that the damping for large amplitudes is less than this, the difference for many purposes not being appreciable.

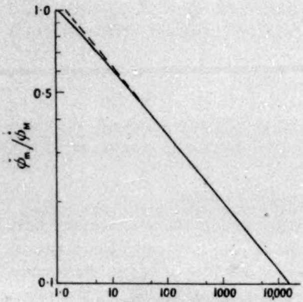

Figure 6. Phase oscillation damping with increasing particle energy, E_s. The dotted line corresponds to damping as $E_s^{-\frac{1}{4}}$.

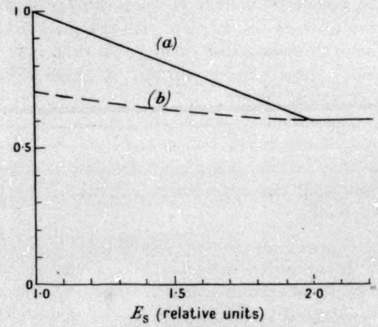

Figure 7. Illustrates the effect of betatron saturation assuming v/V to increase linearly from 0 to 2, while E_s increases from 1 to 2 (relative units). The curve (a) gives $\Phi^{\frac{1}{2}} = \dot{\phi}_M/(4kV)^{\frac{1}{2}}$, which corresponds to the limit of the stable region, while the dotted curve (b) gives $\dot{\phi}_m/(4kV)^{\frac{1}{2}}$, corresponding to the amplitude of oscillation of the particle which is just retained during the process.

The saturation of the betatron flux in general takes place slowly, thus v (and ϕ_s) will increase from zero to some maximum value causing a contraction of the stable region (see Figure 2). The purpose of this section is to determine the area of the initial stable region from which particles may be lost, and it is shown that if V_1 is made somewhat larger than needed, just to trap all of the particles, this area will contain no particles, and thus there will be no loss (ignoring possible space charge effects).

Since ϕ_s will generally be negligible at the time of transition, we really wish to know the effect of slowly increasing ϕ_s from zero to a maximum value ϕ_{sp}. Consider for instance the case for which ϕ_s has initial and final values 0° and 30° respectively, which is probably about as large a change as would be experienced in a conventional electron synchrotron. An examination of the potential curves of Figure 1 shows that the particle which is just lost during such a change is one which initially corresponded to a value of $U(\phi_m)$ within the shaded area. It is clear that we will not be seriously in error in taking the upper limit as representing the initial level for this particle, i.e. in assuming that

$$U(\phi_m) - U(\phi_s) = \dot{\phi}_m{}^2/2kV$$

remains unchanged during the change of shape of the potential well (which is in fact the case for small oscillations).

Taking into account the phase damping during the period of magnetic saturation, which we will assume to be of the order of $E_s^{-\frac{1}{4}}$ (even though large angle oscillations are involved), we see that $[\dot{\phi}_m/(2kV)]E_s^{-\frac{1}{4}}$ remains constant during the change in ϕ_s. If ϕ_s reaches a maximum value ϕ_{sp}, all particles with peak phase velocities greater than

$$\dot{\phi}_m = \left(\frac{E_{sp}}{E_s}\right)^{\frac{1}{4}} (4kV\Phi_p)^{\frac{1}{2}} \qquad \ldots\ldots(29)$$

will be lost, where the subscript p refers to the value when $\phi_s = \phi_{sp}$, all other quantities being evaluated at transition.

Translating phase velocity into radius, (29) becomes

$$\epsilon_m = \Phi_p{}^{\frac{1}{2}} \left(\frac{E_{sp}}{E_s}\right)^{\frac{1}{4}} \epsilon_M \qquad \ldots\ldots(30)$$

(remembering, of course, that $\epsilon_m \not> \epsilon_M$).

The process is illustrated in Figure 7, which depicts the case where v/V increases linearly from 0 to 2, while in the same period the particle energy is doubled.

Let us now consider the case of a betatron beam of half-width ϵ_0 which is captured by a slowly rising resonator voltage V. The extreme particles of phase velocity $\dot{\phi}_0$ will be captured when $V = V_0$, where $\dot{\phi}_0 = (2kV_0)^{\frac{1}{2}}$. As V increases to its final value V_1, the phase oscillations will be damped approximately as $V^{-\frac{1}{4}}$, and at the same time $\dot{\phi}_M$ will increase as $V^{\frac{1}{2}}$, so that $\dot{\phi}_m$ (and ϵ_m) will increase as $V^{\frac{1}{4}}$. Thus in order that the extreme particles are not lost during the period of saturation we must have

$$\Phi_p{}^2 V_1/V_0 = E_s/E_{sp}. \qquad \ldots\ldots(31)$$

The relation between the width of the betatron beam and the width of the stable region immediately subsequent to transition, in order that all of the electrons be retained, is now

$$\epsilon_0 = \left(\frac{E_{sp}}{2E_s}\right)^{\frac{1}{2}} \Phi_p \epsilon_{M1} \qquad \ldots\ldots(32)$$

(where $\epsilon_M = \epsilon_{M1}$ when $V = V_1$), which replaces the condition (20) in cases in which there is a significant change in ϕ_s subsequent to transition. We must again remember that ϵ_0 cannot be greater than $\epsilon_{M1}/\sqrt{2}$, i.e. if $(E_{sp}/E_s)^{\frac{1}{2}}\Phi_p > 1$, the appropriate relation, is (20).

The above result can only be regarded as approximate because of the assumption that the damping is always the same as for small angle oscillations, but its significance is in showing that if the resonator voltage rises slowly to a value somewhat greater than is needed just to capture the betatron beam at the time of transition, there will be no subsequent loss of particles during the magnetic saturation.

The condition that the theory of capture be valid is, of course,

$$t_0(2kV_0)^{\frac{1}{2}} \gg \tfrac{1}{2}, \qquad \ldots\ldots(33)$$

where $t = t_0$ when $V = V_0$, which is equivalent to

$$t_1(2kV_1)^{\frac{1}{2}} \gg \tfrac{1}{2}(V_1/V_0)^{\frac{3}{4}}. \qquad \ldots\ldots(34)$$

§ 3. APPLICATION TO ACTUAL ACCELERATORS

An analysis of a number of existing electron synchrotrons has shown that in all cases the time of rise of resonator voltage satisfies (33), which is in general agreement with the fact that the capture efficiency in all cases approaches 100%.

(i) 70 Mev. *Synchrotron*

An excellent example is the 70 Mev. machine described by Elder *et al.* (1947), who state that increasing V_1 beyond $2v_p$ does not appreciably increase the x-ray output.

The parameters of interest are: $v_p = 170$ volts and thus $V_1 = 340$ volts, $\omega_s/2\pi = 163$ Mc/s., $n = 0{\cdot}75$, and at transition $E_s = 2{\cdot}5$ Mev., giving $(2kV_1)^{\frac{1}{2}} = 2\times 10^7\ \mathrm{sec}^{-1}$. The value of V/v at transition is not given; however, the half-width of the curve of output against time of switching on the R.F. is of the order of 50 μsec., and assuming that this is the order of the time of the orbit radius, in the absence of the accelerating voltage, to contract by an amount equal to the width of the betatron beam, we get $V_1/v \sim 200$ at transition, and thus ϕ_s at this instant may be taken as zero.

The ratio E_{sp}/E_s is not given, but as a rough estimate we shall put it equal to 2, and we should not be greatly in error in calculating ϵ_0 since this ratio only appears in equation (32) to the power one-half.

Putting $V_s/v_p = 2$ and $E_{sp}/E_s = 2$ in (31) we get $V_1/V_0 = 4$. For the capture theory to be valid we need, using (34), $t_1 \gg 0{\cdot}2\ \mu$sec., which should be satisfied by $t_1 \sim 2\ \mu$sec. or longer. In fact, the above authors quote 100% capture for t_1 between 2 and 20 μsec., while for an instantaneously established R.F. voltage we would expect an overall transition efficiency of the order of 50%.

From (7), (11) and (32) we find that the half-width of the betatron beam prior to transition is $\epsilon_0 \simeq 0{\cdot}2$ cm. Since the spread of instantaneous orbits during the betatron acceleration decreases approximately as H^{-1} (i.e. as βE_s^{-1}) (Kerst and Serber 1941), the above figure corresponds to a spread of orbits at injection (injection voltage of 40 kv.) of the order of 4 cm. It is interesting to compare this figure with the width of orbit tube, namely 9 cm., indicating that the spread of orbits is of the order of one-half this width, a result which might be expected in the absence of effects of space charge, azimuthal field irregularities, etc.

In conventional electron synchrotons, irrespective of the final energy, there is not a great deal of variation in the betatron injection voltage, transition energy, and the ratio of orbit tube width to orbit radius, the main variables being the orbit radius and the peak voltage per turn needed to maintain the acceleration, v_p.

Taking the 70 MeV. machine to be typical, (33) may be reduced to

$$\omega_s t_0 \gg 60. \qquad \ldots\ldots(35)$$

This means that the condition for the capture theory to be valid is that the R.F. voltage rises to V_0 in a time which is long compared with ten times the R.F. period, a condition which will in general be satisfied in electron accelerators simply because of the high selectivity of the resonator, quite apart from limitations set by the associated electronic equipment.

(ii) *Heavy Particle Accelerators*

The capture theory is directly applicable to the heavy particle synchrotron, especially if initial betatron acceleration is contemplated in order to reduce the range of frequency modulation and to take advantage of the damping and contraction of the instantaneous orbits during the betatron phase. In this case a suitable choice of the R.F. voltage and its time of rise will give 100% capture and can compensate for the phase antidamping with increasing ω_s in much the same fashion as the compensation for betatron flux saturation in the electron synchrotron.

If injection is to take place directly, without the initial betatron phase, using an injector placed outside the equilibrium orbit, the situation is more complicated. The oscillation amplitude subsequent to injection is the sum of the free and synchrotron amplitudes, and since the damping of these free oscillations in one phase oscillation period will be small, an appreciable phase acceptance angle can only be achieved by first injecting the particles and then establishing the R.F. voltage, otherwise only particles injected near the equilibrium phase will be able to clear the gun structure. We could, for instance, inject until the orbit of the particle executing no free oscillations contracts to the equilibrium orbit, when the spread of instantaneous orbits will be a small fraction of the width of the orbit tube (due to the relatively small betatron induction), and the free oscillation amplitudes will extend from zero up to amplitudes just clearing the injector. If we then instantaneously establish the R.F. voltage (which, in contrast to electron accelerators, is easy to accomplish) the fraction of the particles accepted depends on the maximum phase acceptance angle and the radial width of the stable region. Depending on the machine parameters, there will be an optimum accelerating voltage corresponding to a stable region somewhat narrower than the available orbit space. For the Birmingham synchrotron the optimum acceptance fraction seems to be about one-third.

On the other hand, with a slowly rising R.F. voltage we can accept particles of any initial phase and yet have a final stable region which is narrower than would otherwise be necessary, thus accepting particles with relatively greater free oscillation amplitudes than in the previous case. The drawback here is that since V_1/v will be fairly small at the time of capture, the average orbit contraction during the time of rise may need to be a substantial fraction of the width of the orbit space. We may thus need to displace the equilibrium orbit towards the inner wall of the orbit tube and establish the radio frequency when the displacement of the

instantaneous orbits from the equilibrium orbit equals this desired orbit contraction. The gain in injection efficiency may not be great, but in this case the particle oscillations may have a considerable clearance from the injector, allowing a relaxing of the tolerance on the radio frequency immediately subsequent to injection.

The capture theory is also applicable if we desire to change R.F. sources during the acceleration (e.g. from a varying to a fixed frequency source for extraction purposes). By slowly suppressing one source and switching on the other in the same fashion at a frequency corresponding to a suitable reduced equilibrium radius, the difficult phasing problem disappears, leaving the relatively simple matter of starting off the two events at the right moment.

APPENDIX

Circumstances under which the Integral R (Equation (16)) may be neglected

First let us consider the simple case when v is sufficiently small that $V_1/v \gg 1$ and at the same time the average orbit contraction during the time t_1 is negligible, i.e. from (19):

$$kvt_1 \ll (2kV_1)^{\frac{1}{2}}$$

or

$$t_1(2kV_1)^{\frac{1}{2}} \ll 2V_1/v. \qquad \ldots\ldots(36)$$

Equations (17) and (19) now become

$$\dot{\phi}^2 = \dot{\phi}_r{}^2 + 2kV\cos\phi, \qquad \ldots\ldots(37)$$

$$\dot{\phi}_0 = \pm(2kV_1)^{\frac{1}{2}}, \qquad \ldots\ldots(38)$$

the fractional error in (38) being approximately $R/4kV_1$.

Substituting (37) in the expression for R we get

$$R \simeq 2k\dot{V}\left[\int_{\phi_0}^{\pi} \frac{\cos\phi}{\dot{\phi}_0}\,d\phi + \sum_{r=1}^{q}\int_{-\pi}^{\pi} \frac{\cos\theta\,d\theta}{(\dot{\phi}_r{}^2 + 2kV_r\cos\theta)^{\frac{1}{2}}}\right],$$

where $\theta = \phi - \phi_r + \pi/2$.

Assuming V to be constant at V_r over the periods 2π of θ, all of the elliptic integrals comprising the series drop out and we are left with

$$R \simeq -\frac{2k\dot{V}}{\dot{\phi}_0}\sin\phi_0. \qquad \ldots\ldots(39)$$

Putting $\dot{\phi}_0 \simeq (2kV_1)^{\frac{1}{2}}$, the condition for (38) to be valid becomes

$$t_1(2kV_1)^{\frac{1}{2}} \gg \tfrac{1}{2}. \qquad \ldots\ldots(40)$$

Combining (36) and (40) we have

$$2V_1/v \gg t_1(2kV_1)^{\frac{1}{2}} \gg \tfrac{1}{2}, \qquad \ldots\ldots(41)$$

which is equation (23) of the text.

From (39) we can actually make a second approximation to the limits of $\dot{\phi}_0$ within which particles are trapped, which become, instead of (38),

$$\dot{\phi}_0 \simeq \pm(2kV_1)^{\frac{1}{2}}\left[1 \mp \frac{\sin\phi_0}{2t_1(2kV_1)^{\frac{1}{2}}}\right]. \qquad \ldots\ldots(42)$$

The general case (no restrictions on v or V/v) is more difficult, but we can get an idea of the magnitude of R as follows. We can write

$$R \simeq 2k\dot{V}\int_{\phi_0}^{(2q+1)\pi-\phi_s} \frac{\cos\phi\, d\phi}{[\dot{\phi}_0{}^2+2kV\cos\phi+2kv(\phi-\phi_0)]^{\frac{1}{2}}}, \quad \ldots\ldots(43)$$

and for (18) to be valid the magnitude of R must be small compared with $2\dot{\phi}_q{}^2$ as given by (18). By a similar procedure to that used above we can show that the average value of the integrand of (43) will be nearly zero, except over the first few phase revolutions (this is so even if $\dot{\phi}_0=0$, and also for particles which pass through $\phi=0$ before being captured, since in this latter case, if V is increasing slowly, ϕ will be approximately an even function of $\dot{\phi}$ near $\dot{\phi}=0$). Now, in this initial period, V will be small, and if $\dot{\phi}_0$ is zero or positive (i.e. corresponding to a particle initially on or inside the equilibrium orbit), we can get a reasonable idea of the magnitude of R by writing

$$R \simeq 2k\dot{V}\int_{\phi_0}^{\infty} \frac{\cos\phi\, d\phi}{[\dot{\phi}_0{}^2+2kv(\phi-\phi_0)]^{\frac{1}{2}}}, \quad \ldots\ldots(44)$$

since this integrand has nearly zero average value except over the initial part of the range. For $\dot{\phi}_0$ negative we are still to some extent justified in accepting (44) since even though ϕ is decreasing we shall get approximately the same value over a few phase revolutions whether we integrate over a positive or a negative range of ϕ, although in either case it must be realized that except when V_1/v is fairly large we shall get, at best, only a rough estimate of R.

If we accept (44), the magnitude of R becomes

$$|R| \simeq \frac{2k\dot{V}}{(2kv)^{\frac{1}{2}}}F(z), \quad \ldots\ldots(45)$$

where

$$F(z)=\{2\pi[(C(\infty)-C(z))^2+(S(\infty)-S(z))^2]\}^{\frac{1}{2}};$$

C and S are the Fresnel integrals and $z=\dot{\phi}_0{}^2/2kv$. For large z, $F(z)\simeq z^{-\frac{1}{2}}$, where the approximation is satisfactory for $z>5$.

It is convenient to compute R in terms of a quantity δ defined by

$$kvt_1=\delta(2kV_1\Phi_1)^{\frac{1}{2}},$$

i.e.

$$t_1(2kV_1)^{\frac{1}{2}}=2\delta\Phi_1{}^{\frac{1}{2}}V_1/v, \quad \ldots\ldots(46)$$

which with (19) defines $\dot{\phi}_0$ for the extreme particles captured. It is clear that δ is the ratio of the average orbit contraction during t_1 to the half-width of the region from which particles are captured.

The condition that R be negligible is that $|R| \ll 4kV_1\Phi_1$, which, with (45), gives

$$t_1(2kV_1)^{\frac{1}{2}} \gg \frac{F(z)}{2\Phi_1}\left(\frac{V_1}{v}\right)^{\frac{1}{2}}. \quad \ldots\ldots(47)$$

Further, for the extreme particles,

$$z=(1\pm\delta)^2\Phi_1V_1/v,$$

the most unfavourable value being

$$z=(1-\delta)^2\Phi_1V_1/v. \quad \ldots\ldots(48)$$

Using (46) and (48), the value of $t_1(2kV_1)^{\frac{1}{2}}$ to make (47) an equality has been computed for a range of values of V_1/v and is plotted in Figure 8. The appropriate condition that R be negligible is just that $t_1(2kV_1)^{\frac{1}{2}}$ has a large value compared with the ordinate of Figure 8 corresponding to the given value of V_1/v.

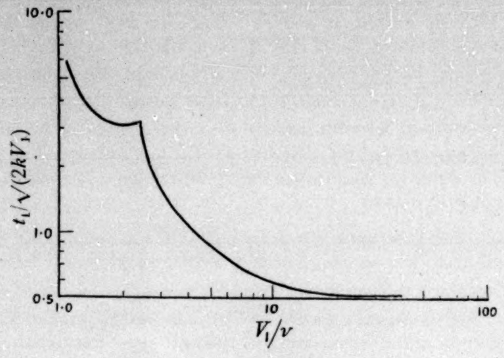

Figure 8. $t_1(2kV_1)^{\frac{1}{2}}$ to make (47) equality. For the capture theory to be valid, $t_1(2kV_1)^{\frac{1}{2}}$ must be large compared with this value.

These restrictions on t_1 leading to the capture theory developed in the text represent one extreme of the capture process, just as the instantaneous rise of the R.F. represents the other extreme; between the two there will be a continuous gradation between the capture of all particles within certain radius limits irrespective of the initial phases, and the capture of only those particles which are initially within the synchrotron stable region.

REFERENCES

Bohm, D., and Foldy, L., 1946, *Phys. Rev.*, **70**, 249.
Dennison, D. M., and Berlin, T. H., 1946, *Phys. Rev.*, **69**, 542.
Elder, F. R., Gurewitsch, A. M., Langmuir, R. V., and Pollock, H. C., 1947, *J. Appl. Phys.*, **18**, 810.
Frank, N. H., 1946, *Phys. Rev.*, **70**, 177.
Gooden, J. S., Jensen, H. H., and Symonds, J. L., 1947, *Proc. Phys. Soc.*, **59**, 677.
Goward, F. K., 1947, *A.E.R.E. Report* No. G/R191.
Kaiser, T. R., and Tuck, J. L., 1948, *Nature, Lond.*, **162**, 616.
Kerst, D. W., and Serber, R., 1941, *Phys. Rev.*, **60**, 53.
Oliphant, M. L., Gooden, J. S., and Hide, G. S., 1947, *Proc. Phys. Soc.*, **59**, 666.

Experiments on Electron Capture and Phase Stability in a 14 Mev. Synchrotron

By T. R. KAISER and J. L. TUCK
Clarendon Laboratory, Oxford

Communicated by Lord Cherwell ; MS. received 11th July 1949

ABSTRACT. Experiments were made by interrupting the radio-frequency accelerating voltage for intervals during the acceleration in a synchrotron, and observing the effects on the output. The process of capture is found to be more efficient than would be expected for an instantaneously developed radio-frequency accelerating voltage. The synchrotron acceleration may be interrupted for a short period without losing more particles than would be accounted for by contraction of the beam radius during the interruption, so that for sufficiently short periods of interruption the loss is negligible. This demonstrates that the phase at which electrons enter the resonator during capture is of no consequence under the conditions prevailing. The results are in quantitative agreement with a theory put forward by Kaiser which takes into account the finite rate of rise of resonator voltage, and with the general theory of synchrotron stability.

§ 1. INTRODUCTION

Measurements of the efficiency of capture of electrons into the stable orbits of a synchrotron have been made using a 14 Mev. electron synchrotron (Abson and Holmes 1947).

In this synchrotron the magnet is energized by 50 c/s. A.C. with a D.C. bias current, the electrons being injected at an energy of about 10 kv. and accelerated by betratron action to a total energy of about 2·5 Mev. when the betatron flux is beginning to saturate. At this point, with an equilibrium orbit radius of about 7·5 cm., R.F. power is supplied to the resonator and synchrotron acceleration begins. The R.F. peak voltage for almost complete capture is found to be 130 v. Other parameters which will be of interest are:

Maximum voltage per turn required by the equilibrium particles	$v_{\mathrm{p}} = 1{\cdot}87$ v.
Magnetic field exponent	$n = 0{\cdot}71$
Resonator frequency	$\omega_s/2\pi = 643$ Mc/s.
Equilibrium radius	$r_s = 7{\cdot}5$ cm.
Width of orbit space at injection time	5 cm.
Resonator voltage	$V = 130$ v.

The notation of the previous paper (Kaiser 1950) is used throughout, and the paper referred to as I.

The technique employed was to suppress the R.F. for a time τ (variable from about 3 to 100 μsec.) at various times T (corresponding to various values of the magnetic guide field H_s) during the acceleration, and to examine the dependence of the X-ray output intensity at $E_s = 14$ Mev. (which is proportional to the number of particles in the beam) on τ. The complete cycle of events was displayed on the screen of a cathode-ray tube, as in Figure 1, horizontal deflection being proportional to the magnet current.

The X-ray intensity was measured by the amplitude of the pulse from a proportional counter placed in the beam, the counter having been calibrated against an ionization chamber type dosemeter. The dosemeter itself could not be used because of the X rays produced earlier in the cycle by the particles lost during the period of R.F. suppression. Since the master oscillator of the R.F. generator was maintained and only the power amplifier suppressed, there was phase coherence before and after suppression. Great pains were taken to ensure that there was no R.F. 'break-through' during the suppression period by suitably biasing the power amplifier, since it was found that quite a small break-through could give spurious results, in particular as regards the time, τ_0, required to suppress the beam completely.

The shape and length of the negative blanking pulse were measured with a crystal rectifier loosely coupled to the resonator, and a cathode-ray oscilloscope containing a generator of 1 μsec. timing pulses. The blanking pulse showing the timing markers is sketched in Figure 2. Both the decay and rise times were of the order of 1 μsec. The actual instant of suppression was known from the calibration of the variable delay in the blanking pulse generator (which was triggered at the instant of transition from betatron to synchrotron acceleration) and was related to the magnet current, and thus to H_s, by measuring the displacement of the blanking pulse along the time-base of Figure 1. This also enabled the R.F. duty cycle to be determined, and the rate of increase of H_s to be checked for each experiment.

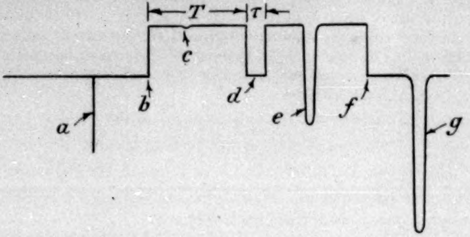

Figure 1. Sequence of operations during the acceleration cycle: *a*, betatron injection pulse; *b*, instant of establishing the R.F.; *c*, X-ray output due to the few betatron electrons not captured; *d*, R.F. suppression; *e*, X-ray output due to electrons lost during suppression; *f*, final R.F. suppression; *g*, X-ray output due to 14 MeV. electrons.

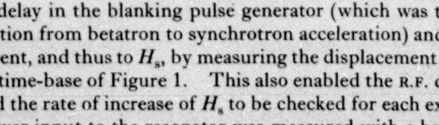

Figure 2. Sketch of the negative blanking pulse with 1 μsec. timing pulses superimposed.

The R.F. power input to the resonator was measured with a bolometer bridge and a wave selector coupled to the transmission line from the power amplifier. In all of the experiments described, this power was adjusted to give almost complete capture, in every case corresponding to a peak input of 28 watts. The measured Q of the quarter-wave resonator was 300 and its characteristic impedance 0·8 ohm, from which we can calculate for the shunt resistance a value of 306 ohms. Using the measured power input we find the peak resonator voltage V to be 130 volts. This value was expected to be very close to the actual peak voltage per turn experienced by an electron, since the conducting surface of the resonator was continuous.* Immediately following the suppression we shall have a beam of electrons spread in radius and phase (relative to the R.F. phase) in a manner dependent on the time of decay of the R.F. voltage. The mean orbit radius will begin to contract at a rate $\dot{r}$, the beam keeping substantially the same width so long as the change in mean radius and the beam width are small compared with r_s. The electron density (averaged with respect to ϕ) will remain substantially the same function of radius, but since particles on the inside and outside of the beam will lose and gain phase respectively, relative to those in the centre, the beam will rapidly become uniform in phase. On re-establishing the radiofrequency the region from which particles may be captured will overlap only a fraction of the beam, this fraction being captured and the remainder spiralling to the inside wall of the orbit vessel. We can examine the fraction recaptured as a function of τ and compare it with that expected, both on the capture theory of paper I and on that for instantaneous R.F. decay and rise. Further, from a knowledge of $\dot{r}$ and τ_0, we can obtain a measurement of the width of the region from which particles may be captured at various times during the period of acceleration, enabling quantitative comparison with the value expected from theory.

§ 2. INSTANTANEOUS FALL AND RISE OF THE R.F. VOLTAGE

Immediately following suppression the bunch shape will be approximately given by

$$\left|\frac{\epsilon}{\epsilon_M}\right| = \cos\tfrac{1}{2}\phi, \qquad \text{since } V \gg v$$

(where ϵ_M is the maximum half-width of the stable region prior to suppression) and is plotted in Figure 3 (*a*). As the mean orbit radius decreases the bunch will spread in phase in the manner indicated in Figure 3 (*b*) which shows the change in shape after the phase gain (or loss), $\delta\phi$, of the extreme electrons in the bunch relative to the central ones has reached 5π radians.

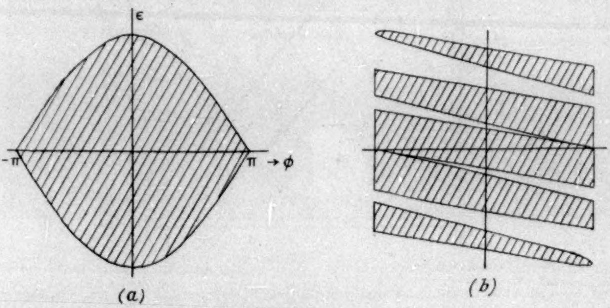

Figure 3.
(*a*) Bunch shape immediately after instantaneous suppression of R.F. voltage.
(*b*) Bunch shape when the phase of the extreme electrons relative to the central ones has advanced or retarded by 5π radians.

---

* The resonator dimensions were such that there was no need to combat eddy currents by subdividing the conducting surfaces.

This phase gain can be shown to satisfy

$$\delta\phi = 4\frac{V\delta r}{v\epsilon_M},$$

where V is the peak voltage prior to suppression and δr is the amount of contraction of the mean orbit radius. We should thus expect the beam to become uniform in phase when $\delta r/\epsilon_M \gg \pi v/2V$, which is equivalent to

$$\frac{\tau}{\tau_0} \gg \frac{\pi v}{4V}, \qquad \ldots\ldots(1)$$

since $\delta r/\epsilon_M = 2\tau/\tau_0$. For this machine, using the least favourable value of v/V, (1) becomes $\tau/\tau_0 \gg 0{\cdot}01$.

When the radiofrequency is instantaneously re-established, the stable region will be of the usual form and will overlap a fraction of the beam. If we adopt the simplifying assumption that the beam becomes uniform in phase immediately after suppression (and that prior to this electrons were uniformly distributed throughout the stable region), the fraction of the electrons recaptured is easily calculated and is plotted in curve (*a*) of Figure 4, giving the expected relative X-ray intensity I/I_0 as a function of τ/τ_0. In fact, we would expect something approximating to the dotted curve of Figure 4, dropping rapidly from unity and approaching the curve (*a*) by a damped oscillation which becomes negligible when (1) is satisfied.

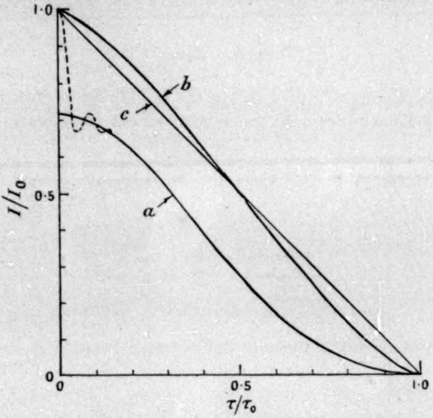

Figure 4. Theoretical curves for relative X-ray output intensity against period of R.F. suppression.
(*a*) Instantaneous suppression.
(*b*) and (*c*) Finite R.F. decay and rise times.

§ 3. FINITE R.F. DECAY AND BUILD-UP TIMES

The actual decay and build-up times t were of the order of 1 μsec., and using the figures given above we find that $t(2kV)^{\frac{1}{2}}$ varies from about 30 to 15 over the period of synchrotron acceleration. In the same period V/v decreases from several hundred to about 70, so that equation (23) of I, i.e. $2V/v \gg t(2kV)^{\frac{1}{2}} \gg \frac{1}{2}$, is fairly well satisfied at all times.

In this case (on the theory of the previous paper) the bunch shape will be destroyed during the R.F. decay time and the half-width of the beam will contract to $1/\sqrt{2}$ times that of the stable region prior to suppression, i.e. to $\epsilon_M/\sqrt{2}$. On re-establishing the radiofrequency all particles will be trapped which lie between the limits $r_s \pm \epsilon_M/\sqrt{2}$, so that we can evaluate the (intensity, τ) curve if we know the density–radius distribution of the electrons during the suppression (which may be similar to that in the original betatron beam). The curves (*b*) and (*c*) of Figure 4 give the expected law for two possible electron distributions, the former on the assumption of a density function proportional to $(1-\epsilon^2)$, where ϵ is the displacement of the particle from the centre of the beam, and the latter on the (less likely) assumption that the density is constant throughout the beam, falling abruptly to zero at the edges.

In the above, the effect of phase damping during the period between capture and R.F. suppression has been neglected, as has also the change in H_s and v during the period of suppression, the latter being negligible during the short time interval involved.

§ 4. EXPERIMENTAL RESULTS

A sample set of experimental results for I/I_0 plotted against τ/τ_0 at various times during the acceleration is given in Figure 5; this comprises three experimental runs taken on different days. The full curves are identical with (*b*) of Figure 4, while the broken curves represent an attempt to take into account the phase damping,

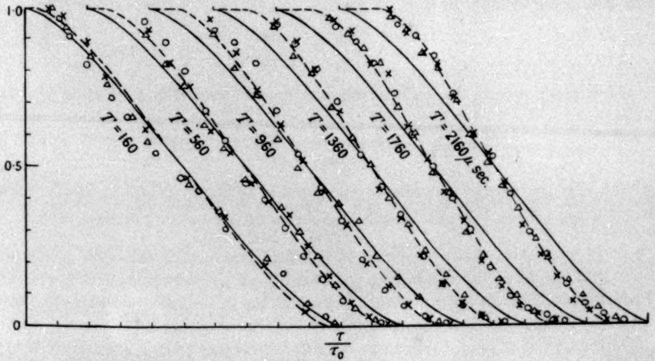

Figure 5. Experimental results for relative X-ray output as a function of period of R.F. suppression, showing agreement with the theory. For convenience the scales of τ/τ_0 for the various curves overlap, so that for each full curve τ/τ_0 has the values 0 and 1 corresponding to ordinates 1 and 0 respectively.

and are obtained from the full curves by assuming that the beam width during R.F. suppression is smaller than that determined from equation (24) of I by a factor proportional to $H_s^{-\frac{1}{4}}$.

The results show that the capture is not of the form to be expected for an instantaneous R.F. decay and rise, and support the conclusion that the initial phase at which the particle enters the resonator is of no consequence, all particles within certain radius limits being captured. The agreement between the experimental and theoretical results seems satisfactory, but is actually not as important as the general form of the results, since any phase dependence would lead, as τ increases, to a rapid fall of I/I_0 from unity followed by a slower decline to zero (as, for instance, curve (*a*) of Figure 4).

The derivative of the experimental curve gives the form of the density–radius distribution in the beam during suppression, and an examination of the results for $T = 160\,\mu$sec. (and to a lesser extent $T = 560\,\mu$sec.) seems to indicate a slight density minimum near the centre of the beam. The fact that this does not appear in later curves may be due to space-charge effects and indicates that it probably derives from the original betatron beam.

From a knowledge of $\dot{r}$ during suppression, and of τ_0, we can calculate the radial width of the region from which particles may be captured and can thus obtain quantitative verification of the theory.

From equations (7) and (24) of I, the expected half-width ϵ of the beam during suppression is

$$\epsilon = \frac{r_s}{\beta_s^2(1-n)}\left(\frac{\mathbf{e}V}{\pi E_s K}\right)^{\frac{1}{2}}, \qquad \ldots\ldots(2)$$

where V, of course, is the voltage immediately prior to suppression.

During this period the orbit radius of a particle in terms of its momentum, p, is

$$r = \frac{p\mathbf{c}}{H\mathbf{e}}, \qquad \ldots\ldots(3)$$

where $\mathbf{c}$ is the velocity of light, so that

$$\frac{\dot{r}}{r_s} = \frac{\dot{p}}{p_s} - \frac{1}{H_s}\frac{dH}{dt}.$$

Now $\dot{p}$ is not zero, due to betatron acceleration, and H is a function of r, thus

$$\frac{\dot{p}}{p_s} = \frac{1}{\beta_s^2}\frac{\dot{E}}{E_s} \qquad \text{and} \qquad \frac{dH}{dt} = \dot{H}_s - nH_s\frac{\dot{r}}{r_s},$$

where $\dot{E}$ is the rate of increase of energy due to betatron action and is related to v by

$$v = \frac{2\pi r_s^2 \dot{H}_s}{\mathbf{c}} - \frac{2\pi\dot{E}}{\mathbf{e}\omega_s}.$$

From (3) $$E_s = \frac{\mathbf{e}H_s r_s}{\beta_s} = \frac{\mathbf{ec}H_s}{\omega_s},$$

giving $$\dot{r} = \frac{-\mathbf{ec}v}{2\pi\beta_s E_s(1-n)}, \qquad \ldots\ldots(4)$$

and since $\epsilon = \tau_0\dot{r}/2$, we get $$\epsilon = \frac{\mathbf{ec}\tau_0 v}{4\pi\beta_s(1-n)E_s}. \qquad \ldots\ldots(5)$$

Although we can evaluate ϵ from (5) and compare it with the value obtained from (2), the following equivalent procedure has been found convenient. From (2) and (5) we get

$$v = \frac{\eta H_s^{\frac{1}{2}}}{\tau_0}, \qquad \ldots\ldots(6)$$

where $\eta = 4(\pi\mathbf{c}V/K\omega_s^3)^{\frac{1}{2}}$, i.e. $V = \dfrac{K\omega_s^3\eta^2}{16\pi\mathbf{c}}$ E.S.U. $\qquad \ldots\ldots(7)$

If η is measured in volt.μsec.gauss^{-1}, (7) becomes

$$V = \frac{10^{-4} K \omega_s^3 \eta^2}{16\pi \mathbf{c}^2} \text{ volt.} \qquad \ldots\ldots(8)$$

In evaluating the results, the particles have been assumed extremely relativistic, i.e. $K = 1/(1-n)$ throughout the acceleration.

The full curve of Figure 6 gives v as a function of H_s as determined by Abson and Holmes (1947)*, while the experimental points are those obtained by substituting the measured values of τ_0 in (6) and choosing η to give a good fit over the flat top of the (v, H_s) curve ($H_s > 2{,}500$). The values of τ_0 were obtained by plotting I/I_0 against τ, and for the first few curves the intersection with the horizontal axis was taken. The later curves correspond to a period of the acceleration when v is almost constant, as also is τ_0; in order to compare the results with the curve of Figure 6 the relative values of τ_0 are more important than absolute values, so that, to obtain greater consistency it was assumed that the graphs of I/I_0 against τ/τ_0 were approximately anti-symmetrical about the line $\tau/\tau_0 = \frac{1}{2}$, τ_0 thus being determined from

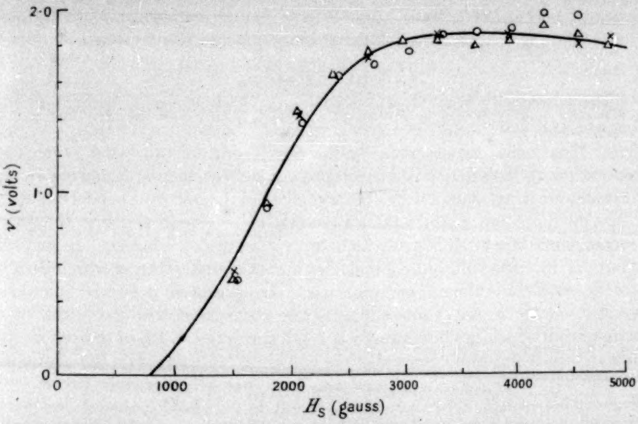

Figure 6. Experimental values of v, as a function of H_s, compared with the result obtained by direct measurement of the residual betatron induction and the rate of increase of H_s.

$$\tau_0 = 2\int_0^\infty (I/I_0)\, d\tau$$

by graphical integration. The results so obtained agreed with the intersection of the curve with the horizontal axis to within the limits of estimation, but the consistency should be somewhat better.

Using the values of η as determined above, the resonator voltage V was evaluated from (8) for each of the sets of results of Figure 6. The values are given in the Table, together with the value determined from the resonator power input.

---

* A numerical error in Abson and Holmes' paper of a factor $\sqrt{2}$ in the value of v has been corrected.

The agreement is well within experimental error, the scatter in the magnitude of V determined from (8) corresponding to a scatter in τ_0 of less than 1 μsec.

Experiment (see Figure 6) ..	○	×	Δ
η	0·49	0·495	0·52
V (volts) (from (8))	122	124	136
V (volts) (from power input)	130	130	130

An extra check on the validity of the capture theory may be obtained by calculating the radial zone of acceptance and comparing it with the expected width of the betraton beam at the instant of transition from betatron to synchrotron. For a resonator voltage of 130 v. the half-width of the acceptance zone is $\epsilon_0 = 0{\cdot}06$ cm., while the assumption that the initial orbit space of width 5 cm. is completely filled at injection, following which the beam contracts approximately as H^{-1} (Kerst and Serber 1941), leads to $\epsilon_0 = 0{\cdot}1$ cm. for the half-width of the betatron beam (neglecting free radial oscillations) immediately prior to transition.

§ 5. CONCLUSIONS

Experiments have been made on the release of electrons from, and their re-capture into, stable orbits in a synchrotron. The capture is found to be more efficient than would be expected by the application of the usual synchrotron equations for an instantaneously developed radio-frequency accelerating voltage. The results are in agreement with a theory (given in the previous paper) taking into account the finite rate at which the R.F. voltage is developed and with the general theory of synchrotron stability on which the capture theory is based. In particular the form of the curves of Figure 5 indicates that the initial phase at which electrons enter the resonator is of no importance, while the agreement between the values of resonator voltage in the Table supports the conclusion that the width of the electron beam which can be captured is $1/\sqrt{2}$ times the width of the synchrotron stable region (it should be noted that the voltage V, calculated on the assumption of instantaneous capture, would be one half that given in the Table). The agreement between the experimental points and the curve of Figure 6 shows that the width of the stable region varies with magnetic field (or particle energy) in the manner required by the general theory.

A modification of the experimental technique that we have used suggests itself for a direct measurement of the distribution of particles with radius in a betatron beam prior to transition to synchrotron acceleration, namely by measuring the output intensity as a function of the time of transition. Provided v remains constant over the interval concerned, the form of this distribution is just the derivative of the (X-ray intensity, time) curve between maximum and zero intensity, while if v does not remain constant, its variation, if known, can be taken into account.

ACKNOWLEDGMENTS

We are indebted to Mr. D. W. Fry (Atomic Energy Research Establishment, Malvern) for permission to use the 14 MeV. synchrotron for these experiments, and one of us (T.R.K.) to the Commonwealth Scientific and Industrial Research Organization (Australia) for a Research Studentship.

REFERENCES

Abson, W., and Holmes, L. S., 1947, *A.E.R.E. (Unclassified) Report*, Ref. A.E.R.E., G/R 192.
Kaiser, T. R., 1950, *Proc. Phys. Soc.* A, **63**, 52.
Kerst, D. W., and Serber, R., 1941, *Phys. Rev.*, **60**, 53.

LETTERS TO THE EDITOR

The Electric Conductivity of Simple Semiconductors

E. H. Putley, in this journal, has recently (1949) drawn attention to a series of papers in which Shifrin (1944) discussed the electric properties of impurity semiconductors, to be expected on the basis of the model originated by Wilson; Shifrin extended the limiting relations originally given so as to cover a much wider range of temperatures and impurity densities. In particular Shifrin has shown that for simple semiconductors the conductivity for the whole range of temperatures should rigorously be given by

$$\sigma=\sigma_0 \ln (1+A), \qquad \ldots\ldots (1)$$

where A is the quantity originally introduced by Sommerfeld (1928) and related to the thermodynamic potential ζ by $\ln A=\mu=\zeta/\boldsymbol{k}T$. Further, he has shown that A and hence the conductivity has a maximum A_{m} at a temperature T_{m} given by

$$\ln A_{\mathrm{m}}=-\Delta\epsilon/\boldsymbol{k}T_{\mathrm{m}}-\ln (\tfrac{2}{3}\Delta\epsilon/\boldsymbol{k}T_{\mathrm{m}}-1). \qquad \ldots\ldots (2)$$

These expressions refer to non-ionic lattices for which the mean free path of the electrons is independent of their energy and inversely proportional to the temperature, with only one kind of impurity centre supplying the electron gas. They take fully into account its degeneracy. It has since been shown by a number of authors (Johnson and Lark-Horovitz 1947, 1942–1949, Busch and Labhart 1946, Putley 1949) that this degeneracy plays in fact an important rôle.

The question then arises how to apply equations (1) and (2) in interpreting measured conductivities in the light of the relation

$$n=n_{\mathrm{b}}/\{1+A \exp (\Delta\epsilon/\boldsymbol{k}T)\}=2C(\boldsymbol{k}T)^{3/2}f_{\frac{1}{2}}(A), \qquad \ldots\ldots (3)$$

where

$$f_{\frac{1}{2}}(A)=\tfrac{1}{2}\int_0^\infty \frac{x^{\frac{1}{2}}\,dx}{A^{-1}\epsilon^x+1}, \qquad \ldots\ldots (4)$$

n_{b} the number of impurity centres, n the number of free electrons, $\Delta\epsilon$ the energy difference between the impurity level and the lower edge of the conduction band,

$$C=4\pi(2\boldsymbol{m})^{3/2}/\boldsymbol{h}^3\simeq 3{\cdot}4\times 10^{39} \text{ C.G.S. units.}$$

Tables of $f_{\frac{1}{2}}$ have been given by McDougall and Stoner (1939) but a tabulated form of $f_{\frac{1}{2}}$ does not lead to an explicit expression for A in terms of n_{b}, $\Delta\epsilon$ and T.

Now, Busch and Labhart have proposed to approximate $f_{\frac{1}{2}}$ by an expression of the form

$$f_{\frac{1}{2}}=A\pi^{\frac{1}{2}}/4(1+bA+cA^2), \qquad \ldots\ldots (5)$$

valid for $A<5$, i.e. in the range which one expects to find in semiconductors. In following this up, however, Busch and Labhart use instead of Shifrin's formula (1) the expression

$$\sigma=\frac{\boldsymbol{e}^2}{\boldsymbol{m}^*}n\tau,$$

which would only be justified if for semiconductors the time of relaxation τ were independent of the energy of the electrons, but which is incompatible with the accepted conclusion that the mean free path is independent of the energy.

Putley, on the other hand, uses Shifrin's relation in connection with the tables of McDougall and Stoner to find σ_0, n_{b}, $\Delta\epsilon$. Inconsistently, however, he suggests obtaining σ_0 from the low-temperature range, whereas the low-temperature approximation of A leads directly only to $\Delta\epsilon$ as the negative slope of $\ln \sigma(\boldsymbol{k}T)^{\frac{3}{4}}$ plotted against $1/2\boldsymbol{k}T$. From $\Delta\epsilon$ and T_{m}, A_{m} can be obtained from (2) and hence n_{b} from (3) and σ_0 from (1). But lacking an analytic expression for A, it is not easy to calculate σ generally.

Busch and Labhart, however, had obtained an analytic expression for A. Following up their suggestion one readily verifies that

$$f_{\frac{1}{2}}=0{\cdot}443/(0{\cdot}25+A^{-1}) \qquad \ldots\ldots (6)$$

reproduces the values of McDougall and Stoner for $A<6$ with an accuracy better than 5%, which is quite satisfactory in the case of semiconductors. With (6), the temperature dependence of the conductivity of semiconductors becomes very clear. Equation (3) leads on the one hand to

$$n=0{\cdot}886C(\boldsymbol{k}T)^{3/2}/(0{\cdot}25+A^{-1}), \qquad \ldots\ldots(7)$$

and on the other hand to a quadratic equation for A or A^{-1},

$$A^{-1}=0{\cdot}443C(\boldsymbol{k}T)^{3/2}/n_b-0{\cdot}125 \\ +[(0{\cdot}443C(\boldsymbol{k}T)^{3/2}/n_b-0{\cdot}125)^2+0{\cdot}886C(\boldsymbol{k}T)^{3/2}\exp(\Delta\epsilon/\boldsymbol{k}T)/n_b]^{\frac{1}{2}}, \qquad \ldots\ldots(8)$$

so that, using (1), an explicit expression for σ can be written down.

When (8) is specialized for high or low T and the resulting value is inserted into (1) and (7), the well-known limiting expressions for the conductivity and the number of free electrons are obtained. Equation (2) follows at once from (8) by equating $\partial A^{-1}/\partial T=0$. Further

$$n_b=0{\cdot}883C(\boldsymbol{k}T_m)^{3/2}[1+A_m\exp(\Delta\epsilon/\boldsymbol{k}T_m)]/(0{\cdot}25+A_m^{-1}). \qquad \ldots\ldots(9)$$

Hence, by combining an approximate expression for $f_{\frac{1}{2}}$ of the Busch and Labhart type with Shifrin's results, an analytic expression for the conductivity of semiconductors valid for all temperatures becomes available, as well as a simple procedure for obtaining the constants. It should, however, be borne in mind that it is derived under the assumptions that the mean free path of the electrons is determined exclusively by collisions with acoustic lattice vibrations, that only one kind of impurity centre supplies the electron gas and that conductivity takes place in one band only.

Birkbeck College,
University of London.
1st November 1949.

W. EHRENBERG.

BUSCH, G., and LABHART, H., 1946, *Helv. Phys. Acta*, **19**, 463.
JOHNSON, V. A., and LARK-HOROVITZ, K., 1947, *Phys. Rev.*, **71**, 374; see also 1942–1949, *Progress Reports* (Dept. of Physics, Purdue University).
MCDOUGALL, J., and STONER, E. C., 1939, *Phil. Trans.* A, **237**, 67.
PUTLEY, E. M., 1949, *Proc. Phys. Soc.* A, **62**, 284.
SHIFRIN, K., 1944, *J. Phys. USSR*, **8**, 242; *J. Tech. Phys. USSR*, **14**, 40, 43, 49.
SOMMERFELD, A., 1928, *Z. Phys.*, **47**, 1.

REVIEWS OF BOOKS

The Freezing of Supercooled Water, by N. Ernest Dorsey. Pp. 82. Reprinted from Transactions of the American Philosophical Society, **38**, 247. (Philadephia: American Philosophical Society, 1948.) $1.75.

In 1938 Dr. Dorsey published a preliminary account of experiments on the supercooling of water. In this he showed that the extent to which a given sample could be supercooled without freezing was determined by the presence of foreign particles or nuclei, and that these could be removed or influenced by further purification, by allowing the sample to stand, or by heating. Very pure water could be supercooled to −21°. The determining factor was thought to be the size of these nuclei. The present longer (82-page) account describes his further experiments carried out intermittently over the last ten years. The style is more discursive than is usual in an account of original research but he presents a large number of results which undoubtedly help to fill in the complicated picture which has arisen from his earlier work and from the more recent work of Cwilong, Rau (extended to much lower temperatures), Weickmann, etc. Dorsey's experiments are all measurements of t_{sf}, the temperature of spontaneous freezing, and for water in his temperature range this means that they are investigations of nucleation, the rate of crystallization being always very large after initiation. He has investigated carefully the effect of prolonged maintenance at particular (higher) temperatures and of various other forms of pre-treatment, and has also established the existence of 'preferred temperatures' for the freezing of his samples. Only speculative suggestions are offered about the actual nature of the nuclei, and some of his experiments are of qualitative rather than quantitative interest—as for instance his tests on "ordinary distilled water containing an unknown amount of alcohol and an unperforated glass bead" and "vacuum distilled water into which ethyl alcohol from the bath leaked through a crack".

While the experimental results presented are useful and extensive, the theoretical discussion is of less value. Dr. Dorsey is critical of previous theories of nucleation, particularly of the 'homogeneous' theory arising from the work of Gibbs, J. J. Thomson, Frenkel, Becker, etc., which considers the onset of crystallization to be due to spontaneous nucleation. Favouring in general some form of 'heterogeneous' theory, that is, one in which nuclei already present are assumed to be responsible for crystallization, he has (to use his own phrase) 'worked up' a new detailed theory in which ice embryos are assumed to be formed in various ways from water molecules adsorbed on larger foreign particles. He is probably right in saying that the 'homogeneous' theory is inapplicable to his experimental results, but is unduly polemical on this and other points. G. O. JONES.

Foundations of Modern Physics, by T. B. Brown. Pp. xvi + 391. Second Edition. (New York: John Wiley and Sons; British Agents: Chapman and Hall, 1949.) 30*s*.

Professor Brown's book is successful if its aim is to give to science students, in their last year at school or in their first year at the university, a sketch of the type of experiments and an outline of the ideas which form the basis of modern physics.

The production of the present work is excellent, the printing is good, the diagrams are clear and concentrate on fundamentals, and there are extremely few errors of any kind. There does not seem to be any way in which the treatment of so wide a subject could be substantially improved within the limits of 400 pages. Yet it does not seem possible to deny that the analysis is shallow; also the contribution of American workers is over-emphasized in the last few chapters. Perhaps the author can hardly be blamed for this since the advance of modern physics has been so rapid and on so wide a front that some selection is inevitable. Indeed, the reviewer feels that the days when a semi-popular exposition of physics can be undertaken are rapidly drawing to a close. No one expects advances in modern mathematics to be made generally intelligible or available to first-year students, and certainly the number and quality of those engaged in advancing modern physics is such that the breadth, content and complexity of the subject are likely to increase still further. F. C. CHAMPION.

Einführung in die Atomphysik, by W. Finkelnburg. Pp. viii + 339. (Berlin: Springer-Verlag, 1948.) 28 *D.M.*

The appearance of this excellent text by Professor Finkelnburg is a welcome sign of the revival of scientific activity in post-war Germany. The book is based on courses given for ten years to classes of physicists, chemists, engineers and biologists. It is approximately of the standard required for a first degree in physics in this country. There are now a number of works in English covering similar subject-matter of about the same standard, but this book compares favourably with any of them in breadth and interest of presentation.

Professor Finkelnburg aims at presenting atomic physics, not as a series of isolated topics, but as a subject with an underlying internal unity. Chapters of the book deal with atomic structure and atomic spectra, nuclear physics, molecular physics and the physics of the solid and liquid states. The outlook is predominantly experimental, and a chapter on the basic ideas of quantum theory enable the author to show how the multitude of experimental data on atomic physics, which twenty-five years ago seemed to defy attempts at rationalization, can now be reduced to a rational form in terms of quantum mechanics

The book as a textbook is thoroughly up to date and contains sections on nuclear fission, isotope separation and the betratron.

It is attractively printed and shows that the great reputation built up by Messrs. Springer as publishers of scientific literature in former days is likely to be maintained in these post-war years.

E. H. S. BURHOP.

CONTENTS FOR SECTION B

PAGE
Editorial 1
Mr. J. K. Mackenzie. The Elastic Constants of a Solid containing Spherical Holes 2
Prof. Friedrich Blaha. On Movements of Small Ferromagnetic Particles in Inhomogeneous Magnetic Fields 12
Mr. B. Collinge. Dead Times of Self-Quenching Counters 15
Mr. F. G. Heymann. Breakdown in Cold-Cathode Tubes at Low Pressure . 25
Mr. W. E. Willshaw and Mr. R. G. Robertshaw. The Behaviour of Multiple Circuit Magnetrons in the Neighbourhood of the Critical Anode Voltage . 41
Mr. D. G. Kiely. Measurements of the Reflection Coefficient of Water at a Wavelength of 8·7 mm 46
Mr. T. L. Eckersley. Coupling of the Ordinary and Extraordinary Rays in the Ionosphere 49

Letters to the Editor:

Mr. A. N. Hunter. The Debye Effect in Electrolytes 58
Mr. C. E. Challice. Electron Optics of the Three-Stage Electron Microscope 59
Reviews of Books. 62
Contents for Section A 63
Abstracts for Section A 63

ABSTRACTS FOR SECTION B

The Elastic Constants of a Solid containing Spherical Holes, by J. K. MACKENZIE.

ABSTRACT. The effective bulk and shear moduli are calculated by a self-consistent method due to Fröhlich and Sack. The bulk modulus k is determined by applying a hydrostatic pressure, and the shear modulus μ by applying a simple homogeneous shear stress, to a large sphere. Each hole is surrounded by a spherical shell of real material, and the reaction of the rest of the material is estimated by replacing it by equivalent homogeneous material. For consistency, both the density and the displacement of the outer spherical boundary must be the same whether the hole and its surrounding shell are replaced by equivalent material or not. The effective elastic constants calculated from these conditions are

$$1/k = 1/k_0\rho + 3(1-\rho)/4\mu_0\rho + O[(1-\rho)^3],$$
$$(\mu_0-\mu)/\mu_0 = 5(1-\rho)(3k_0+4\mu_0)/(9k_0+8\mu_0) + O[(1-\rho)^2],$$

where k_0 and μ_0 refer to the real material and ρ is the density of the actual material relative to that of the real material ; in the next approximation k depends on the standard deviation of the volumes of the holes.

The dilatation due to a distribution of pressures in the holes is $\bar{p}(1/k-1/k_0)$, where $\bar{p}$ is the mean obtained when the pressure in each hole has a weight proportional to the volume of the hole. By using the hydrodynamic analogue of the elastic problem, the theory is briefly applied to the theory of sintering, and used to discuss the effective viscosity of a liquid containing small air bubbles.

On Movements of Small Ferromagnetic Particles in Inhomogeneous Magnetic Fields, by FRIEDRICH BLAHA.

ABSTRACT. Ferromagnetic particles of diameter from 10^{-3} to 10^{-5} cm. when exposed to light move along the lines of force of an inhomogeneous magnetic field. It does not seem possible to explain the movement when only dipole properties of the particles are taken into account. Field strengths of 10^{-2} gauss are sufficient to cause distinct movement. The motions resemble those of electrically charged particles in electric fields.

Dead Times of Self-Quenching Counters, by B. COLLINGE.

ABSTRACT. Experiments on Geiger counters are described in which localization of the ion sheath was brought about by reducing the wire potential immediately after each count. The effect on the dead time is discussed. The dead time of a counter 30 cm. long was found to be 20 μsec. and independent of the counting rate up to $1{\cdot}8 \times 10^6$ counts per minute. The reduction of the dead time of short counters was also investigated.

Breakdown in Cold-Cathode Tubes at Low Pressure, by F. G. HEYMANN.

ABSTRACT. When, in cold-cathode discharge tubes, electrode spacings and surface areas deviate from the ideal of infinite parallel planes, it is found that the breakdown voltage between electrodes increases. This is explained as a decrease in the effective η of the gas due to loss of electrons and positive ions by diffusion to the walls of the container. The loss factor per unit potential difference is shown theoretically to be inversely proportional to the field strength and tube radius, although this is not fully verified by experiment.

Paschen curves obtained experimentally for potassium and nickel cathodes in argon and in a neon–argon mixture at low pressures are shown and from these, values of γ for the two cathode surfaces are obtained as a function of E/p_0. The apparatus used for measuring breakdown voltage is described.

Earlier theories of statistical and formative time delays are extended to cover the case of a rising overvoltage and also the case where the primary electrons appear in bursts as with ionization by α-particles. The shape of the statistical distribution curve is an indication of whether the primary electrons have been produced singly or in bursts. The overvoltage ΔV of breakdown due to formative lag and the rate of rise of the uniformly increasing applied voltage V are found to bear the relation $\Delta V \propto \sqrt{(dV/dt)}$. This has been experimentally verified.

The Behaviour of Multiple Circuit Magnetrons in the Neighbourhood of the Critical Anode Voltage, by W. E. WILLSHAW and R. G. ROBERTSHAW.

ABSTRACT. It is pointed out that the mechanism of operation of the multiple circuit magnetron oscillator in the region of minimum magnetic field and voltage, where the efficiency is commonly assumed to approach zero, should approach that of an oscillator of the travelling wave tube type, providing that a cathode of suitable size is used. Useful efficiencies should thus be obtainable under these conditions.

Details of experiments are given in which an electronic efficiency of 12% was obtained at a wavelength of 3 cm. at values of magnetic field and voltage several times lower than those used for high efficiency operation. The mode of operation was determined by the value of the magnetic field, a given mode being maintained over a range of magnetic field of the order of 8%. The anode voltage was about 70% of the critical value.

The experimental results generally support the hypothesis and suggest that the minimum voltage regime should be of extreme importance for work at the highest radio frequencies.

Measurements of the Reflection Coefficient of Water at a Wavelength of 8·7 *mm.*, by D. G. KIELY.

ABSTRACT. An account is given of measurements (carried out in March 1947) of the reflection coefficient of water at a wavelength of 8·7 mm. over a range of angles of incidence.

The method employed is to measure the relative field strengths of the direct waves and waves reflected from a trough of water using free-space propagation and high-gain aerials.

The following electrical constants of water have been computed from the measured results (water temperature 11·1° c.): refractive index 4·40±0·24, dielectric constant 10·86±2·21, absorption coefficient 2·91±0·06, conductivity/frequency 12·82±0·42, Brewster angle 79°.

Coupling of the Ordinary and Extraordinary Rays in the Ionosphere, by T. L. ECKERSLEY.

ABSTRACT. In this paper an approximate solution to the wave equation is given for propagation in an ionosphere in which the gradient of the density N is in the vertical, z, direction only, and in which account is taken of the earth's magnetic field. It corresponds exactly to the ray theory and expresses a quantity Z, which is the z derivative of the phase function S, by a quartic equation. Z can be represented as a function of ζ (which is proportional to N) on a four-sheeted Riemann surface, and the branch points are studied for the case of vertical incidence for which Z becomes the refractive index. By considering the branch points in the complex ζ plane, the amount of the coupling between the ordinary and the isolated extraordinary branches of the (Z, ζ) curves can be expressed as a function of the obliquity of the magnetic field. The triple splitting of rays reflected from the ionosphere, observable where the field is nearly vertical, can thus be explained, and the theory is substantiated by the observation that the polarizations of the echoes on the (P', f) records are ordinary, ordinary and extraordinary in order of increasing critical frequencies, as given by the branches of the (Z, ζ) curves.